Università degli studi di Padova
Department of information Engineering
Master's course in Bioengineering

A model of intraperitoneal insulin kinetics in patients with type 1 diabetes treated by implanted insulin pumps

Supervisor
Prof. Chiara Dalla Man

Student
Filippo Moret

Co–Supervisor
Michele Schiavon

Academic Year 2018–2019

Abstract

Type 1 Diabetes (T1D) is an autoimmune disease which affects about 5–10% of all diabetic patients in the world (422 million according to the World Health Organization), commonly occurring in childhood and adolescence. It is characterized by the destruction of the insulin–producing pancreatic beta cells, leading to chronic hyperglycaemia. As a consequence, a strict glycaemic control is needed in order to maintain the glucose homeostasis approximately in 80–140 mg/dl (4.4–7.8 mmol/l) range, avoiding both the risk of hyperglycaemia, leading to micro– and macro–vascular complications and the risk of hypoglycaemia, potentially leading to coma and death. In this regard, several insulin therapies are available, mainly based on exogenous subcutaneous insulin administration through the common Multiple Daily Injection (MDI) or the more recent Continuous Subcutaneous Insulin Infusion (CSII) therapy. However, in some patients with T1D, the subcutaneous insulin therapy is not sufficient to avoid excessive glycaemic excursions, both due to the delay and large inter–/intra–subject variability in the insulin appearance in plasma as well as subcutaneous insulin resistance. Recently, solution has been proposed for this problem, represented by Continuous Intraperitoneal Insulin Infusion (CIPII). The two main insulin infusion systems adopting the intraperitoneal route are the implantable pumps and Diaport systems. In the treatment of patients with T1D, several studies have demonstrated that the CIPII therapy mimics more closely physiological conditions, allowing also to reduce hypoglycaemic events, improve glycaemic control and thus, increase patients satisfactory and Quality of Life (QoL) than standard therapies. However, so far, a mathematical model of intraperitoneal insulin absorption is still lacking thus limiting the optimization of insulin therapy in this population. The aim of this thesis is to develop a mathematical model to describe the intraperitoneal insulin absorption in patients with T1D, who are treated by CIPII therapy. In this regard, a database of eight patients, studied fro three days in a hospitalized setting with basal and meal insulin administered via intraperitoneal route, is used. A battery of compartmental models with increasing complexity are developed and compared based on standard metrics. Finally, the best model, i.e. the one able to describe the data with the minimum number of parameters, is selected.

Sommario

Il diabete di tipo 1 è una malattia autoimmune che colpisce circa il 5–10% di tutti i pazienti diabetici nel Mondo (422 milioni secondo l'Organizzazione Mondiale della Sanità), comunemente bambini ed adolescenti. Si caratterizza per la distruzione delle beta cellule pancreatiche, responsabili della produzione di insulina, che porta ad eventi cronici di iperglicemia. Di conseguenza, è richiesto un ferreo controllo della glicemia al fine di mantenere un livello della concentrazione di glucosio nel sangue approssimativamente nel range di 80–140 mg/dl (4.4–7.8 mmol/l), evitando sia il rischio di iperglicemia, che può provocare complicanze micro e macrovascolari, sia il rischio di ipoglicemia che può potenzialmente indurre al coma e alla morte. A questo proposito, diverse terapie insuliniche sono disponibili, nelle quali tale ormone viene somministrato tramite iniezione sottocutanea: la comune terapia di "iniezioni multiple giornaliere" (MDI) oppure la più recente "infusione di insulina sottocutanea continua" (CSII). Tuttavia, in alcuni soggetti con diabete di tipo 1, la terapia insulinica sottocutanea non riesce ad evitare eccessive escursioni della glicemia, sia per il ritardo sia per la grande variabilità inter– e intra–soggetto nella comparsa di insulina nel plasma, così come per la loro marcata resistenza sottocutanea all'insulina. La soluzione che è stata recentemente proposta per questo problema prende il nome di "infusione intraperitoneale continua di insulina" (CIPII). I due principali sistemi di infusione di insulina che adottano la via intraperitoneale sono le pompe implantabili e il sistema DiaPort. Nel trattamento dei pazienti con diabete di tipo 1, diversi studi hanno infatti già dimostrato che la terapia CIPII rappresenta un sistema in grado di mimare meglio, rispetto alle terapie standard, le condizioni fisiologiche, permettendo anche di ridurre gli eventi di ipoglicemia, di migliorare il controllo glicemico e perciò, di aumentare il livello di soddisfazione percepito dai pazienti e la qualità di vita. Tuttavia, finora, non è presente in letteratura alcun modello matematico dell'infusione di insulina per via intraperitoneale, limitando perciò l'ottimizzazione della terapia insulinica in questa popolazione. Lo scopo di questa tesi è quindi quello di sviluppare un modello matematico in grado di descrivere l'assorbimento di insulina per via intraperitoneale nei pazienti con diabete di tipo 1, trattati utlizzando la terapia CIPII. A tal proposito, è stato utilizzato un database di otto pazienti ospedalizzati e studiati per tre giorni, attraverso una terapia insulinica bolo-basale somministrata per via

intraperitoneale. Differenti configurazioni di modelli compartimentali di crescente complessità sono state quindi proposte e comparate secondo criteri standard. Infine, è stato scelto il miglior modello, cioè quello in grado di descrivere i dati con il minor numero di parametri.

Contents

Glossary

AP Artificial Pancreas

CBG Capillary Blood Glucose

CGM Continuous Glucose Monitoring

CIPII Continuous Intraperitoneal Insulin Infusion

CSII Continuous Subcutaneous Insulin Infusion

GH Growth Hormone

HbA1c Glycated Hemoglobin

HE Hepatic Extraction

HIU Hepatic Insulin Uptake

IGF–1 Insulin–like Growth Factor–1

IP Intraperitoneal

IV Intravenous

IVGTT Intravenous Glucose Tolerance Test

MAP Maximum A Posteriori

MDI Multiple Daily Injection

NSIO Net splanchnic insulin output

PID Proportional–Integral–Derivative

QoL Quality of Life

SAP Sensor–Augmented Pump

SC Subcutaneous

SHBG Sex Hormone–Binding Globulin

SR Secretion

SS Steady–State

T1D Type 1 Diabetes

WRSS Weighted Residual Sum of Squares

Chapter 1

Introduction

1.1 Diabetes mellitus

T1D mellitus is characterized by an (almost) absent secretion of insulin due to autoimmune mechanisms [49]. In particular, the immune system attacks and destroys the insulin producing cells called *beta cells* in the islets of Langerhans in the pancreas. To better understand what's going on type 1 diabetes, in Figure 1.1 is represented the glucose–insulin mechanism. Carbohydrates that we ingest through food are broken down into simple sugars, primarily glucose, that is an important source of energy for the body's cells. To leave the bloodstream and to enter into the cells, glucose needs insulin, a key hormone that promotes its absorption by the cells. Normally, the pancreas secrets more insulin when glucose levels in the blood rise. However, in patients with T1D, due to the lack of insulin secretion, glucose accumulates in the bloodstream leading to hyperglycaemia.
The causes of T1D are unknown and the possible explanatory theories are related to genetics and environment such as particular viral and bacterial infections and dietary agents that may, precisely, trigger this autoimmune disease. The incidence in the World indeed represents an epidemiological conundrum: T1D is most common in Finland (>60 cases per 100 000 people each year) while its incidence in Estonia, separated from Finland by less than 120 km, is less than one–third. The global incidence of T1D is estimated 5–10% of all diabetes cases and in Italy it is most common in Sardinia (around 40 cases per 100 000 people each year). This type of diabetes, also known as "juvenile diabetes" or insulin–dependent diabetes, tends to occur in childhood, adolescence or early adulthood (before age 30) but it may have its clinical onset at any age. The classic symptoms are excessive excretion of urine (polyuria), weight loss, blurry vision, increased thirst (polydipsia), excessive hunger (polyphagia), and fatigue. Symptoms typically develop over a short period of time. The life expectancy is 11 years less for men and 13 years less for women with type 1 diabetes [28]. Diabetes complications are classified as macrovascular or microvascular. In par-

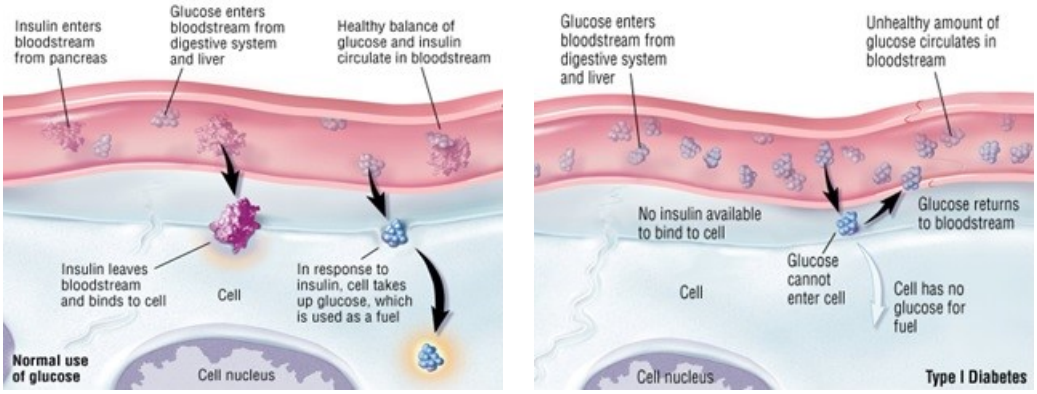

(a) *Healthy subject* (b) *Type 1 diabetes patient*

Figure 1.1: Representation of the glucose-insulin molecular mechanism. Retrieved from https://www.health.harvard.edu/media/content/images/cr/205333.jpg. Author: Wendy Hiller Gee. Copyright 2007 Krames

ticular, as patients with T1D live longer, cardiovascular disease is becoming a more common macrovascular complication with a ten–times higher risk than age–matched non-diabetic populations. The microvascular ones include retinopathy and nephropathy [1]. It has been proven that those complications are unambiguously linked to the duration and severity of hyperglycaemia [49], so it's crucial to guarantee insulin injection, after disease onset, through intensive insulin therapy (diet and exercise are not enough although important). Moreover, also hypoglycaemia can lead to both short and long–terms consequences: for example, since the brain is completely dependent upon glucose supply, it can alter cerebral activity, damage the cells and even cause death. This risk is increased with the increasing duration of the disease and strict glycaemic control. Hence, diabetes therapy focuses on maintain glucose in the tight target range, approximately 80–140 mg/dl (4.4–7.8 mmol/l) avoiding hypo and hyper–glycaemia phenomena.

Nowadays several strategies are adopted for the treatment of T1D via insulin therapy: *Multiple Daily Injection (MDI)* of insulin in the Subcutaneous (SC) tissue and *Continuous Subcutaneous Insulin Infusion (CSII)* with externally placed pumps. With the first exogenous insulin replacement modality, a short–acting insulin analogue is administered in the postprandial period to compensate glucose increase, due to meal ingestion and/or hyperglycaemic events as bolus insulin, while a long–acting insulin analogue is administered once daily to keep glucose stable in the post–absorptive state as basal insulin. On the other hand, CSII uses a portable electromechanical pump infusing short–acting insulin into the subcutaneous tissue at preselected rates. A randomised controlled trial in adults reported that a greater proportion of patients

reached the targeted levels of Glycated Hemoglobin (HbA1c) using *Sensor–Augmented Pump (SAP)*, i.e. through Continuous Glucose Monitoring (CGM) sensors and CSII pumps therapy instead of MDI [5]. Nevertheless, outcomes reported in various studies don't agree whether CSII is better, overall, than MDI. In fact, another recent randomised trial and economic evaluation of infants, children and young people in the first year of T1D, demonstrated CSII treatment was not more clinically effective than treatment with MDI and that glycaemic control was suboptimal in both treatments [7]. Actually, with both MDI and CSII, pharmacokinetic and pharmacodynamic properties of SC administered insulin cause deviations from the normal response. This is generally due to the high intra and inter subject variability in the rate of SC absorption, together with differences in insulin absorption between injections sites and insulin preparation [49]. Therefore, it's not uncommon to detect unpredictable fluctuations in blood glucose concentrations that globally reduce the quality of life (*QoL*). The current and future challenge is to avoid, as much as possible, these fluctuations and to increase the time in normoglycaemia that translates into a better QoL and a reduction in complications. In this framework, alternative insulin infusion routes have been developed such as the Intraperitoneal (IP) one which is thoroughly analysed in the following section 1.2.

1.2 Insulin infusion using intraperitoneal route

As previously mentioned, the researchers' goal is to build an *Artificial Pancreas (AP)* capable to achieve long–term strict glycaemic regulation. Nowadays, the aim pursued via SC glucose sensing and SC insulin delivery. However, even the most sophisticated control algorithms in on–body AP systems are not able to maintain tight glycaemic control because of the high delays introduced by the SC route in compensating exogenous glucose disturbances like meals and exercise. Moreover, some patients with T1D do frequently experience unexpected hypoglycaemia, despite an intensive SC insulin treatment. Therefore, the need for a more physiological route of insulin delivery has opened the door to the IP insulin delivery.

1.2.1 Physiological justification

Before focusing on the main physiological reasons underlying IP route, it is useful to make some essential introductory remarks to the kinetics of insulin, represented schematically in the Figure 1.2. Endogenous insulin Secretion (SR) in healthy subjects is pulsatile (bursts approximately every 4 minutes) and occurs into the portal vein. The liver, for its special anatomical position, receives the entirety of *de novo* secreted insulin, introducing a "first pass" effect. Studies have shown that 50–80% of the endogenous portal insulin is extracted by the liver before the subsequent systemic

entry [8], [18], [32]. Then, after each recirculation, systemic insulin is again extracted by the liver. In order to quantify these intuitive facts in humans, some technical and theoretical issues are evident, such as the inaccessibility of the ports of entry and exit of the liver. Thus, the kinetics is measured in the system circulation and some assumptions have to be made to estimate the various parameters of insulin metabolism. On the assumption of Steady–State (SS) and by direct hepatic vein and artery sampling (invasive direct measurement), it was possible to calculate the Net splanchnic insulin output (NSIO) as the product of hepatic plasma flow (F) and the difference between the arterial insulin concentration $\left(I_a^{SS}\right)$ and the insulin concentration in the hepatic veins $\left(I_{hv}^{SS}\right)$: $NSIO = F\left(I_a^{SS} - I_{hv}^{SS}\right)$. This balance equation is only valid at SS and so applicable in conditions in which SS is not significantly perturbed. AS it can be clearly seen in the Figure 1.2, pancreatic insulin reaches the hepatic veins before distribution to body periphery, so this leads to a considerable positive portal to systemic insulin gradient (insulin concentrations ratio 4:1). The gradient assists in balancing peripheral glucose disposal and hepatic glucose output, ensuring daily glucose homeostasis. The net effect of insulin secretion and Hepatic Extraction (HE) determine the peripheral insulin concentrations. So, the extraction ratio (h) can be interpreted as the ratio of Hepatic Insulin Uptake (HIU) to total insulin delivery to the liver, i.e. $SR + FI_a^{SS}$. As mentioned above, the direct measurement of F or HE is not possible because of the catheterization invasive procedure, so estimation is a reasonable alternative exploiting the fact that C–peptide is secreted equimolarly with insulin, but the former is not extracted by the liver. It has been proven that with a hepatic fractional extraction of 55% and a $4:1$ portion of splanchnic blood flow between the portal vein and the hepatic artery, all the available information on insulin are confirmed [17]. The HE is a dynamic process which is affected by the mass (and therefore amplitude) of insulin pulses and hyperglycaemia. Moreover it declines linearly with the logarithm of insulin concentration and saturates at levels approximately higher than $400 - 500\mu U/ml$. However, probably the liver saturates at lower insulin concentrations than those of peripheral tissues but it may work under saturation conditions since it receives an higher insulin amount.

Taking into account these considerations, IP insulin administration seems to be a nearly physiological solution, since insulin is directly infused in the IP space and then, via the capillaries, is absorbed into the portal vein, so restores partially the positive portal to systemic insulin gradient. Liebl *et al.* showed that emulating this insulin gradient may be beneficial also for weight management, since increase in body weight is linked to high level of peripheral insulin [27]. Actually, IP insulin delivery represents a similar but less invasive way of portal insulin administration via the umbilical vein that has been proven to be beneficial. The speed of the IP insulin absorption depends on factors such as concentration of insulin solution, injected volume and duration of injection, but it is mostly directly absorbed into the portal system and detectable within 1 minute after administration. For this reason, after absorption, an

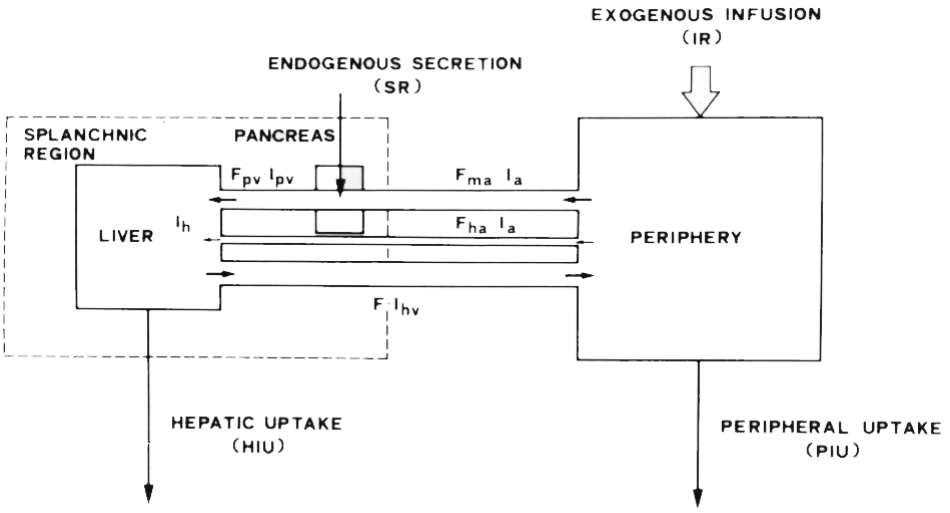

Figure 1.2: Block diagram of the insulin system. Retrieved from [17].

higher hepatic uptake of insulin occurs, with fist–pass liver insulin extraction. Consequently, this achieves a lower peripheral insulin concentration than the conventional SC insulin delivery. The latter aspect is very important because the peripheral overinsulinization, caused by SC insulin administration, shifts the primary site of insulin action toward the skeletal muscle instead of the liver. So, considering that skeletal muscle is a larger glucose sink than the liver and that it takes up glucose regardless of glycaemic levels, also glucose storage shifts towards the muscles. This contributes to excess hepatic glucose output and so to a predisposition to hypoglycaemia. To mention, some other positive physiological effects (that will be further explored in the subsection 1.2.3) related to *CIPII*, include a more rapidly return to blood glucose baseline values, since insulin takes 15/20 minutes to reach its peak effect. Thus, insulin profile is more predictable and reproducible compared to SC insulin. Then, there is an improvement of glucose production in the liver in response of exercise and hypoglycaemia, and of the glucagon secretion. Finally, there are some studies that indicate how a long–term use of IP therapy positively influences the *Insulin–like Growth Factor–1 (IGF–1)* concentrations, increasing them, in a more pronounced effect than SC insulin treatment [23], [45].

1.2.2 Target population

Currently, CIPII therapy is only used by a small number of patients with T1D due to limited evidence, high costs and risks of complications. Experts, including EVAluation dans le Diabète des Implants ACtifs group [22], have published guidelines for

patients selection for IP therapy. CIPII therapy is recommended for patients with T1D who have frequent episodes of severe hypoglycaemia during SC insulin therapy, who are unaware of it and also who experience fear of it (in fact their subsequent behaviour leads to chronic hyperglycaemia). Moreover, this is suitable for patients who have *brittle diabetes*, thus they show sustained suboptimal glucose control with the result of recurrent hospitalizations, despite intensive SC therapy. Then it is recommended for patients with T1D who have SC insulin resistance or other SC site defects/issues such as allergies, lipoatrophy and lipohypertrophy, that alter insulin absorption with the conventional therapy. In this regard, in [26] it is reported a case study of a 36 years old Caucasian man, who developed two areas of significant lipohypertrophy around his umbilicus. This inflammation led to poor insulin absorption and subsequently to ketoacidosis. Even though the injections sites were changed, local inflammation and pain were reported together with a higher difficulty in the management of diabetes. CSII treatment helped in the first four–year time period but then inflammation recurred. Therefore, only CIPII device let him to go back to his normal life.

However, there are some contraindications that avoid the large use of CIPII treatment for every diabetes patient. Among them, there is the presence of high insulin–antibodies levels, pregnancy, gastrointestinal disorders including peritoneal adhesions and immunodeficiency syndromes.

1.2.3 Effects of continuous intraperitoneal insulin infusion

Several studies and clinical trials have been carried out with the purpose of comparing IP with SC insulin infusion therapy and to find out some proven benefits of IP insulin delivery. Just for simplicity's sake, it's possible to split the effects in *on glycaemic control* and *beyond glycaemic control*.

With regard to the first ones, a randomized trial conducted by Selam *et al.* on twenty–one T1DM patients aged 24–61 years old, showed an improvement of HbA1c levels to near-normal with both treatments but intraperitoneal therapy resulted to be more effective for limiting glycaemic fluctuations [43]. In another 6–month randomised, crossover, controlled study performed by Haardt *et al.* on ten adult patients reduced glycaemic fluctuations were observed, together with improved glycaemic control (lower HbA1c levels) and fewer hypoglycaemic events with CIPII [21]. In 2008, Logtenberg *et al.*, in a longer (16 months) randomized, prospective, cross-over trial on twenty–four patients, found a decline of HbA1c levels, with a mean difference 0.76% and an 11% increase in the time spent in euglycaemic range in favour of IP. No increase in hypoglycaemic events has been reported [31]. Moreover, Logtenberg *et al.*, in a long–term retrospective analysis (over 20 years) in Zwolle, found that CIPII improves glycaemic control showing a decline in self–reported hypoglycaemic events in patients with poorly controlled diabetes [29]. It is also remarkable to report the case

of a 26–year–old woman, who, 15 months after IP pump implantation, decided to become pregnant. As anticipated in 1.2.2, CIPII therapy is not indicated in pregnancy because it may be associated with an increased risk of fetal mortality. However, in this case, no complications were observed and CIPII was maintained during the whole pregnancy [42]. Finally, besides the implantable insulin pump, it has been noted that also DiaPort system, that will be developed in more detail in the subsection 1.2.4, improves (slightly) HbA1c levels and reduces the number of severe episodes of hypoglycemia, as found by Liebl *et al.* during a 12–month trial. In this study, for instance, severe hypoglycaemic episodes with CIPII were 34.8/100 patient years, while with CSII they were 86.1 ($p = 0.013$). Thus, to sum up, a considerable number of observational studies (also long–term ones as previously cited and confirmed by the 6–year follow–up on nineteen patients [47]) reported that CIPII, instead of CSII therapy, ensures a lower occurrence of hypoglycemia and an improved glycaemic control, in terms of both reduction/stabilization of HbA1c levels and lower glycaemic variability. The latter, expressed as the standard deviation of the capillary glucose, has been demonstrated to be lower also using CGM as proven by the 26–week, prospective, observational case–control on 176 patients [48].

As already mentioned in the subsection 1.2.1, CIPII treatment positively affects some physiological processes, besides glycaemic control. In addition to the previously cited increasing of the sensitivity of the liver to the Growth Hormone (GH) and the subsequent higher IGF–1 production and bioactivity, also production of the hepatic glycoprotein Sex Hormone–Binding Globulin (SHBG) is influenced by insulin. In particular, it has been proven that CIPII significantly lowers SHBG concentrations, since portal insulin concentrations inhibit SHBG production, regardless of glycaemic control [25]. It could be a potential advantage for male patients with T1D but the clinical significance on reproductive function has to be further tested. Moreover, CIPII improves also lipoprotein metabolism. The key factor, in this case, is the lower peripheral plasma insulin concentration that normalizes cholesteryl–ester–transferase and lipoprotein lipase increasing the hepatic lipase [2], [38]. Finally, another study by Colette *et al.* showed a correlation between vitamin D metabolism and IP insulin infusion [14]. In fact, patients with T1D treated with CIPII had higher values of calcidiol, a prehormone that physicians measure to determine vitamin D status. Apart from all these effects described so far, there are other two beneficial aspects of CIPII: QoL and treatment satisfaction. Many case studies and randomized trials such as [27], [29], [37] report that both are substantially improved during CIPII as compared to CSII.

1.2.4 Intraperitoneal insulin infusion systems

The first implantable pump was applied in 1979 and early IP utilised either IP or Intravenous (IV) routes [3]. However, IP has prevailed because of its lower risk of

Figure 1.3: The MIP 2007D implantable pump system and patients-pump communicator. Retrieved from [49].

thrombosis and infection. Nowadays, the only available commercial implantable system is the *MIP 2007D pump*, visible in figure 1.3. It has a diameter of 8 cm, thickness of 2 cm, its clinical use is limited to few countries of Europe (France, the Netherlands, Sweden, and Belgium) and contains up to 15 ml of insulin. Implantable systems are put, under general anaesthesia, at the lower quadrants of the abdomen in which the insulin is delivered via a catheter towards the liver, as can be seen in figure 1.4. The implantable device components are biocompatible in order to avoid adverse reactions or rejections. The insulin reservoir is refilled transcutaneously through a refill port at least every three months and it has also an additional side-port for the technical maintenance. Finally, the user has the possibility to control insulin delivery remotely using a hand–held device. For implantable systems it is necessary a highly concentrated insulin such as *U–400* (Sanofi–Aventis, Frankfurt Germany) since the higher ambient temperature, interactions with surface materials and fluid turbulence aggravate the risk of insulin precipitation. Among preliminary and early studies on implanted insulin pumps, a pilot one in 18 participants showed that glycaemic control was sustained, glucose variability reduced without episodes of sever hypoglycaemia or diabetic ketoacidosis and the total mean daily insulin dose was maintained constant. The authors also noted 80% of catheters were usable for seasons not longer than 1.5 years, due to their obstruction [40]. A relevant issue for IP therapy consists in having limited data from randomised controlled trials, although for several decades it has been available in clinical practise. These limitations concern the small number of participants and the short duration of studies ranging from 9 to 16 months. Nevertheless, it has been demonstrated that IP delivery is clinically feasible and improve not only pharmacokinetic and pharmacodynamic, but it also better mimics physiological insulin delivery compared to SC insulin.

Besides the reported positive effects using implantable pumps, various studies ad-

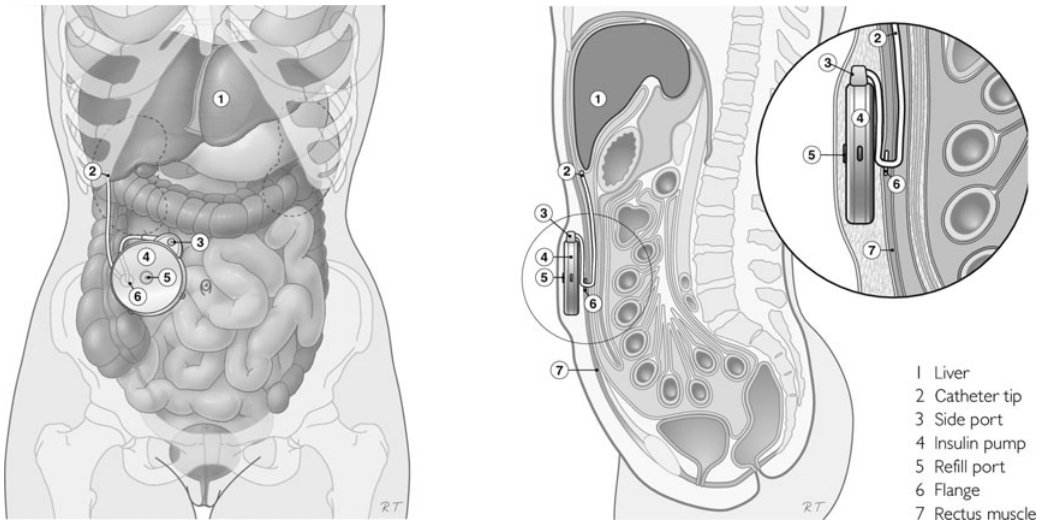

Figure 1.4: Illustration of the implantable pump system. Retrieved from Diabetes Care 2009 Aug;32(8):1372–1377. Copyright 2009 The American Diabetes Association[3].

dressed also some technical issues that limited widespread use of CIPII in the past. For instance, a retrospective observational cohort study performed by van Dijk *et al.* on 56 patients over the period from 2000 to 2011, found that the most frequent complications were catheter occlusion (32.9%), pump dysfunction (17.1%), pain at the pump site (15.7%) and infections (10.0%). The same study also included sub–analyses to compare patients starting CIPII from 2000 to 2007 and from 2007 onwards. A significant decrease in pump dysfunction and explanation was seen after 2007 compared to the previous subperiod [46]. In fact, the ongoing development of the technology has helped to address these problems, thus modern IP devices have fewer of them. Another recent study with an observational time window from 1990 to 2006 confirmed this improvement over the years, in terms of an increase of the median operation free period (from 21 to 78 months from 2000 onwards; p=0.039) and the reduction of the complication rate (only 19%). One more issue that was reported in several studies in 1990s is the increased production of anti–insulin antibodies during implantable systems use. Even if the exact cause remains unknown, the possible explanations are related to the fact that peritoneum is a macrophage-rich area so that it may increase the antibody production, or to the insulin modification that occurs during storage in the pump, or this issue can be due to insulin aggregates which are known to be antigenic [24]. Anyway, this immune reaction is highly variable and it does not affect the number of hypoglycaemic episodes or insulin requirements. Finally, a relevant problem of IP therapy is its high cost per year (during a 7-year period): in 2010 direct

pump and procedure associated costs were estimated at 10910 Euros compared with 4810 Euros for CSII [30]. This high price is mainly due to implantable pump and the insulin used.
Therefore, due to this high cost, the invasive nature (a surgical procedure is needed to put the pump in the peritoneum and also to replace the pump battery when it is depleted), the risk of complications and the invasive procedures (insulin refill or rinsing in case of catheter occlusion), an alternative approach for intraperitoneal insulin delivery has been developed: *DiaPort*. As depicted in figure 1.5, the Accu–Chek DiaPort system consists of a flexible catheter that is placed in the peritoneal space and a small titanium port–body which is biocompatible and it is implanted into the subcutaneous tissue. The membrane and polyester felt, on which patient skin grows, are needed to prevent skin infections. The port, that is stabilized by a flower–shaped plate, can connect to the Spirit Combo pump, which delivers insulin through a special stainless steel ball canula infusion set. Infused insulin is a regular U–100 insulin solution (Insuman Infusat, Sanofi).
Significant advantages of CIPII via this system compared with via implantable pumps (considering the similar efficacy on glucose control) are related to the lower cost and the higher flexibility and patient autonomy. In fact, insulin refill and battery replacement can be carry out by the patients on their own. Moreover, due its less invasive application procedure, it is more feasible in clinical practice. On the other hand, among the severe complications associated with DiaPort use, infections at the port implantation site was the most reported one. However, the second generation of this system, introduced in 2011 and used, for instances, in Dassau *et al.* study [16], has shown less frequent adverse events [20] than DiaPort of the first generation used by Liebl *et al.* [27]. Manufacturer improved the implantation method, materials and design in order to simplify the implantation procedure in addition to reduce the complications, precisely. Therefore, for its apparent low side effects and economic reasons, specific interest for this system is relevant, although still pending data from the clinical field does not allow a thorough assessment of its risks [34].

1.2.5 Future use of continuous intraperitoneal insulin therapy

CIPII as a valuable treatment option for patients with T1D is, nowadays, more than just a promising researchers' idea. As seen, several studies have confirmed its benefits on glucose control and positive effects in terms of pharmacokinetic and pharmacodynamic properties. At the same time, they have emphasised the overcoming of historical drawbacks of CIPII such as long–term efficacy and complications. So, the promising approach would be using CIPII to enhance closed–loop system, known as *Artificial Pancreas*, so far developed. In fact, all the efforts of the research in this field aim to an optimal glucose control, without patient involvement, that is performed with an insulin pump, a control algorithm and a CGM sensor. Most AP so far devel-

Figure 1.5: Illustration of the Accu-Chek DiaPort system (Roche Diabetes Care). Retrieved from [20].

oped are based on CSII delivery and SC glucose sensing. Limitations in CSIIinclude slow insulin clearance and insulin absorption due to delays in the interstitial fluid. This can cause a non–satisfactory postprandial glycaemic control. Some early studies [36], [35] have demonstrated, on the contrary, that CIPII, due to its ability to restore the physiological portal–systemic insulin gradient, leads to an improvement on both problems and they have ensured the feasibility of a hybrid implantable artificial pancreas. Moreover, recently, Burnett *et al.*, using Intravenous Glucose Tolerance Test (IVGTT) in eight swine, have provided evidence that IP glucose–sensing are significantly faster than sensing in the SC space [9]. This is due to the fact that blood vessels in the peritoneal cavity are unaffected by slow and variable blood flow during sensing and external fluctuations such as temperature and mechanical pressure. Also Fougner *et al.* reached the same conclusion underlining an even faster peritoneal fluid reaction to changes in intravascular glucose levels than previous studies on animals reported [19]. Therefore, in order to make a safe artificial pancreas with a robust, rapid and accurate glucose control, sensing glucose and delivering insulin in the IP space could be used. Furthermore, considering the advantages of IP insulin delivery and the restoration of glucagon secretion, IP insulin infusion could make possible a fully automated close–loop system, as suggested by Renard [34].
Consequently, even if there are authors (Garcia–Verdugo *et al.*) which are already very optimistic about CIPII future, it seems clear that nowadays more research and well–conducted studies on CIPII are needed to confirm short and long–term effects and to provide an irrefutable scientific evidence for its subsequent wider use in clinical practice. In the meantime, also an increased awareness of the availability of CIPII as a valid solution is needed, as emphasised by Lee *et al.* for UK country [26].

1.3 Aim of the thesis

The aim of this work is to develop a mathematical model of insulin absorption from the IP space in patients with T1D. Recently, in order to improve the available knowledge and the understanding of the underlying physiology, a powerful research tool, i.e. a mathematical model, is utilized. Moreover, it can provide insight into the various mechanisms and may help in suggesting new experiments. In this respect, a first model is proposed, based on a unique database of eight patients with T1D in a hospitalized setting, treated by implanted pumps in a two–day closed–loop and one–day control phase in randomised order. The main purpose has been to determine the insulin kinetics related to the insulin boluses and to assess the inter and intra–variability of the patients. Thus, considering all the positive aspects of IP route and the recent efforts to develop a fully automated and implantable AP, this model can be thought as an additional step towards that direction.
In detail, in the following chapter the description of the database used is provided. Then, chapter 3 is dedicated to report a battery of models. In chapter 4 the methods for the *a priori* model identifiability, the parameters estimation and criteria for the model selection are described. Finally, in chapter 5 and 6 the discussion of the obtained results together with the future developments are outlined.

Chapter 2

Database

In this thesis a small database of eight type 1 diabetic patients is used. They are all treated by implanted pumps and monitored by a subcutaneous glucose sensor for a total of 86 hour–period in a hospital setting. The subjects and protocol characteristics are explored more thoroughly below.

2.1 Patients

The database consists of eight patients with T1D treated by implanted pumps (model MMT–2007D; Medtronic Diabetes) and infusing U–400 regular insulin (Insuplant; Sanofi–Aventis) for at least 3 months. The process of enrolling in the study foresaw some inclusion and exclusion criteria. Among the former ones, there were the age (18–70 year–interval allowed), the plasma anti–insulin antibody level, which had to be lower than 30%, the insulin delivery expected accuracy for the 60 days preceding the trial (within 15% allowed), health insurance and written informal consent. Among the exclusion criteria, there were obviously the suspected allergy to glucose sensor components, any cardiovascular event within the last 6–month period and evolving ischemic or diabetic retinopathy within the last year. Then also pregnant and feeding women together with subjects with plasma creatinine > 150 $\mu mol/l$, total blood Hb < 12 g/dl, aspartate aminotransferase and serum alanine aminotransferase above twice the highest limit of the normal range, were not admitted [36].

2.2 Study protocol

The study protocol was approved on 11 September 2007 by the regional ethics committee Comité de Protection des Personnes Sud Mediterranée IV, France. It consists of three phases summarized in the Table 2.1, for a total of 86 hours.

To measure plasma insulin and blood glucose, frequent blood samples were drawn

Table 2.1: Phases of the study protocol and their main characteristics

Phase	Duration	Characteristics
Preparation	14 h	Calibration and patients instructions
Control	24 h	Pumps programmed according to patient–monitoring data
Closed–loop	48 h	Pump's insulin infusion rate *automatically* modulated by algorithm and 15–min premeal *manual* bolus (HyPID)

using an intravenous catheter: every 20 minutes in the *early postprandial periods* (8:00–10:00, 13:00–15:00, 19:00–21:00), every hour from 8:00 to 22:00, excluding early postprandial periods, every two hours in the *non–postprandial periods* (22:00–8:00). Moreover, for a mere safety's sake, two SC glucose sensors (one of them used as a backup) were inserted in the patients' abdominal area and calibrated against a Capillary Blood Glucose (CBG) in order to perform CBG tests every hour from 8:00 to 22:00 and every two hours from 22:00 to 8:00.
In further detail, during the *control phase* (also called *open–loop*), diabetes was monitored by 7 CBG tests performed by patients before and after each meal and at bedtime. Then, according to these data, they programmed themselves their pump, in fact sensor glucose data were patient blinded.
On the other side, in the *closed–loop phase*, the implanted pump was driven by a SC glucose sensor and the only manual operation was the insulin bolus, given approximatively 15 minutes before meal time, which consisted of 30% of the amount the patient–programmed. Thus, the Proportional–Integral–Derivative (PID) algorithm, running on a laptop computer, received sensor data using a radiofrequency protocol and automatically modulated the pump's insulin infusion rate. The pump, in turn, was set up to receive commands via Bluetooth and its minimum basal infusion rate was 0.2 unit/h. To sum up, three components were used in the closed loop phase: SC glucose sensors, a PID algorithm and an implanted pump. This system, because of the hybrid PID due to manual premeal boluses, was called *HyPID system*. As with control phase, also in the closed–loop phase, the sensor glucose data were patient blinded. Closed–loop phases and control phases were in a randomised order: the control phase therapy for the patients 1,4,5,6 was before the closed–loop one, vice versa for the other four patients. Finally, the amount of carbohydrates for breakfast was 40 grams, while both for lunch and dinner it was 70 grams.

Chapter 3

Models of intraperitoneal insulin kinetics

As mentioned in the introduction, in this chapter a number of compartmental models describing intraperitoneal insulin kinetics will be provided. In particular, in the first section, two models of whole–body insulin kinetics are reported. In the second section, instead, a battery of models developed with the purpose to describe the insulin absorption via intraperitoneal route in patients with T1D. For all the models, it will be specified the number of compartments, their interconnections and the sites where insulin absorption and loss occur.

3.1 Plasma and Liver subsystem

3.1.1 One–compartment model

The simplest model configuration for the insulin kinetics is the one–compartment linear model, depicted in Figure 3.1. Insulin kinetics is described by a unique pool which corresponds to the liver and plasma considered together. This is a reasonable approximation since the exchange between them is very rapid. This simple model does not account for first–pass hepatic insulin extraction. However, this is a reasonable approximation in T1D subjects where insulin is not secreted by the pancreas into the portal vein but it is usually exogenously administered in the periphery (e.g. subcutaneous route).
This model is described by the following equations:

$$\begin{cases} \dot{I}_p(t) = -nI_p(t) & I_p(0) = I_{pb} \\ I(t) = \dfrac{I_p(t)}{V_I} \end{cases} \tag{3.1}$$

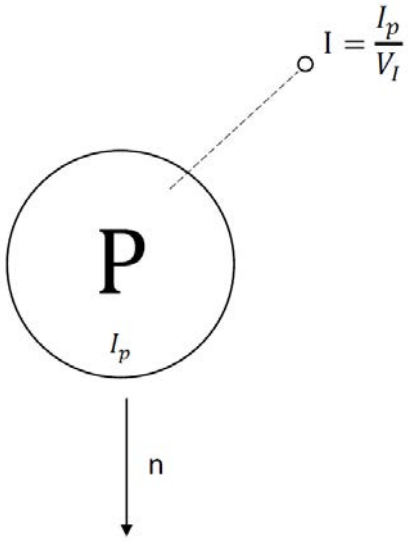

Figure 3.1: The one–compartment linear model for the insulin kinetics [11]

where n (min^{-1}) is the only rate parameter and I_p is the insulin mass in plasma and in the liver considered as an unique pool. In fact, the liver is not modeled as a true kinetics compartment with its own size and exchange rates, as the following model. Therefore, in this mono–compartment model, the insulin is considered to be distributed into a unique compartment in the body, that is characterized by the distribution volume V_I and the clearance can be considered as: $\mathrm{CL} = n \cdot V_I$.

3.1.2 Two–compartment model

The two–compartment model of whole–body insulin kinetics, described in [15], [50], is represented in Figure 3.2. Is is described by the following equations:

$$\begin{cases} \dot{I}_p(t) = -(m_2 + m_4)I_p(t) + m_1 I_l(t) & I_p(0) = I_{pb} \\ \dot{I}_l(t) = -(m_1 + m_3(t))I_l(t) + m_2 I_p(t) & I_l(0) = I_{lb} \\ I(t) = \dfrac{I_p(t)}{V_I} \end{cases} \tag{3.2}$$

In details, the two compartments represent the *liver* (L) that is non accessible to direct measurement, and the *plasma* (P), where both sampling and testing occur. I_p and I_l (mU/kg) are respectively the insulin masses in plasma and in the liver, V_I (l/kg) is the distribution volume of insulin, I (mU/l) is the plasma insulin concentration and m_1, m_2, m_3 and m_4 (min^{-1}) are the rate parameters. The parameters m_3 and m_4 represent respectively the insulin degradation in liver and plasma. Then, in particular,

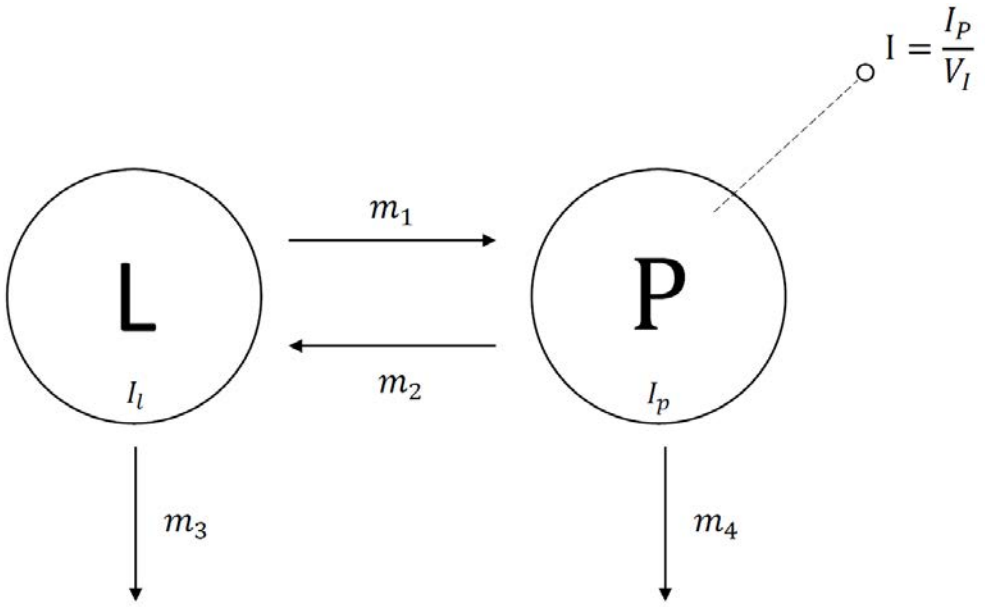

Figure 3.2: The two–compartment linear model for the insulin kinetics [15], [50]

m_3 is given by:

$$m_3(t) = \frac{\mathrm{HE(t)} \cdot m_1}{1 - \mathrm{HE(t)}} \tag{3.3}$$

where $\mathrm{HE(t)}$ is the HE of insulin. In T1D subjects, HE is fixed to 0.6, as reported in [15], [50], assuming that the liver is responsible for 60% of insulin clearance.
This model has been already implemented in the UVA/Padova T1D simulator [15], [50], allowing in silico testing and so accelerating the development of artificial pancreas control algorithms.

3.2 Intraperitoneal subsystem

In this section, a battery of models are proposed in order to describe the IP insulin absorption kinetics. These models are linked to the mono–compartment model of whole–body insulin kinetics, represented in Figure 3.1, with the purpose of reproducing the data presented in the Chapter 2. In a future work, the chosen model, i.e. able to better describe the experimental data with the minimum number of parameters, will be linked to the two–compartment model of whole–body insulin kinetics, so that the IP insulin absorption model can be implemented in the UVA/Padova T1D simulator.

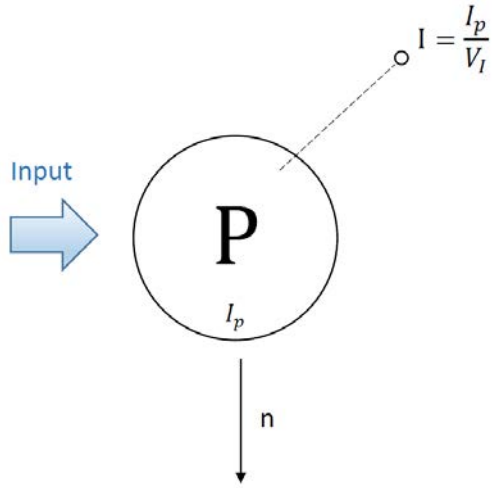

Figure 3.3: The linear model for the direct intraperitoneal absorption

3.2.1 Model I: direct absorption model

The first easiest assumption made is shown in Figure 3.3. Since insulin absorption from the IP route is known to be very fast, it is assumed to be directly absorbed into the circulation. The equations are the same of the mono–compartment model with the exogenous input, given by the IP route:

$$\begin{cases} \dot{I}_p(t) = -nI_p(t) + Input(t) & I_p(0) = Input(0)/n \\ I(t) = \dfrac{I_p(t)}{V_I} \end{cases} \tag{3.4}$$

3.2.2 Model II: one–compartment linear model

Another developed model is depicted in Figure 3.4. Compared to the previous model, it has been added a compartment that is able to describe a slower insulin absorption than the direct configuration model. In this case, the model equations are:

$$\begin{cases} \dot{I}_p(t) = -nI_p(t) + k_a I_q(t) & I_p(0) = Input(0)/n \\ \dot{I}_q(t) = -k_a I_q(t) + Input(t) & I_q(0) = Input(0)/k_a \\ I(t) = \dfrac{I_p(t)}{V_I} \end{cases} \tag{3.5}$$

where I_q (mU) is the insulin mass in intraperitoneal space, k_a (min^{-1}) is the rate parameter and $Input$ is the total exogenous insulin administered, i.e. insulin basal and bolus (mU/min).

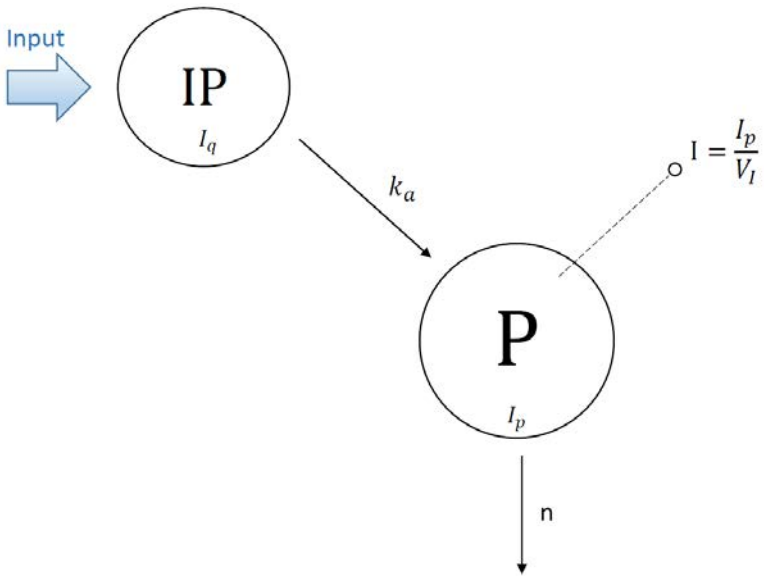

Figure 3.4: The linear one–compartment model for the intraperitoneal absorption

3.2.3 Model III: two–compartment linear model

A third linear model, which is made up of two compartments to represent the intraperitoneal space, as can been seen in Figure 3.5, has been developed. The underlying idea is to take into consideration, with a one more compartment, the physiological route and time period between the insulin injection site (where the flexible catheter is placed) and its absorption via the capillaries of the visceral peritoneum. The equations that describe this model are:

$$\begin{cases} \dot{I}_p(t) = -nI_p(t) + k_a I_{q2}(t) & I_p(0) = Input(0)/n \\ \dot{I}_{q2}(t) = -k_a I_{q2}(t) + k_d I_{q1}(t) & I_{q2}(0) = Input(0)/k_a \\ \dot{I}_{q1}(t) = -k_d I_{q1}(t) + Input(t) & I_{q1}(0) = Input(0)/k_d \\ I(t) = \dfrac{I_p(t)}{V_I} \end{cases} \tag{3.6}$$

where I_{q1} and I_{q2} (mU) are respectively, the insulin masses in the first absorption site (IP_1) and in the second pool (IP_2), representing both the IP space. As can been seen in Figure 3.5, between these two IP compartments, insulin flow is expected to be unidirectional and no insulin degradation occurs, so that all the exogenous insulin enters the circulation. The two rate parameters are k_a and k_d (min^{-1}), which are interchangeable from *a priori* identifiability analysis, thus in the model identification, the assumption $k_d \geq k_a$ has been made.

So far, only linear models for the intraperitoneal subsystem have been proposed.

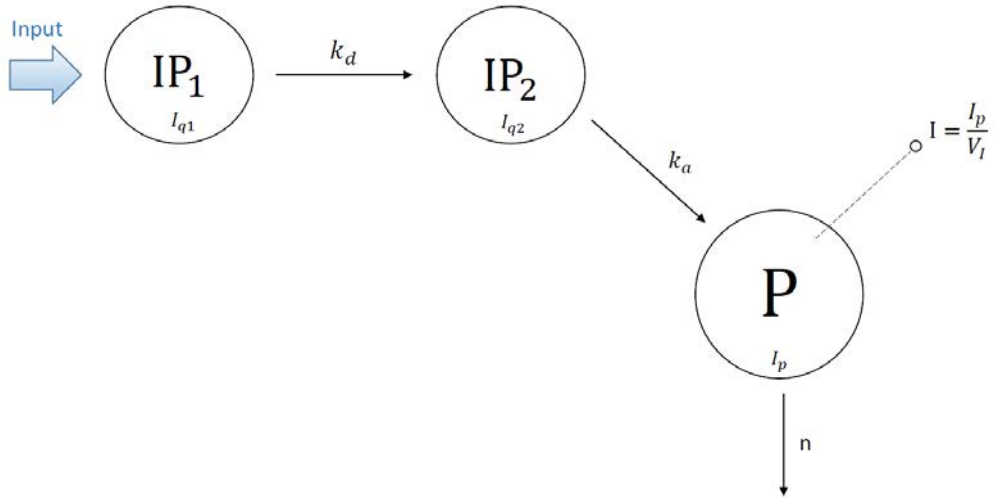

Figure 3.5: The two–compartment linear model for the intraperitoneal absorption

However, it has been deemed useful to further increase the model complexity, considering also some nonlinearities, in order to evaluate any possible correlation between the rate parameters and insulin and/or glucose concentrations. Thus, some nonlinear strategies have been developed starting from the two–compartmental model described in Figure 3.5.

3.2.4 Model IV: Michaelis–Menten kinetics between the intraperitoneal compartments

Firstly, the question concerning the saturation has been examined and the chosen approach was the *Michaelis–Menten*. The underlying idea can be summarised as follows: by increasing the insulin concentration, the speed of the insulin absorption increases until its maximum value is reached, assuming that, increasing insulin concentration, its absorption reaches a saturation level. Thus, in this case, a correlation between the rate parameter k_d and an eventual saturation of the insulin mass I_{q1} (first compartment IP_1) is evaluated. The equations that describe the model are the following:

$$\begin{cases} \dot{I}_p(t) = -nI_p(t) + k_a I_{q2}(t) & I_p(0) = Input(0)/n \\ \dot{I}_{q2}(t) = -k_a I_{q2}(t) + \dfrac{V_{\max} I_{q1}(t)}{K_m + I_{q1}(t)} & I_{q2}(0) = Input(0)/k_a \\ \dot{I}_{q1}(t) = -\dfrac{V_{\max} I_{q1}(t)}{K_m + I_{q1}(t)} + Input(t) & I_{q1}(0) = \frac{Input(0)K_m}{V_{\max} - Input(0)} \\ I(t) = \dfrac{I_p(t)}{V_I} \end{cases} \tag{3.7}$$

where $V_{\max}$ (mU/min) represents the maximum value of the speed of the insulin absorption, K_m (mU) is a mass parameter and by definition, it represents the insulin concentration needed for the speed value of the insulin absorption to be half than its maximum. Therefore, using this nonlinear technique, the pool which controls the rate parameter k_d is the first one, i.e. IP_1.

3.2.5 Model V: Langmuir kinetics between the intraperitoneal compartments

Another nonlinear strategy to describe the possible insulin saturation is based on the *Langmuir* relation. The main difference compared with Michaelis–Menten is that the intraperitoneal compartment which regulates the rate parameter k_d is the second one, i.e. the IP_2 in Figure 3.5. In fact, in this case, the underlying idea consists in evaluating whether, as the insulin concentration in IP_2 increases, the rate parameter k_d starts to decrease down to zero, due to a saturation phenomenon. In mathematical terms, the equations describing this kind of nonlinearity are the following:

$$\begin{cases} \dot{I}_p(t) = -nI_p(t) + k_a I_{q2}(t) & I_p(0) = Input(0)/n \\ \dot{I}_{q2}(t) = -k_a I_{q2}(t) + k_d(I_{q2}(t), \alpha, \beta) I_{q1}(t) & I_{q2}(0) = Input(0)/k_a \\ \dot{I}_{q1}(t) = -k_d(I_{q2}(t), \alpha, \beta) I_{q1}(t) + Input(t) & I_{q1}(0) = \frac{Input(0)}{\alpha\left(1 - \frac{Input(0)}{\beta k_a}\right)} \\ I(t) = \dfrac{I_p(t)}{V_I} \end{cases} \tag{3.8}$$

and $k_d(I_{q2}(t), \alpha, \beta)$ is given by:

$$k_d(I_{q2}(t), \alpha, \beta) = \begin{cases} \alpha\left(1 - \dfrac{I_{q2}(t)}{\beta}\right) & if \quad \beta \geq I_{q2}(t) \\ 0 & if \quad \beta < I_{q2}(t) \end{cases} \tag{3.9}$$

where α (min^{-1}) represents the rate parameter between the two IP compartments and β (mU) is the threshold value above which there is no insulin absorption because of saturation.

3.2.6 Model VI: fractional insulin clearance modulated by glucose concentration

In this case, a nonlinearity on the rate parameter n, i.e. the irreversible insulin removal from the circulation, has been introduced. In this case, it has been taken as a reference a recent literature study of Piccinini et al. [33], who found a relation between the insulin HE and plasma glucose concentration. Consider that, as previously specified, assuming a mono–compartment description for the insulin kinetics

as in this specific case, the HE parameter is not directly estimated, but it is partially included in the rate parameter n. Thus, the model equations are the following:

$$\begin{cases} \dot{I}_p(t) = -(a_G G(t) + a_{oG}) I_p(t) + k_a I_{q2}(t) & I_p(0) = Input(0)/n_b \\ \dot{I}_{q2}(t) = -k_a I_{q2}(t) + k_d I_{q1}(t) & I_{q2}(0) = Input(0)/k_a \\ \dot{I}_{q1}(t) = -k_d I_{q1}(t) + Input(t) & I_{q1}(0) = Input(0)/k_d \\ I(t) = \dfrac{I_p(t)}{V_I} \end{cases} \tag{3.10}$$

where G (mg/dL) is the glucose concentration in the pool, a_G $(min^{-1}dL/mg)$ represents the control of glucose on n and a_{oG} (min^{-1}) is obtained from the SS constraint:

$$a_{oG} = n_b + a_G G_b \tag{3.11}$$

where n_b is the fractional insulin clearance in the basal state.

3.2.7 Model VII: saturable fractional insulin clearance

The Michaelis–Menten kinetics has been also used in order to describe the irreversible insulin degradation from the accessible pool. Thus, in this case, the underlying idea consists in evaluating whether, increasing insulin concentration, its disposal increases until a maximum value. So, a correlation between the rate parameter n and an eventual saturation of the insulin mass I_p is evaluated. The equations that describe the model are the following:

$$\begin{cases} \dot{I}_p(t) = -\left(\dfrac{V_{\max} I_p(t)}{K_m + I_p(t)}\right) + k_a I_{q2}(t) & I_p(0) = \frac{Input(0) K_m}{V_{\max} - Input(0)} \\ \dot{I}_{q2}(t) = -k_a I_{q2}(t) + k_d I_{q1}(t) & I_{q2}(0) = Input(0)/k_a \\ \dot{I}_{q1}(t) = -k_d I_{q1}(t) + Input(t) & I_{q1}(0) = Input(0)/k_d \\ I(t) = \dfrac{I_p(t)}{V_I} \end{cases} \tag{3.12}$$

where $V_{\max}$ (mU/min) and K_m (mU) are the Michaelis–Menten parameters previously described.

3.2.8 Model VIII: Fractional insulin clearance modulated by insulin concentration

Finally, the last nonlinear strategy which has been developed, takes as a reference the recent literature study of Piccinini et al. [33] outlined previously. In this case, the focus has been put on the relation between the insulin HE and plasma insulin

concentration, with the same considerations applied. The equations describing this kind of nonlinearity are the following:

$$\begin{cases} \dot{I}_p(t) = -(a_I I(t) + a_{oI}) I_p(t) + k_a I_{q2}(t) & I_p(0) = Input(0)/n_b \\ \dot{I}_{q2}(t) = -k_a I_{q2}(t) + k_d I_{q1}(t) & I_{q2}(0) = Input(0)/k_a \\ \dot{I}_{q1}(t) = -k_d I_{q1}(t) + Input(t) & I_{q1}(0) = Input(0)/k_d \\ I(t) = \dfrac{I_p(t)}{V_I} \end{cases} \tag{3.13}$$

where I ($\mu U/mL$) is the insulin concentration in the pool, a_I ($min^{-1}mL/\mu U$) represents the control of insulin on n and a_{oI} (min^{-1}) is obtained from the SS constraint:

$$a_{oI} = n_b + a_I I_b \tag{3.14}$$

where n_b is the fractional insulin clearance in the basal state.
The last remark: implementing this strategy evaluating both the glucose and insulin dependency on n, the parameter n can mathematically reach any minimum value. However, a negative one is physiologically unacceptable, so it has been added a constraint to avoid it.

Chapter 4

Model Identification

In order to analyse dynamics of complex systems such as those in biological and physiological fields, and to understand their regulatory processes, mathematical models are required. A simple schematic illustration of the framework for building models of complex physiological processes is outlined in Figure 4.1. The inverse process of designing models from experimental time course data is called system identification. Since the focus of the thesis is to investigate the insulin absorption, models have a parametric description and take the form of a set of ordinary differential equations involving parameters. Many of these parameters are not directly accessible to measurement, so their values can only be obtained by designing a structural model and estimating its parameters. Thus, in this chapter, a briefly introduction to the theory of the criteria for the optimal model selection, will be reported.

4.1 *A priori* identifiability

In parametric models, the first bottleneck is to verify whether the unknown parameters of the postulated model can be uniquely determined from the input–output experiment, under the ideal conditions of noise–free observable variables, continuous–time measurements and error–free model structure. This is a model–related property called *structural identifiability* or *a priori identifiability*. The identifiability assessment is certainly a necessary but not sufficient prerequisite to guarantee an accurate identification of the model. Of course, if there is no structural identifiability, the parameter estimation will be totally casual and meaningless. Moreover, in clinical practice, data are affected by measurement error, hence, after verifying *a priori* identifiability, one must verify that the model is a posteriori identifiable from the data, i.e. that model parameters can be estimated with a good precision.

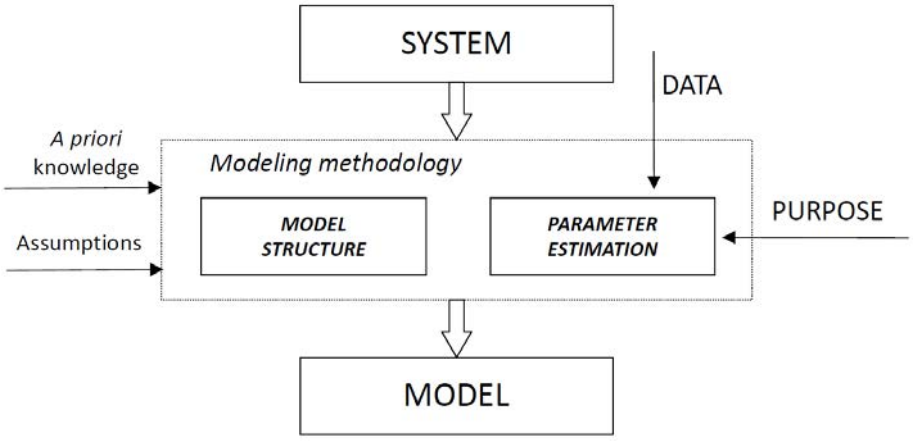

Figure 4.1: Framework for building mathematical models of complex systems. Retrieved by [13]

In mathematical terms, a dynamical model can be described by:

$$\begin{cases} \dot{x} = f(x(t), \theta) + \sum_{i=1}^{n} g_i(x(t), \theta) u_i(t) \\ y(t) = h(x(t), u(t), \theta) + \varepsilon(t) \end{cases} \tag{4.1}$$

where $x(t) \in R^n$ is the state function, $y(t) \in R^m$ is the output, $u(t) \in R^q$ is the input data function, $\varepsilon(t) \in R^m$ is the random measurement noise, f is the function which defines the model structure, g defines the input data function, h is the function which connects model with measurements and finally $\theta \in R^p$ is the unknown parameter vector that characterizes the process.
The methods to study the *a priori* identifiability are based on a definite mathematical procedure [12], [6], [4], [39]. Let's assume for the sake of simplicity, only one known input $u(t) = \delta(t)$, one output and the following parameterized deterministic model:

$$\begin{cases} \dot{x} = f(x, u; \theta) \\ y = h(x, u; \theta) \\ x(0^-) = x_0(\theta) \end{cases} \tag{4.2}$$

A set of functions $\rho_1, \rho_2, \ldots, \rho_q$ called *observational parameters* are extracted by the output of the system. These parameters are functions of the basic model parameter θ, they can be estimated uniquely from the data by definition, i.e. they are uniquely associated to known observable values $\hat{\rho}_i$. Moreover, they should sum up the whole information about θ included in the model output. The latter is a crucial point for nonlinear systems since, in this case, the number of observational parameters could be

infinite and there is no criteria to know which is the correct number of parameters ρ_i needed to study the *a priori* identifiability. Thus, it is necessary to study the preimages or inverse images of the set ρ_i, that is, to solve the system of nonlinear algebraic equations in the unknown ρ_i, called *exhaustive summary*.

$$\begin{cases} \rho_1(\theta) = \hat{\rho}_1 \\ \rho_2(\theta) = \hat{\rho}_2 \\ \vdots \\ \rho_q(\theta) = \hat{\rho}_q \end{cases} \tag{4.3}$$

The extension to the case of multiple–input and multiple–output models is immediate: for each k input channel and j output channel, we obtain the functions ρ_i which characterise the output $y_j(t)$, considering the latter is generated by all null input except $u_k(t) = \delta(t)$. Then, the previous exhaustive summary is obtained by the union of all the algebraic equations related to the various values of k and j. We can now generalize definitions, first defining a single parameter of the model and then the model as a whole. So, the single parameter θ_i is *a priori*

globally identifiable if and only if the system of 4.3 has one and only *one* solution for θ_i;

locally identifiable if and only if θ_i is not globally identifiable but the system of 4.3 has a *finite* number of solutions for θ_i;

nonidentifiable if and only if the system of 4.3 has an *infinite* number of solutions for θ_i.

Focus on the whole model, it is *a priori*

globally identifiable if all of its parameters are globally or uniquely identifiable;

locally identifiable if all of its parameters are identifiable, either globally or locally and at least one θ_i is locally identifiable;

nonidentifiable if at least one θ_i is nonidentifiable.

The mathematical procedure just described, is applied to study the *a priori* identifiability, both in the case of linear and nonlinear dynamic models. The different methods to perform it are in detail reported below.
Consider a *linear dynamic model* with only one input and one output, described by:

$$\begin{cases} \dot{x}(t) = F(\theta)x(t) + G(\theta)u(t) \\ y(t) = H(\theta)x(t) \end{cases} \tag{4.4}$$

where F, G, H are constant coefficient matrices parametrized by θ and there is a non linear relationship between θ and y in general. Moreover, for sake of simplicity assume that the system remains at rest until disturbed by an impulse ($x(0^-) = 0$), but all results and comments hold for the general case. In this case, the commonly used method to study *a priori* identifiability is the *transfer function method* which requires the Laplace transform of the output. Since the transformation of input $u(t) = \delta(t)$ is $U(s) = 1$, the output coincides with the transfer function $W(s)$ of the system, thus:

$$\begin{aligned} Y(s) &= H(\theta)(sI - F(\theta))^{-1}G(\theta) \\ &= \frac{\beta_d(\theta)s^{d-1} + \cdots + \beta_2(\theta)s + \beta_1(\theta)}{s^d + \alpha_d(\theta)s^{d-1} + \cdots + \alpha_1(\theta)} \end{aligned} \tag{4.5}$$

where I is the identity matrix, d is the state space dimension and the $2d$ coefficients are the observational parameters $\{\alpha_i, \beta_i\}_{i=1}^d$ to whom the known values $\{\hat{\alpha}_i, \hat{\beta}_i\}_{i=1}^d$ can be associated. Therefore, the exhaustive summary can be written as:

$$\begin{cases} \alpha_1(\theta) = \hat{\alpha}_1 \\ \alpha_2(\theta) = \hat{\alpha}_2 \\ \vdots \\ \alpha_d(\theta) = \hat{\alpha}_d \\ \beta_1(\theta) = \hat{\beta}_1 \\ \beta_2(\theta) = \hat{\beta}_2 \\ \vdots \\ \beta_d(\theta) = \hat{\beta}_d \end{cases} \tag{4.6}$$

With p inputs and q outputs, the transfer function must have p by q dimensionality and thus has a total of pq rational functions. All the elements of the matrix has the same denominator and each numerator provides d adding new algebraic equations so that the number of observational parameters ρ_i is d x $(pq + 1)$.

On the other hand, the problem to test *a priori* identifiability becomes harder if it is considered a *non linear dynamic model*. The method is based on the Taylor expansion. As usual, for sake of simplicity, it is considered only one input and one output and our interest is the resulting overall systems' behaviour to the Dirac delta function application. Thus, the Taylor series expansion in $t = 0^+$ interval and θ parametrized, is:

$$y_\theta(t) = y_\theta(0^+) + \dot{y}_\theta(0^+)t + \ddot{y}_\theta(0^+)\frac{t^2}{2} + \dots \tag{4.7}$$

where derivatives of all orders are known and can be interpreted as the observational

parameters ρ_i. In the latter case, the exhaustive summary is described by:

$$\begin{cases} y_\theta(0^+) = \hat{\rho}_1 \\ \dot{y}_\theta(0^+) = \hat{\rho}_2 \\ \ddot{y}_\theta(0^+) = \hat{\rho}_3 \\ \vdots \end{cases} \tag{4.8}$$

Again, in case of p inputs and q outputs, for each function with k as entry and j as output, it is computed the Taylor series expansion of y_j. The latter one, in turn, is generated by all null input except $u_k(t) = \delta(t)$. Then, the exhaustive summary is obtained by the union of all the algebraic equations to varying of the values of k and j. The crucial aspect of this method is the lack of criteria to know how many parameters ρ_i are needed to study the *a priori* identifiability handling independent equations. In other words, there is no theory that provides a stop–value for the order of derivatives, except for some cases such as d–dimensional linear systems (where it can be demonstrated it is sufficient to stop at $2d - 1$ order of the derivatives).

4.1.1 The Daisy software

The Laplace transform method discussed above is a handy and simple approach to test *a priori* identifiability for linear models of low dimensions. For more complex models, the nonlinear algebraic equations increase both in degree of linearities and number of terms so that their solution becomes increasingly difficult. In this framework, the software *DAISY* (Differential Algebra for Identifiability of SYstems) has been developed as a structural identifiability test of linear and nonlinear models involving polynomial and rational functions [4], [39]. This tool (available on the web site `https://daisy.dei.unipd.it`) implements a differential algebra algorithm, the Buchberger algorithm, which allows to compute a Gröbner basis , i.e. a set of polynomials allowing to assess the global or local identifiability or the nonidentifiability of the system of differential equations. In fact, the algorithm allows to find the input–output relation involving only the (u, y) variables, eliminating the non–observed state variables. This is possible because of the knowledge of a characteristic set (that is a "minimal" set of differential polynomials) whose computation is performed via the Ritt's pseudodivision algorithm. Together with the system of differential equations, also initial condition can play a fundamental role, so, if available, they should be used to test the *a priori* identifiability of the model. Without going into too much details, it is sufficient knowing that the input of the algorithm are the differential equations defining the dynamic system, the list of the unknown parameters and the number of inputs, outputs and state variables, while the output is the number of solutions for each unknown parameter of the model. The software DAISY manages to check the global identifiability of the original model in only a few seconds and

it does not require an in–depth understanding of the mathematical tools but only a minimum prior knowledge of mathematical modelling. See the article [4] for further details concerning the algorithm.

In conclusion, in this section we have ascertained the essential role of the *a priori*identifiability analysis in model identification, although many researchers often neglect it.

4.2 Parameter estimation

In the section 4.1 it was pointed out the importance of *a priori* identifiability, as a necessary prerequisite for well posedness of parameter estimation. Once the model has passed this test, it is possible to proceed with the parameter estimation adopting one of the available techniques. Any of them is called an *estimator* which is a statistic that is applied to a set of data (represented by the m–dimensional random vector z) to construct an estimate $\hat{\theta}$. An estimator has three key properties: *consistency*, *bias* and *variance*. Briefly, consistency is a nearly always desired property that requires the convergence of the estimate to the true parameter value θ as the number of items in the data set (to which it is applied) increases. The bias is defined as the deviation of the expectation from the true value, that is the difference between the estimator's expected value and the true value of the parameter being estimated: $Bias_\theta(\hat{\theta}) = E[\hat{\theta}] - \theta$. An estimator is said to be *unbiased* if its bias is equal to zero for all values of parameter θ. Finally, the variance of an estimator is the expected value of the squared sampling deviations: $Var(\hat{\theta}) = E[(\hat{\theta} - E[\hat{\theta}])^2]$. One measure which is used to reflect both types of difference is the mean square error: $MSE(\hat{\theta}) = Var(\hat{\theta}) + (Bias(\hat{\theta}, \theta))^2$. The parameter estimation problem can be mathematically formalized in the following way. Since the model includes a set of unknown parameters and the experimental data are available, the discrete–time noisy output measurements z_i are:

$$z(t_i) = z_i = y_i + v_i = g(t_i, \theta) + v_i \tag{4.9}$$

where $g(t_i, \theta)$ is related to the model of the system and v_i is the measurement error of the i–th measurement, which is modeled as a random variable with zero mean and known statistics distribution. The random vector v has a covariance matrix $\Sigma_v = E[(v - E[v])(v - E[v])^T] = E[vv^T] = \sigma^2 B$, where σ is scalar quantity and B is a NxN diagonal matrix if the entries of v are uncorrelated. In vector form, the equation 4.9 can be expressed as follows:

$$z = y + v = G(t, \theta) + v \tag{4.10}$$

There are two main estimation approaches: the Fisher (deterministic) approach is based on the estimation of θ, for which exits a "true" value, only using the experimental data, so the estimator gives a point estimate for the parameter of interest θ. The

Bayes (stochastic) approach refers to the situation in which a stochastic realization of the parameter vector is assumed as opposed to the deterministic approach previously described. In particular, it is known not only the data of the experiment, called *a posteriori information*, but also some *a priori information* on θ that is a random vector and so it is expressed in probabilistic terms. Focusing on the Bayesian approach, which can be used also for small data records and it allows to improve the estimate sequentially as new data arrives, three statistical concepts are presented below in order to describe how it is possible to obtain Bayesian point estimators.

4.2.1 A priori information

On the unknown parameters vector θ, $\theta \in \Theta \subseteq \mathbb{R}^M$, there is some expectation/belief (often from the scientific literature) before seeing any data z, which is described by its *a priori* probability density:

$$f_\theta(\theta) = f_{\theta_1,\theta_2,\ldots,\theta_M}(\theta_1, \theta_2, \ldots, \theta_M) \tag{4.11}$$

Consider the particular case in which it is known that the prior for the vector θ has a normal distribution with μ_θ mean and Σ_θ covariance matrix, the 4.11 can be rewritten as:

$$f_\theta(\theta) = \frac{1}{\left((2\pi)^M det(\Sigma_\theta)\right)^{\frac{1}{2}}} \exp\Big(-\frac{1}{2}(\theta - \mu_\theta)^T \Sigma_\theta^{-1}(\theta - \mu_\theta)\Big) \tag{4.12}$$

4.2.2 Likelihood function

The likelihood function or simply likelihood, expresses how probable a given set of observations z (available after the experiments) is for different values of statistical parameters θ. Thus, it depends on the model $g(t_i, \theta)$ and on the probability density of the measurements error $f_v(v)$ and it is expressed as:

$$f_{z|\theta}(z|\theta) = f_{z_1,z_2,\ldots,z_M|\theta_1,\theta_2,\ldots,\theta_M}(z_1, z_2, \ldots, z_M|\theta_1, \theta_2, \ldots, \theta_M) \tag{4.13}$$

Consider the particular case in which the random vector v, $v \in \mathbb{R}^N$, has a Gaussian distribution with $\mu_v = 0$ mean and Σ_v covariance matrix. The 4.13 can be rewritten as:

$$f_{z|\theta}(z|\theta) = \frac{1}{\left((2\pi)^N det(\Sigma_v)\right)^{\frac{1}{2}}} \exp\Big(-\frac{1}{2}\big(z - G(\theta)\big)^T \Sigma_v^{-1}\big(z - G(\theta)\big)\Big) \tag{4.14}$$

4.2.3 A posteriori information

A posteriori information is the conditional probability of the parameters θ_i which takes into account the observed data (e.g. given the evidence z):

$$f_{\theta|z}(\theta|z) = f_{\theta_1,\theta_2,\ldots,\theta_M|z_1,z_2,\ldots,z_M}(\theta_1, \theta_2, \ldots, \theta_M|z_1, z_2, \ldots, z_M) \tag{4.15}$$

Consequently, it must be expected that the initial *a priori* expectation changes. Using both 4.11 and 4.13, it is possible to determine the latter probability density applying the Bayes' rule, which forms the heart of Bayesian inference:

$$f_{\theta|z}(\theta|z) = \frac{f_{z|\theta}(z|\theta)f_\theta(\theta)}{f_z(z)} = \frac{f_{z|\theta}(z|\theta)f_\theta(\theta)}{\int f_{z|\theta}(z|\theta)f_\theta(\theta)\,d\theta} \tag{4.16}$$

where $f_z(z)$ is the probability density of the measurements vector z which is just a constant, in fact it does not depend on θ. In general, posterior densities are too complex to work with analytically, thus it is used a numerical simulation method called *Markov Chain Monte Carlo* with which it is possible to generate samples from an arbitrary posterior density and to use them to approximate the expectations of quantities of interest. However, it can be demonstrated that there is a particular case in which the a posteriori probability density can be handled analytically, that is when prior and error v have Gaussian distribution. From 4.15 it is possible to define confidence intervals and different point estimators such as *Mean value a posteriori (minimum variance)* and *Maximum A Posteriori (MAP)*, the latter one chosen to be used in the models reported in this thesis. Bayesian estimators are defined by a minimization problem which seeks for the value of θ that minimizes the posterior expected value of a loss function. In particular, the MAP estimator minimizes Bayes risk for a "hit or miss" loss function and estimates θ as the *mode* (the highest value) of the posterior distribution. It is defined as

$$\hat{\theta}_{MAP} = \underset{\theta}{\operatorname{argmax}}\, f_{\theta|z}(\theta|z) \tag{4.17}$$

So, the MAP estimate, known the data measurements z, is given by the value of θ that maximises the a posteriori probability density. Considering 4.16 and the remark concerning $f_z(z)$, the equation 4.17 can be simplified:

$$\hat{\theta}_{MAP} = \underset{\theta}{\operatorname{argmax}}\, f_{z|\theta}(z|\theta)f_\theta(\theta) \tag{4.18}$$

It is worth noting that maximizing the *log* of a function is equivalent to maximizing the original function, since log is a monotonic transformation. The log distribution is often convenient to work with because it is less prone to numerical problems and closer to an ideal quadratic function that optimizers like. Then, usually, we find the *mode* of the distribution by minimizing an *'energy'*, which is the negative log–probability of the distribution up to a constant. Taking into account these observations and in the particular case in which prior and v have Gaussian distributions, MAP estimator becomes a minimization problem as follows:

$$\hat{\theta}_{MAP} = \underset{\theta}{\operatorname{argmin}}\big(z - G(\theta)\big)^T\Sigma_v^{-1}\big(z - G(\theta)\big) + (\theta - \mu_\theta)^T\Sigma_\theta^{-1}(\theta - \mu_\theta) \tag{4.19}$$

where the first addend represents the *a posteriori information*, while the second one the *a priori information*. So Bayesian estimator realizes a trade–off between these two type of informations underlying how, in the situation of 'poorer and poorer' prior, MAP estimator tends to Maximum Likelihood Estimation (MLE). In fact, at the limit, $f_\theta(\theta)$ tends to a constant, prior function becomes flat and thus it is like not having *a priori* information.

The models which have been reported in the chapter 3 are *nonlinear* in the parameters, thus a closed–form solution does not exist. Consequently, it is needed iterative linearizations such as Gauss–Newton method, used to solve nonlinear least squares problems. Moreover, another critical aspect may also concern the error structure of the data. Since, generally, it is partially or totally unknown, assumptions must be made and the common one is that the errors are independent with zero mean. Then, considering that the natural choice is to weight each datum according to the inverse of the variance, it is necessary to distinguish between the case in which variance is known (*absolute weights*) and when it is known up to a proportionality constant (*relative weights*).
Using the MAP formulation, in the absolute weights case, the loss function is expressed by 4.19, where the first addend is related to the measurements data adherence, while the second one represents the prior adherence.
In the relative weights case, as seen before, the covariance matrix Σ_v can be rewritten as:

$$\Sigma_v = \sigma^2 \begin{bmatrix} b_1 & 0 & 0 & \dots & 0 \\ 0 & b_2 & 0 & \dots & 0 \\ 0 & 0 & b_3 & \dots & 0 \\ 0 & 0 & 0 & \dots & 0 \\ 0 & 0 & 0 & \dots & b_M \end{bmatrix} = \sigma^2 B \tag{4.20}$$

where B is a known matrix and σ^2 is an unknown scalar that can be estimated a posteriori by dividing the value of the cost function $F(\hat{\theta})$ by the degrees of freedom of the model $M - N$:

$$\hat{\sigma}^2 = \frac{\big(z - G(\hat{\theta})\big)^T B^{-1} \big(z - G(\hat{\theta})\big)}{N - M} \tag{4.21}$$

The previous formula is valid when the Maximum Likelihood (ML) estimator is used. However, in case of MAP estimation, the following cost function $F(\theta)$ is used [41]:

$$F(\theta) = \frac{1}{M+N} \left\{ \sum_{k=1}^{M} \left(\frac{\big(z_k - g(t_k, \hat{\theta})\big)^2}{V_k\big(g(t_k, \hat{\theta}), z_k, \hat{\sigma}^2\big)} + \log\Big(V_k\big(g(t_k, \hat{\theta}), z_k, \hat{\sigma}^2\big)\Big) \right) + \sum_{j=1}^{N} \left(\frac{\big(\theta_j - \mu_j\big)^2}{\sigma_j^2} + \log(\sigma_j^2) \right) \right\} \tag{4.22}$$

where, as usual, θ is the parameters vector, z_k is the $k-th$ measurement and $g(t_k, \theta)$ is the model prediction at time k. Then, M and N are the number of data measurements and Bayesian parameters respectively and $V_k\big(g(t_k, \hat{\theta}), z_k, \hat{\sigma}^2\big) = \sigma^2$ is the variance term of the $k - th$ datum that is a posteriori estimated as:

$$\hat{\sigma}^2 = \frac{1}{M} \sum_{k=1}^{M} \left(\frac{\big(z_k - g(t_k, \hat{\theta})\big)^2}{V_k\big(g(t_k, \hat{\theta}), z_k, 1\big)} \right) \tag{4.23}$$

At this stage, an estimate $\hat{\theta}$ of the parameter vector has been obtained, so both numerical values of the parameters and, obviously, the equations are known. Thus, in order to consider whether the model is valid, it is necessary to assess the quality of the identification results.

4.3 Analysis of the identification results

The quality evaluation of the parameters estimates can be performed in two main steps which are described in this section.

4.3.1 Residuals

The first step is to analyse the *residuals* vector defined as:

$$r = z - g(\hat{\theta}) \tag{4.24}$$

that is the difference between the observed data and the model prediction obtained with the "optimal" estimated value of the parameter of interest. Considering the definition 4.24 and observing 4.10, residuals vector can be thought of as sort of estimate of the vector v, i.e. it may be compatible with the statistical description of v. For instance, if it is known or expected that v has uncorrelated elements, a significant correlation among the residuals cannot be acceptable and it can be associated to a bad modelling of the system. Thus, a first important step in the analysis of residuals is to assess their whiteness. In practical cases, it is always performed by visual inspection, then also some statistical tests such as the Anderson–Darling whiteness test and the runs test are used [13], above all if a large number of data is available. Residuals assessment is facilitated if weighted residuals are considered. In fact, assuming that errors are uncorrelated and their variance σ_k^2 is known and defining weighted residuals as $wres_k = \frac{r_k}{\sigma_k}$, then:

$$var\Big(\frac{r_k}{\sigma_k}\Big) = \frac{1}{\sigma_k^2} \cdot var(r_k) = \frac{1}{\sigma_k^2} \cdot var(v_k) = \frac{\sigma_k^2}{\sigma_k^2} = 1 \tag{4.25}$$

Thus, weighted residuals should be uncorrelated and with an amplitude comparable to the $[-1, +1]$ band. Finally, observing the first addend of the MAP loss function 4.19, it can be noted that the residual vector is also connected to the *Weighted Residual Sum of Squares (WRSS)*:

$$WRSS = r^T B^{-1} r \tag{4.26}$$

which provides a measurement of the goodness of fit, regardless how $\hat{\theta}$ is obtained.

4.3.2 Precision of the estimates

Since the data z_i are uncertain because affected by error, also estimated parameter vector is uncertain in any case. Therefore, another important aspect to take into consideration is the precision of the estimates in order to assess how much $\hat{\theta}$ is reliable. Starting with the definition of the estimation error as $\tilde{\theta} = \theta - \hat{\theta}$, where $\tilde{\theta}$ is a random vector (since $\hat{\theta}$ is random), the uncertainty affecting the estimates can be measured by using the covariance matrix of $\tilde{\theta}$:

$$\Sigma_{\tilde{\theta}} = E[\tilde{\theta}\tilde{\theta}^T] \tag{4.27}$$

However, in the nonlinear case, it has no closed–form solution, so analytical approximate computations are feasible only under restrictive assumptions, for example of Gaussianity. Therefore, for the MAP estimator, the approximation often utilized is:

$$\Sigma_{\tilde{\theta}} = \Sigma_{\hat{\theta}} \approx \left(S^T \Sigma_v^{-1} S + \Sigma_\theta\right)^{-1} \tag{4.28}$$

where S is the sensitivity M x N matrix of the linearized system given by:

$$S = \begin{bmatrix} \left.\frac{\partial g(t_1,\theta)}{\partial \theta_1}\right|_{\theta=\hat{\theta}} & \left.\frac{\partial g(t_1,\theta)}{\partial \theta_2}\right|_{\theta=\hat{\theta}} & \cdots & \left.\frac{\partial g(t_1,\theta)}{\partial \theta_N}\right|_{\theta=\hat{\theta}} \\ \left.\frac{\partial g(t_2,\theta)}{\partial \theta_1}\right|_{\theta=\hat{\theta}} & \left.\frac{\partial g(t_2,\theta)}{\partial \theta_2}\right|_{\theta=\hat{\theta}} & \cdots & \left.\frac{\partial g(t_2,\theta)}{\partial \theta_N}\right|_{\theta=\hat{\theta}} \\ \cdots & \cdots & \cdots & \cdots \\ \left.\frac{\partial g(t_M,\theta)}{\partial \theta_1}\right|_{\theta=\hat{\theta}} & \left.\frac{\partial g(t_M,\theta)}{\partial \theta_2}\right|_{\theta=\hat{\theta}} & \cdots & \left.\frac{\partial g(t_M,\theta)}{\partial \theta_N}\right|_{\theta=\hat{\theta}} \end{bmatrix} \tag{4.29}$$

and the quantity in the right side is the inverse of the Fisher information matrix [13]. Finally, it should be noted that the mathematical expression 4.28 is also equal to $(J^T J)^{-1}$ in the absolute weights case, while it is necessary consider also a scale factor σ^2 in relative weights case. Therefore, in order to provide a measure of the precision, i.e. uncertainty, it is possible to obtain the expression of the *standard deviation* (SD) from the diagonal elements of the $\Sigma_{\hat{\theta}}$ matrix which contain the variances of the parameters:

$$SD(\hat{\theta}_i) = \sqrt{var(\hat{\theta}_i)} \qquad\qquad i = 1, 2, \ldots, N \tag{4.30}$$

Moreover, precision is often given in terms of the coefficient of variation (CV), as follows:

$$CV(\hat{\theta}_i) = \frac{SD(\hat{\theta}_i)}{\hat{\theta}_i} \qquad i = 1, 2, \ldots, N \tag{4.31}$$

4.4 Criteria for model selection

There is often the need of selecting which model can be defined the most suitable among a number of competing one, such as in this thesis. In this regard, it is interesting to cite a famous Box and Draper' statement: "All models are wrong but some are useful", where usefulness of a model can be intended as its ability to make predictions about unseen observations. Thus, the aim is to find a model which is useful, able to fit the data with the minimum number of parameters and physiologically plausible. To evaluate the model fit, it is used the WRSS, since it minimizes the difference between the observed and predicted value for each sample time t_i with $i = 1, 2, \ldots, M$. Then, under hypothesis that the measurement error is zero mean and uncorrelated, also weighted residuals should be almost zero mean, uncorrelated with most of them lying in the $-1 + 1$ interval. Finally, it is assumed the parameters are estimated with good precision if their CV is less than 100%. Criteria based on principle of *parsimony* are used in order to obtain a trade–off between goodness of fit and precision of the parameter estimates. When MAP estimation is applied as in the models developed in the chapter 3, the Generalized Information Criterion (GIC) can be employed. It is an extension of the Akaike Information Criterion (AIC) (used in the Fisher approach) and requires the following index to be minimized:

$$\mathrm{GIC} = \frac{2M}{N} + J_{\mathrm{MAP}}(\hat{\theta}) \tag{4.32}$$

where M is the number of unknown parameters, N is the number of data and $J_{\mathrm{MAP}}(\hat{\theta})$ is the value of the cost function at its minimum. The relation 4.32 consists in two terms: the first one takes into consideration the number of parameters, while the second term represents the trade–off between the adherence to *a priori* knowledge and data fit. In case of smaller sample size, as in this thesis work, a corrected version of Akaike Information Criterion (AICc) should be used [10]:

$$\mathrm{AICc} = \mathrm{AIC} + \frac{2M(M+1)}{N - M - 1} \tag{4.33}$$

where M is the number of unknown parameters, N is the number of data points and AIC is defined as $\mathrm{AIC} = \mathrm{WRSS} + 2M$. Finally, another possible criterion is the Bayesian information criterion (BIC) or Schwarz information criterion which introduces a penalty term for the number of parameters in the models, larger than in

AIC. It is formally defined as:

$$\text{BIC} = \text{WRSS} + Mlog(N) \tag{4.34}$$

where again M is the number of unknown parameters and N is the number of data points.
Thus, each of these criteria are computed for each model and the model with the smallest criterion value is preferred.

4.5 Identification strategy and statistical analysis

As it has been described in the Chapter 2, the study protocol consisted in two main therapy phases: the control one and the closed–loop one. The identification of all the developed models which have been provided in the Chapter 3, has been applied at the control phase data and performed using MAP estimation. In particular, at the beginning, it has been considered these data in their entirety, then, for a simplicity's sake and a greater clarity, the 24 hour–period has been divided into three time sub-periods, each including a meal. Then, the identification process has been performed as follows: the parameters related to the insulin kinetics, i.e. the Volume and the fractional insulin clearance, have been assumed constant in the whole control phase and thus identified one time. The parameters related to the IP insulin absorption instead, have been identified three times, one for each time subinterval, in order to evaluate their inter and intra–variability. Moreover, this data partition has been made trying to begin each sub–period in a condition of SS. Then, the model adopted to describe the error in insulin is based on the assumption the error samples are uncorrelated, Gaussian with zero mean known standard deviation, in particular equals to:

$$\text{SD} = \sqrt{\frac{1}{6} + 0.0055 \cdot I^2} \tag{4.35}$$

where I ($\mu U/mL$) is the insulin concentration [44]. Finally, to investigate the intra–subject variability in the intraperitoneal absorption, *one–way analysis of variance* (one–way ANOVA) was performed in order to test the *null hypothesis* that k_{a1}, k_{a2} and k_{a3} values (corresponding to the three time subintervals), in each subject, are drawn from populations with the same mean values (using the F distribution). Similarly for the k_{d1}, k_{d2} and k_{d3} values.

Chapter 5

Results

In this chapter, for each model developed (Chapter 3), the results of the *a priori* and a posteriori model identification, together with model selection, are reported.

5.1 *A priori* identifiability

Firstly, the results of the *a priori* identifiability are outlined for each of the eight models, showing the final part of the DAISY software (version 1.5) report as proof. In this regard, it is worth recalling that one basic step of the differential algebra identifiability algorithm consists in choosing a set of pseudo–randomly numerical values for the unknown parameter vector and then calculating the corresponding value of the coefficients of the input–output relation. This provides a system of algebraic nonlinear equations, which is solved by the Buchberger algorithm. Finally, by repeating this procedure for an adequate set of parameter values, if, for example, a unique value for the Groebner basis is obtained, then the model is globally identifiable. Therefore, the numerical values reported in the Figures below, simply refer to this mathematical procedure performed by the DAISY software.

Model I

As expected, the model with direct insulin absorption into circulation, which has 2 parameters to be estimated, i.e. the ones related to plasma kinetics (V_I, n), is a priori globally identifiable. A screenshot of the output of the DAISY software is showed in Figure 5.1. It has been also exploited the *a priori* information (retrieved by [11]) concerning the uncertainty equal to 20% affecting as the insulin kinetics parameter V_i.

```
MODEL PARAMETER SOLUTION(S)

g_ := {{n=18,vi=21}}

SYSTEM GLOBALLY IDENTIFIABLE
```

Figure 5.1: Model I: output of the DAISY software

Model II

The model with a mono-compartment description for the intraperitoneal insulin absorption together with a single–compartment description of plasma kinetics, has 3 parameters to be estimated (V_I, n, k_a) and it is *a priori* locally identifiable, since it can admit two different solutions. The Daisy software in fact shows (Figure 5.2) two possible numerical solutions for the parameter set. As previously reported, the *a priori* information on V_I has been used to help a numerical identifiability.

```
MODEL PARAMETER SOLUTION(S)

g_ := {{ka=18,n=21,vi=18},{ka=21,n=18,vi=21}}

SYSTEM LOCALLY IDENTIFIABLE
```

Figure 5.2: Model II: output of the DAISY software

Model III

The model with a two-compartment description for the intraperitoneal insulin absorption, together with a single–compartment description of plasma kinetics, has 4 parameters to be estimated (V_I, n, k_a, k_d) and it is *a priori* locally identifiable, since it can admit six different solutions. The Daisy software in fact shows (Figure 5.3) six possible numerical solutions for the parameter set. Again, the *a priori* information on V_i helps numerical identifiability but, the model is still *a priori* locally identifiable with two possible different solutions. This is due to the fact that the parameters k_a and k_d are interchangeable, so, as we will see in the following section, it has been assumed that $k_d \geq k_a$, without loss of generality.

```
EXHAUSTIVE SUMMARY


flist_ := {ka*kd*n - 6375,
( - ka*kd + 255*vi)/vi,
ka*kd + ka*n + kd*n - 1055,
ka + kd + n - 57}


MODEL PARAMETER SOLUTION(S)


g_ := {{ka=17,kd=15,n=25,vi=1},
{ka=25,kd=15,n=17,vi=25/17},
{ka=15,kd=17,n=25,vi=1},
{ka=25,kd=17,n=15,vi=5/3},
{ka=15,kd=25,n=17,vi=25/17},
{ka=17,kd=25,n=15,vi=5/3}}


SYSTEM LOCALLY IDENTIFIABLE
```

Figure 5.3: Model III: output of the DAISY software

Model I, II and III are linear models, thus, the *a priori* information can be studied with the transfer function method, which requires the Laplace transform of the output. As an example, for the model III, the mathematical procedure is reported below. The model equations can be written as:

$$\begin{cases} \dot{x}_1(t) = -n \cdot x_1(t) + k_a \cdot x_2(t) \\ \dot{x}_2(t) = -k_a \cdot x_2(t) + k_d \cdot x_3(t) \\ \dot{x}_3(t) = -k_d \cdot x_3(t) + u(t) \\ y(t) = \dfrac{1}{V_I} \cdot x_1(t) \end{cases} \tag{5.1}$$

where $x_1(t), x_2(t), x_3(t)$ and $y(t)$ represent $I_p(t), I_{q2}(t), I_{q1}(t)$ and $I(t)$, respectively. Then, $u(t)$ is the input and it can be supposed equal to the Dirac impulse multiplied by a known constant value D: $u(t) = D \cdot \delta(t)$. Using the matrix representation 4.4, the F matrix is:

$$F = \begin{bmatrix} -n & k_a & 0 \\ 0 & -k_a & k_d \\ 0 & 0 & -k_d \end{bmatrix} \tag{5.2}$$

the vector $G = [0\ 0\ D]^T$ and the vector $H = \left[\frac{1}{V_I}\ 0\ 0\right]$. From this matrix–vector

representation, we can calculate the determinant of the matrix $(sI - F)$:

$$\det(sI - F) = \det \begin{pmatrix} s+n & k_a & 0 \\ 0 & s+k_a & k_d \\ 0 & 0 & s+k_d \end{pmatrix} = (s+n)(s+k_a)(s+k_d) \quad (5.3)$$

Now, for simplicity's sake, rename $(sI - F)$ with A, so that:

$$A^{-1} = \frac{1}{\det(A)}(A^*)^T = \frac{1}{\det(A)} \begin{bmatrix} a_{11} & a_{21} & a_{31} \\ a_{12} & a_{22} & a_{32} \\ a_{13} & a_{23} & a_{33} \end{bmatrix} \quad (5.4)$$

where A^* is the attached matrix, i.e. a matrix where each of the elements a_{ij} is replaced by their smallest complementaries multiplied by -1 elevated to the sum of the row i plus the column j. Thus $(sI - F)^{-1}$ is obtained by:

$$\frac{\begin{bmatrix} s^2 + (k_a + k_d)s + k_a k_d & -k_a s - k_a k_d & k_a k_d \\ 0 & s^2 + (n + k_d)s + nk_d & -(s+n)k_d \\ 0 & 0 & s^2 + (n + k_d)s + nk_a \end{bmatrix}}{s^3 + (k_a + k_d + n)s^2 + (k_a k_d + nk_d + nk_a)s + nk_a k_d} \quad (5.5)$$

and the transfer function $W(s)$ is:

$$W(s) = Y(s) = \frac{\frac{1}{V_I} k_a k_d D}{s^3 + (k_a + k_d + n)s^2 + (k_a k_d + nk_d + nk_a)s + nk_a k_d} \quad (5.6)$$

Finally, the exhaustive summary is:

$$\begin{cases} \frac{1}{V_I} k_a k_d D = \hat{\beta}_1 \\ k_a + k_d + n = \hat{\alpha_3} \\ k_a k_d + nk_d + nk_a = \hat{\alpha_2} \\ nk_a k_d = \hat{\alpha_1} \end{cases} \quad (5.7)$$

that is the same one obtained by the Daisy Software provided in the Figure 5.3. At this point, it is possible to obtain the model parameters V_I, n, k_a, k_d as a function of $\beta_1, \alpha_1, \alpha_2, \alpha_1$ with a finite possible number of solutions.

Model IV

The model with the non–linear (Michaelis–Menten) absorption between the two intraperitoneal compartments, governed by the first compartment, has 5 parameters to be estimated (V_I, n, k_a, $V_{\max}$, k_m) and it is *a priori* locally identifiable, since it can admits two different solutions. The Daisy software in fact shows in the Figure 5.4 two possible numerical solutions for the parameter set.

```
MODEL PARAMETER SOLUTION(S)

g_ := {{ka=25,km=21,n=18,vi=75/2,vmax=18},
{ka=18,km=21,n=25,vi=27,vmax=18}}

SYSTEM LOCALLY IDENTIFIABLE
```

Figure 5.4: Model IV: output of the DAISY software

Model V

The model with the non–linear (Langmuir) absorption from the two intraperitoneal compartments, governed by the second compartment, has 5 parameters to be estimated (V_I, n, k_a, α, β) and it is *a priori* globally identifiable. The Daisy software in fact shows, in the Figure 5.5, a unique numerical solution for the parameter dataset.

```
MODEL PARAMETER SOLUTION(S)

g_ := {{alpha=18,beta=21,ka=18,n=25,vi=27}}

SYSTEM GLOBALLY IDENTIFIABLE
```

Figure 5.5: Model V: output of the DAISY software

Model VI

This model is represented by a two–compartment model of intraperitoneal absorption and accounts for a possible correlation between the glucose concentration and the rate parameter which describes the insulin clearance from the accessible pool, has 5 parameters to be estimated (V_I, k_a, k_d, a_G, n_b) and it is *a priori* locally identifiable. The Daisy software in fact shows, in the Figure 5.6, two possible numerical solutions for the parameter set. In particular, it is evident how the software is not able to assign a unique numerical value to the rate parameters k_a and k_d. This underlines the fact that the parameters k_a and k_d are interchangeable, as previously seen in the model III. Therefore, also in this model, the assumption $k_d \geq k_a$ has been made in the identification procedure.

```
MODEL PARAMETER SOLUTION(S)

g_ := {{ag=6,ka=11,kd=8,nb=20,vi=3},
{ag=6,ka=8,kd=11,nb=20,vi=3}}

SYSTEM LOCALLY IDENTIFIABLE
```

Figure 5.6: Model VI: output of the DAISY software

Model VII

This model is represented by a two–compartment model of intraperitoneal adsorption and accounts for a non–linear (Michaelis–Menten) insulin disposal from the accessible pool, has 5 parameters to be estimated (V_I, k_a, k_d, $V_{\max}$, k_m) and it is *a priori* locally identifiable. The Daisy software in fact shows, in the Figure 5.7, two possible numerical solutions for the parameter set and in particular, underlines the interchangeability between the two rate parameters k_a and k_d. So, also for this model, the assumption $k_d \geq k_a$ has been made in order to guarantee the *a priori* unique identifiability.

```
MODEL PARAMETER SOLUTION(S)

g_ := {{ka=21,kd=18,km=25,vi=27,vmax=18},
{ka=18,kd=21,km=25,vi=27,vmax=18}}

SYSTEM LOCALLY IDENTIFIABLE
```

Figure 5.7: Model VII: output of the DAISY software

Model VIII

[htp] Finally, this model is represented by a two–compartment model of intraperitoneal adsorption and accounts for a possible correlation between the insulin concentration and the rate parameter which describes the insulin disposal from the accessible pool, has 5 parameters to be estimated (V_I, k_a, k_d, a_I, n_b) and it is *a priori* locally identifiable. The Daisy software in fact shows, in the Figure 5.8, two possible

```
MODEL PARAMETER SOLUTION(S)

g_ := {{ai=10,ka=23,kd=8,nb=25,vi=15},
{ai=10,ka=8,kd=23,nb=25,vi=15}}

SYSTEM LOCALLY IDENTIFIABLE
```

Figure 5.8: Model VIII: output of the DAISY software

numerical combinations for the 5 parameters. Also in this model, as seen in model III, VI and VII, the local identifiability is due to the interchangeability between k_a and k_d. So, in the identifiability procedure, the assumption $k_d \geq k_a$ is used in order to guarantee the *a priori* unique identifiability.

5.2 A posteriori identification

The model differential equations integration has been carried out by *ode45* solver implemented in Matlab® (R2017a). Considering the low number of subjects in the database, in this section, for each model, both model predictions and weighted residuals, together with the parameter estimates related to each patient, are provided. Note that, in subject 6, data related to the first time interval have not been taken into account, because some of them have been considered outliers.

Model I

Model I was not able to satisfactorily predict plasma insulin profiles, due to a slower IP insulin absorption into the circulation, which is not well described with this configuration of direct absorption model. In fact, the model predicts insulin peaks in correspondence of meal (or correction) boluses in which insulin concentration increases and decreases too rapidly, as shown in Figures 5.9–5.16. As a consequence, the pattern of weighted residuals is not acceptable since their amplitude is almost always larger than expected, i.e. ± 1. Subject 3 shows a better model fit and weighted residuals (Figure 5.11) than the others subjects, due to its more rapid kinetics with respect to the other subjects. The inability of the model to predict the data leads also to unphysiological parameter values. In fact, the volume of distribution achieves very high values (0.833 ± 0.336 with respect to the prior value around 0.131 L/Kg), while the fractional clearance achieves very low values (0.131 ± 0.321 with respect to the expected value around 0.105 min^{-1}) but with a great variability since the SD is

higher than the average value. In addition to this, also a very high variability in model parameters is observed.

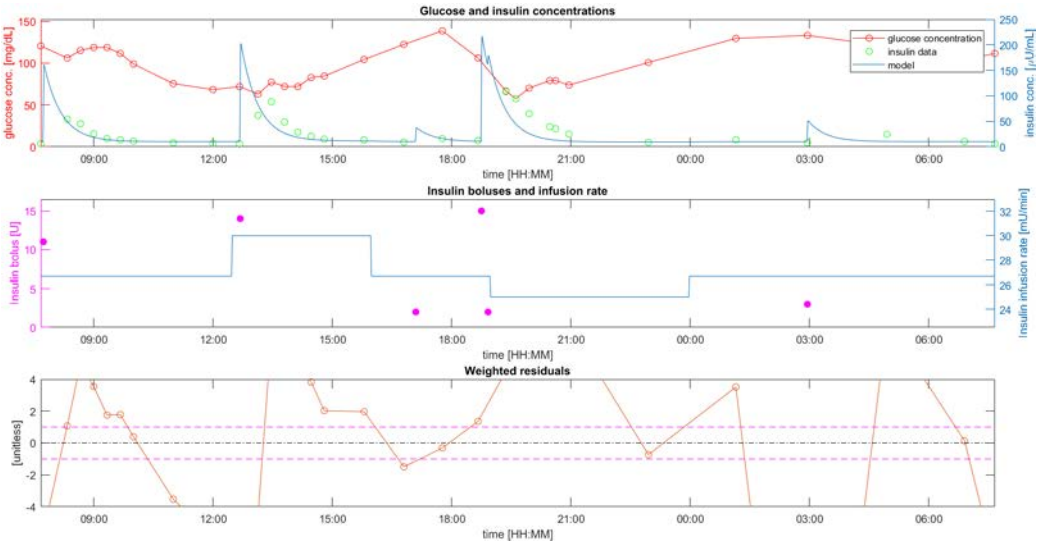

Figure 5.9: Model I: Subject 1

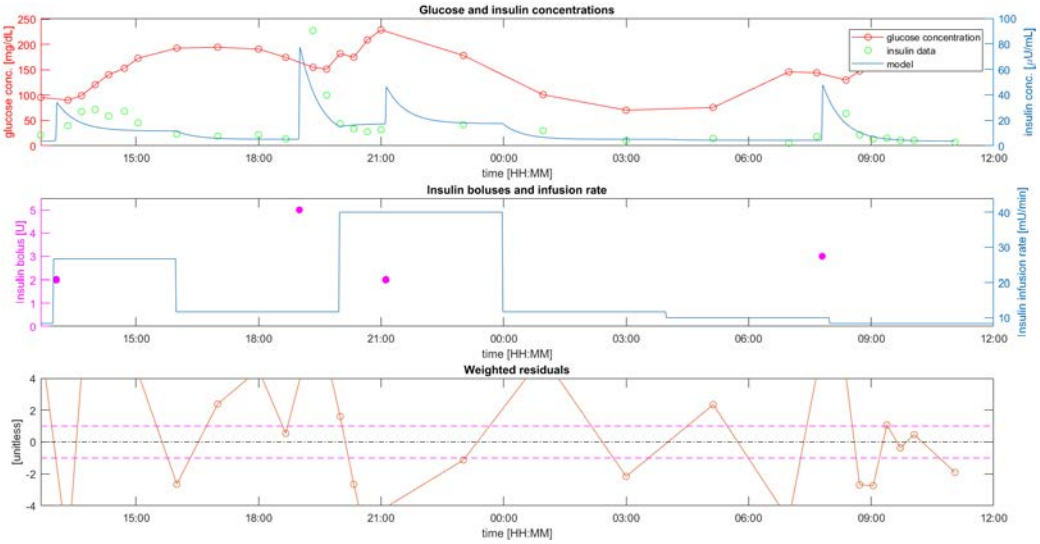

Figure 5.10: Model I: Subject 2

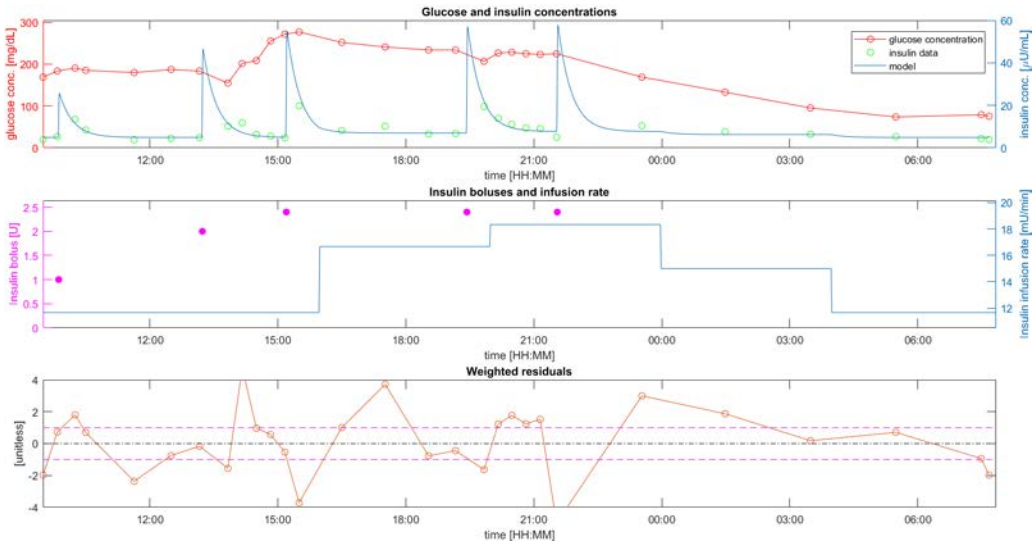

Figure 5.11: Model I: Subject 3

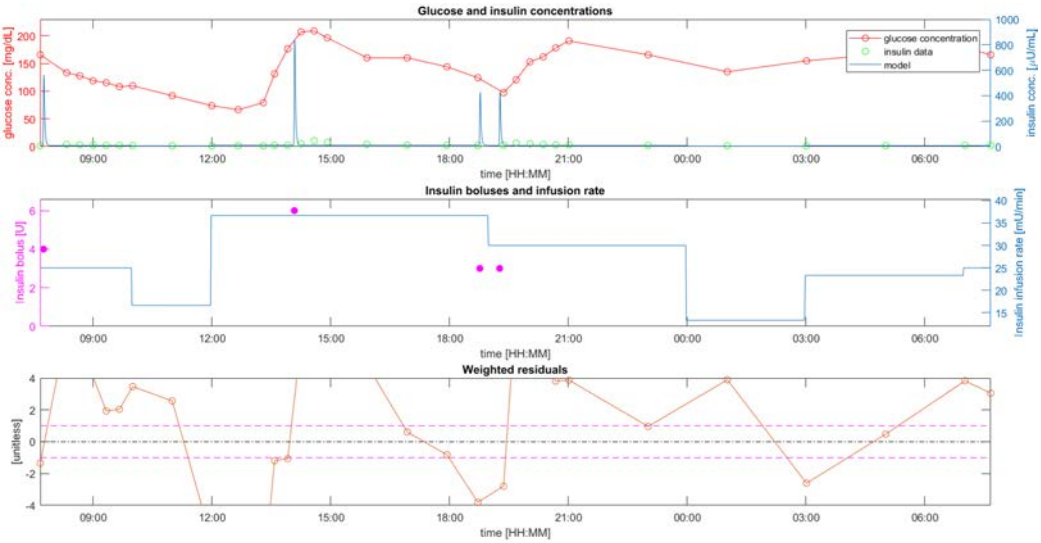

Figure 5.12: Model I: Subject 4

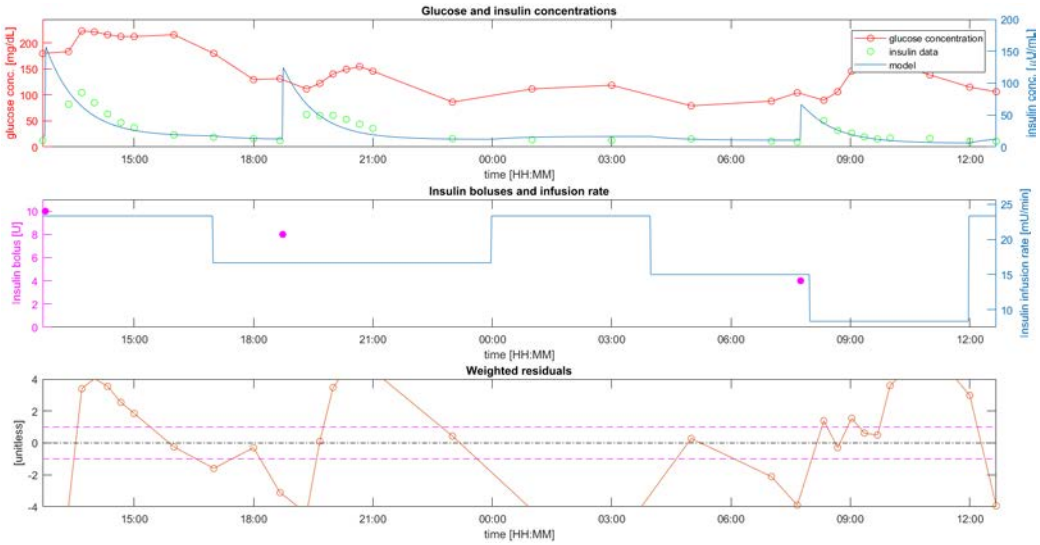

Figure 5.13: Model I: Subject 5

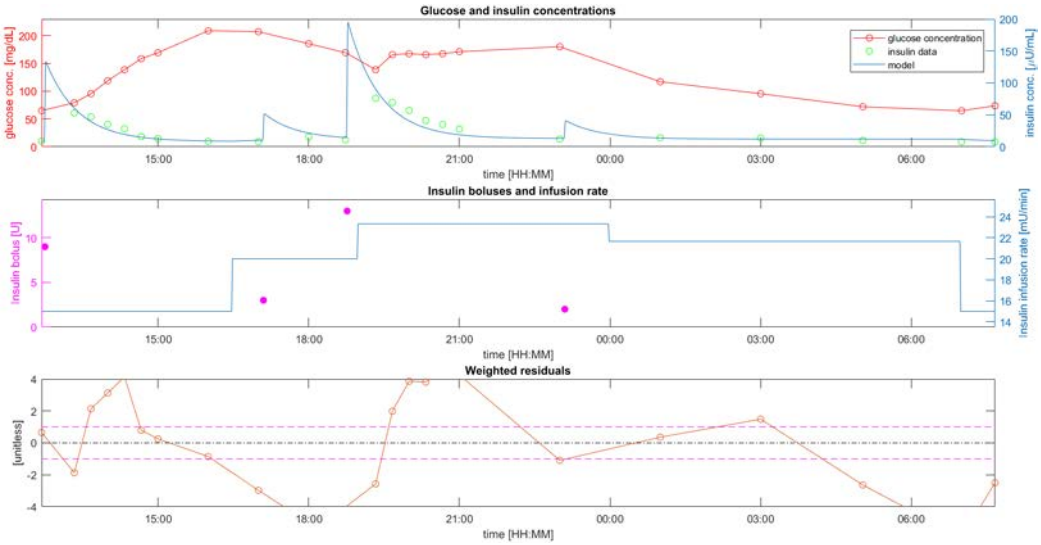

Figure 5.14: Model I: Subject 6

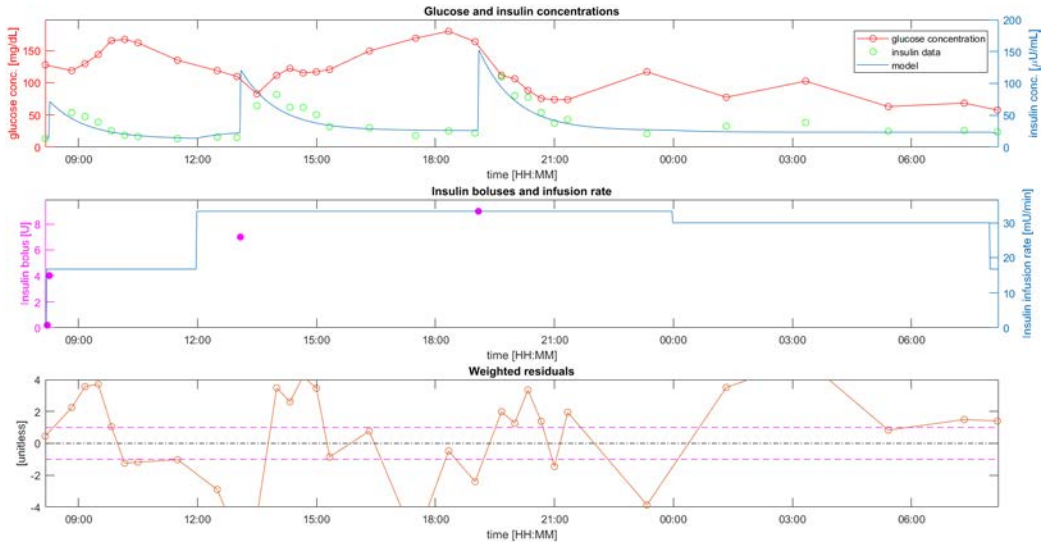

Figure 5.15: Model I: Subject 7

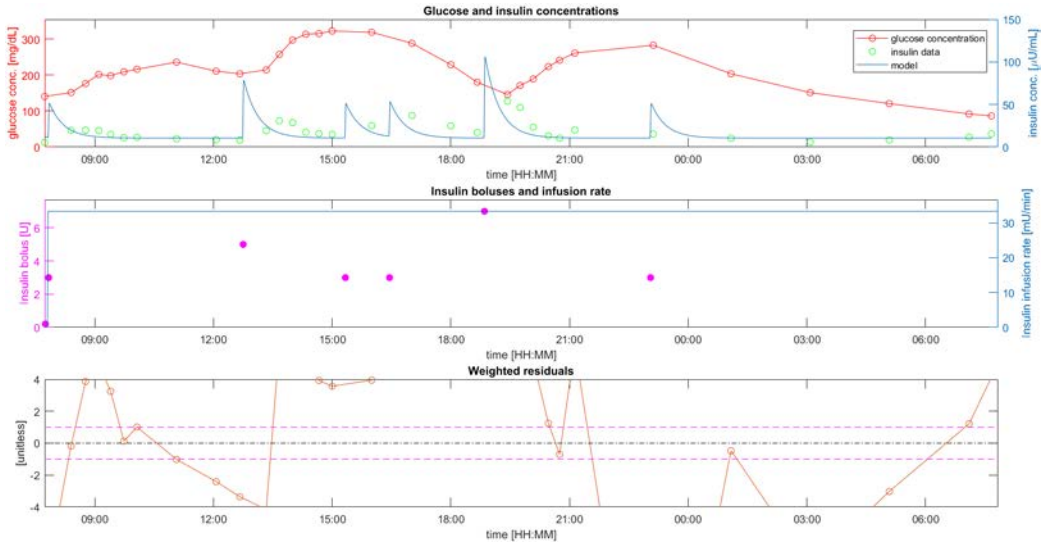

Figure 5.16: Model I: Subject 8

Table 5.1: *Model I*: parameter estimates and their precisions (CV)

Subjects	*Parameters*	
	V_i (L/kg)	n (min^{-1})
1	1 (3)	0.038 (3)
2	0.954 (6)	0.035 (5)
3	0.649 (10)	0.053 (8)
4	0.058 (11)	0.817 (11)
5	1 (5)	0.020 (5)
6	1 (6)	0.026 (5)
7	1 (6)	0.018 (6)
8	1 (4)	0.045 (4)
MEAN ± SD (CV)	0.833 ± 0.336 (6)	0.131 ± 0.321 (6)

Model II

Model II was not able to satisfactorily predict plasma insulin profiles, due to a slower IP insulin absorption into the circulation, which is not described with a single–compartment configuration model. Although model fit has visibly improved compared to model I, in most of the subjects, the insulin concentration predicted by the model in correspondence of insulin boluses increases and decreases too rapidly compared to the experimental data. This is also confirmed by their weighted residuals pattern. In Table 5.2 parameters estimates and their precisions are reported. In particular, all the parameters are well estimated and V_i (0.357 ± 0.153 L/Kg) is much closer to the prior value than in Model II. The same applies to the fractional clearance (0.122 ± 0.078 with respect to the prior value around 0.131 min^{-1}). The variability of the IP rate parameter estimates in each of the three subintervals (k_{a1}, k_{a2} and k_{a3}) is quite small, since their dispersion (SD) is always lower than their aver-

age value (0.025 ± 0.013, 0.023 ± 0.014, 0.027 ± 0.023 min^{-1} respectively). Finally, considering that, for each subject, k_a is identified three times (one for each time subinterval), *one–way analysis of variance* (one–way ANOVA) was performed in order to test the *null hypothesis* that values in the k_{a1}, k_{a2} and k_{a3} columns (Table 5.2) are drawn from populations with the same mean values (using the F distribution). Since $F = 0.13 < F_{\text{crit}} = 3.49$, the null hypothesis was accepted, concluding that the differences between k_{a1}, k_{a2} and k_{a3} means are nonsignificant at the 5% significance level (the p–value is 0.8817).

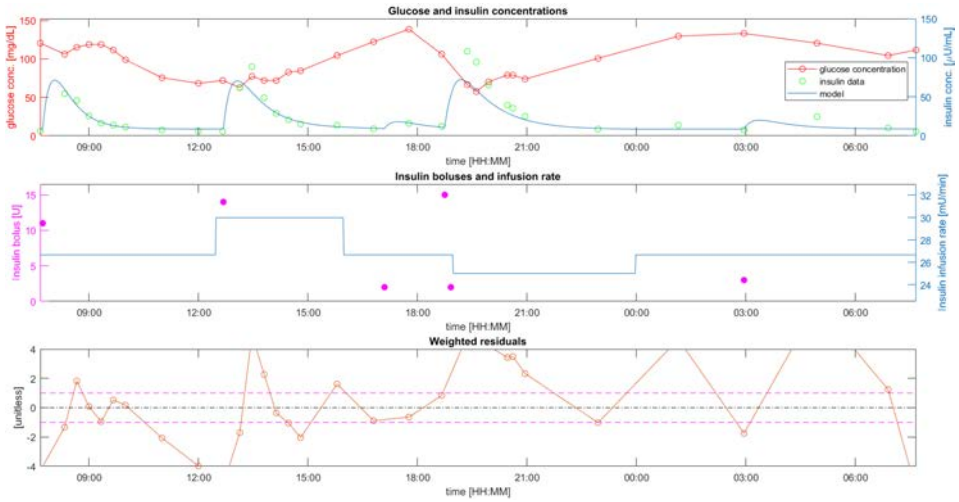

Figure 5.17: Model II: Subject 1

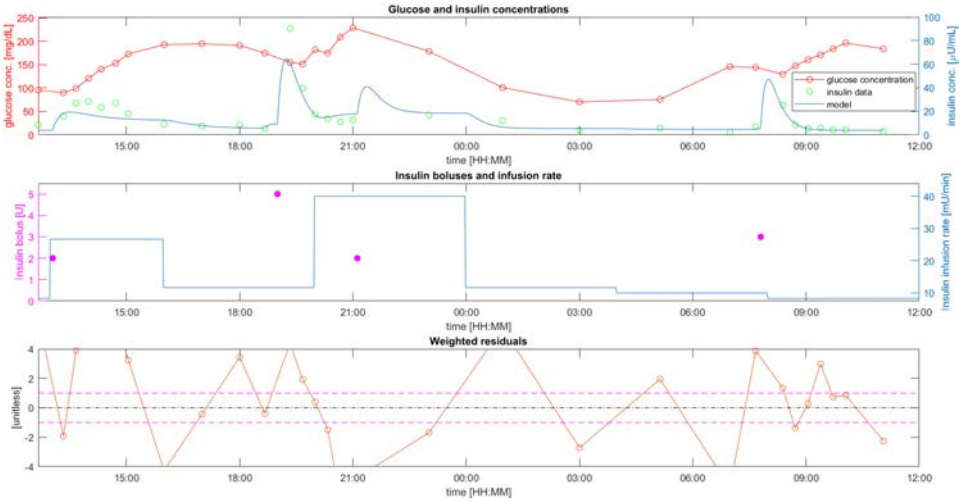

Figure 5.18: Model II: Subject 2

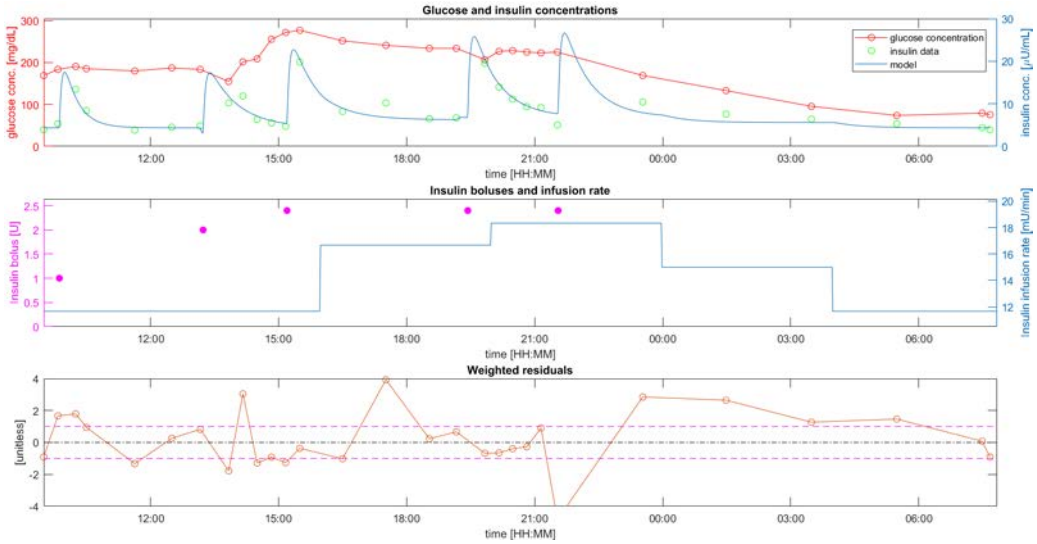

Figure 5.19: Model II: Subject 3

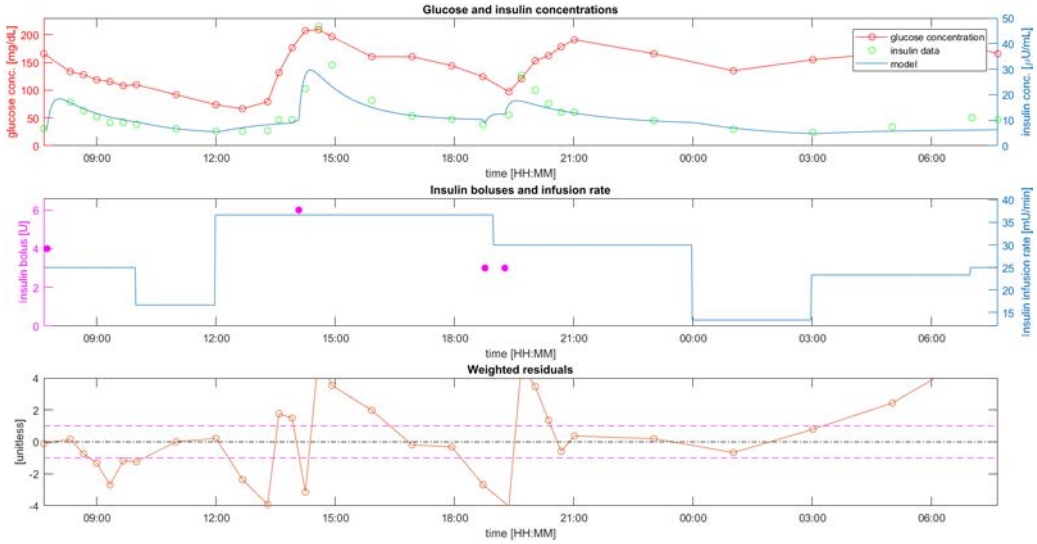

Figure 5.20: Model II: Subject 4

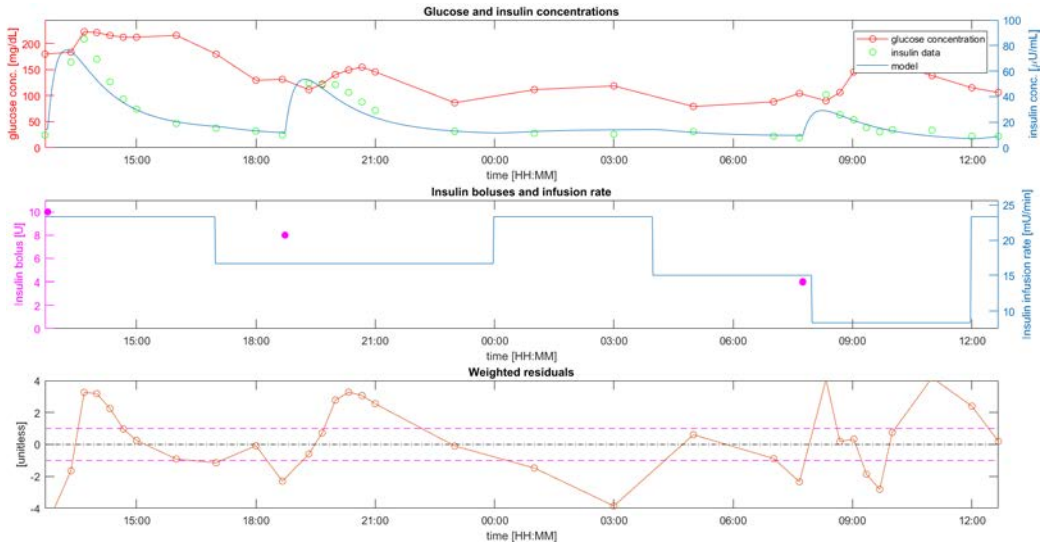

Figure 5.21: Model II: Subject 5

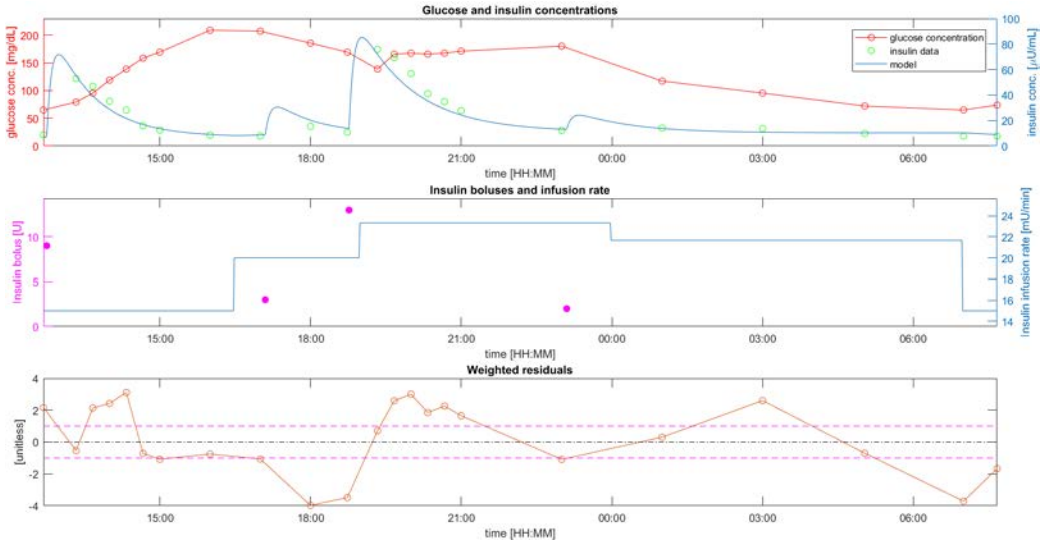

Figure 5.22: Model II: Subject 6

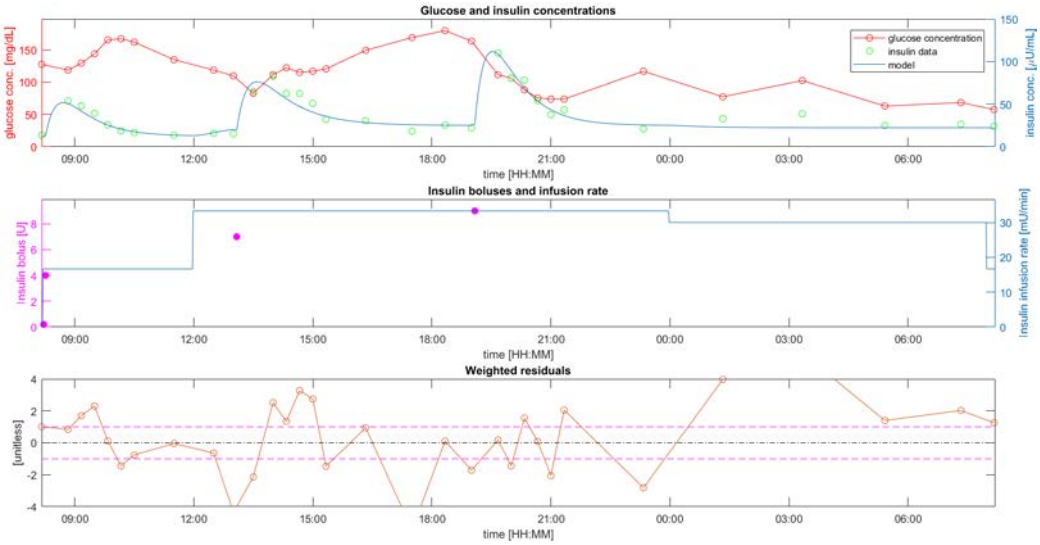

Figure 5.23: Model II: Subject 7

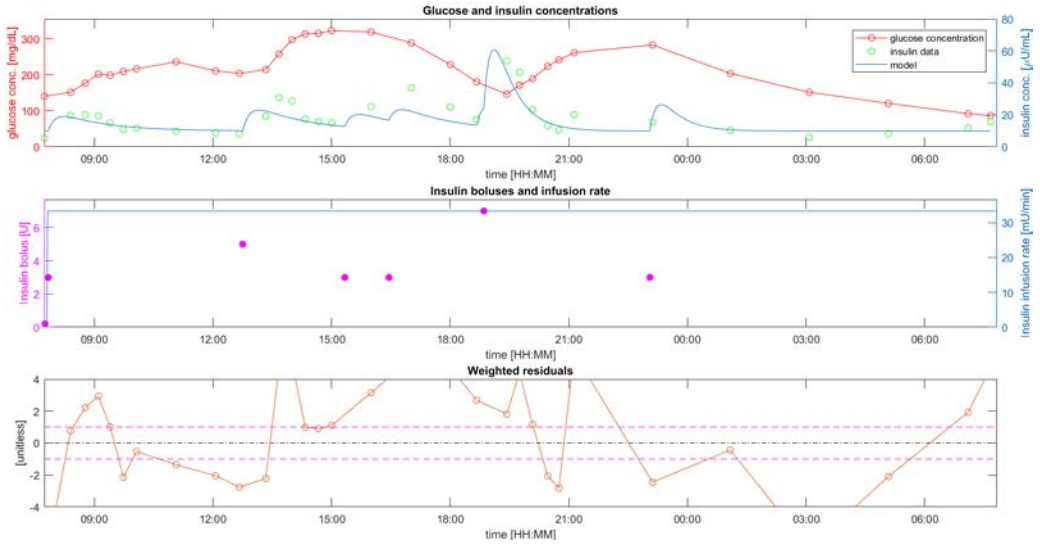

Figure 5.24: Model II: Subject 8

Table 5.2: *Model II*: parameter estimates and their precisions (CV)

Subjects	*Parameters*				
	V_i (L/kg)	n (min^{-1})	k_{a1} (min^{-1})	k_{a2} (min^{-1})	k_{a3} (min^{-1})
1	0.593 (14)	0.073 (14)	0.033 (9)	0.023 (8)	0.018 (9)
2	0.372 (17)	0.083 (17)	0.023 (12)	0.056 (16)	0.082 (20)
3	0.132 (19)	0.289 (19)	0.051 (30)	0.025 (11)	0.027 (12)
4	0.375 (16)	0.141 (16)	0.014 (11)	0.016 (8)	0.009 (7)
5	0.345 (15)	0.067 (14)	0.016 (7)	0.013 (8)	0.012 (8)
6	0.176 (19)	0.171 (18)	N/A (N/A)	0.020 (6)	0.015 (8)
7	0.350 (15)	0.055 (15)	0.024 (12)	0.019 (10)	0.023 (11)
8	0.508 (15)	0.095 (15)	0.014 (17)	0.013 (10)	0.033 (9)
MEAN ± SD (CV)	0.357 ± 0.153 (16)	0.122 ± 0.078 (16)	0.025 ± 0.013 (13)	0.023 ± 0.014 (10)	0.027 ± 0.023 (10)

Model III

The Model III was able to quite satisfactorily predict plasma insulin profiles in all of the subjects. This two–compartment model can better predict the absorption kinetics with respect to the previous models, as can be observed by the model fit, which is able to describe the experimental data (clearly visible in subject 5, Figure 5.29). This is also confirmed by weighted residuals, which are smaller than Model I and II, even if their profile presents some correlated sequences positive/ negative residuals (Figure 5.27, 5.28, 5.29, 5.30, 5.32) and the amplitude is larger than expected in some time intervals (Figure 5.25, 5.26, 5.32). In table 5.3 model parameter estimates and their precisions are reported, in particular: only k_{d1} in subject 4 is estimated with poor precision (CV>100%), V_I ($0.163 \pm 0.023\ L/Kg$) is estimated close to the prior value (around $0.131\ L/Kg$), the same applies to the fractional clearance (0.224 ± 0.068

with respect to the prior value around 0.131 min^{-1}). The variability of k_a in each of the three subintervals (k_{a1}, k_{a2} and k_{a3}) is quite small, since their dispersion (SD) is always lower than their average value (0.036 $\pm$ 0.016, 0.033 $\pm$ 0.018, 0.031 $\pm$ 0.019 min^{-1} respectively). On the other hand, the variability of k_d in the second and third subinterval (k_{d2} and k_{d3}) is large since their standard deviation is greater than their average value (0.114 $\pm$ 0.164, 0.213 $\pm$ 0.298 min^{-1} respectively). Finally, one–way ANOVA was performed in order to test the *null hypothesis* that values in the k_{a1}, k_{a2} and k_{a3} columns (Table 5.3) are drawn from populations with the same mean values (using the F distribution). Since $F = 0.13 < F_{\text{crit}} = 3.49$, the null hypothesis was accepted, concluding that the differences between k_{a1}, k_{a2} and k_{a3} means are nonsignificant at the 5% significance level (the p–value is 0.8757). Then, one–way ANOVA was performed also to compare means of k_{d1}, k_{d2} and k_{d3}. Also in this case, $F = 0.77 < F_{\text{crit}} = 3.49$, the null hypothesis was accepted, concluding that the differences between k_{d1}, k_{d2} and k_{d3} means are nonsignificant at the 5% significance level (the p–value is 0.4758).

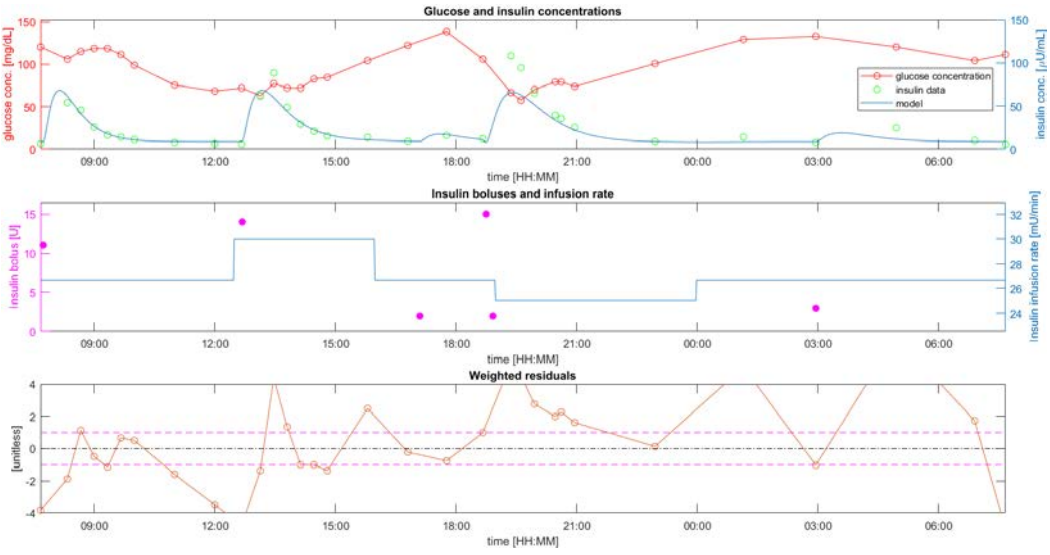

Figure 5.25: Model III: Subject 1

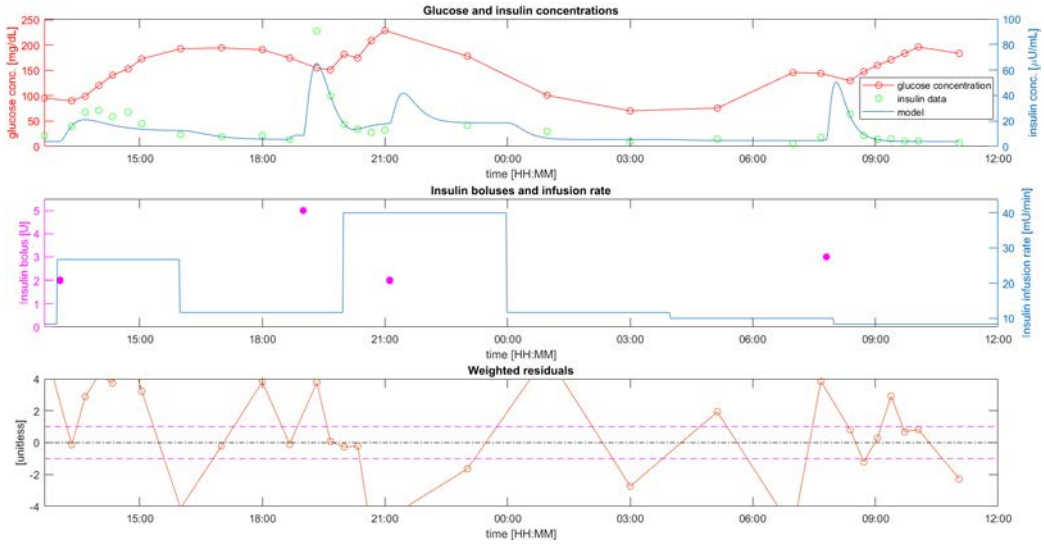

Figure 5.26: Model III: Subject 2

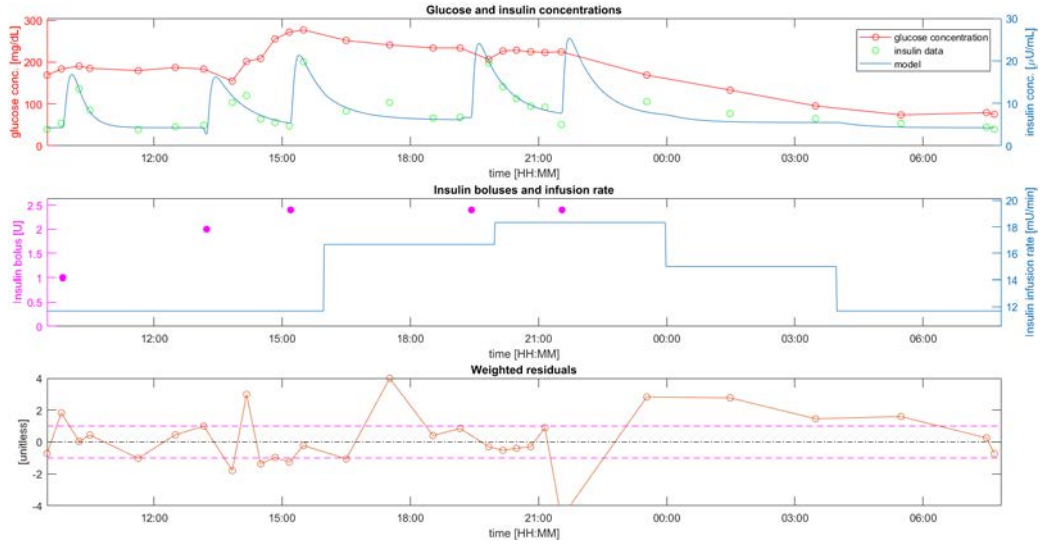

Figure 5.27: Model III: Subject 3

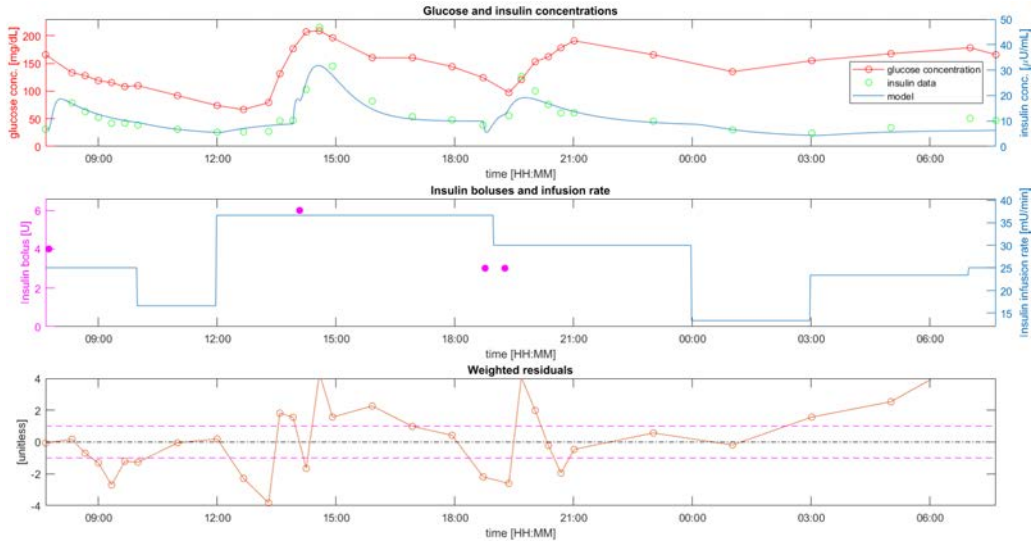

Figure 5.28: Model III: Subject 4

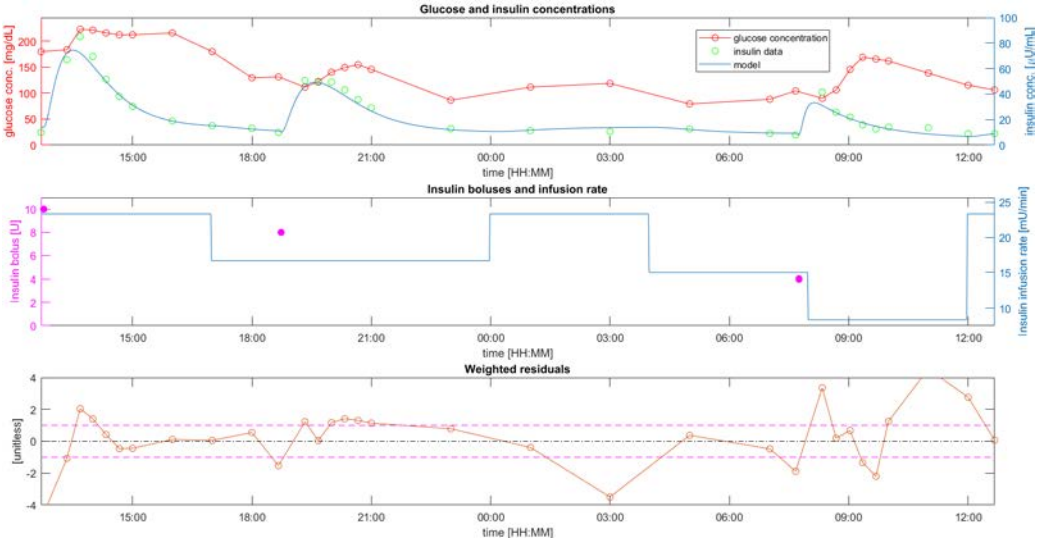

Figure 5.29: Model III: Subject 5

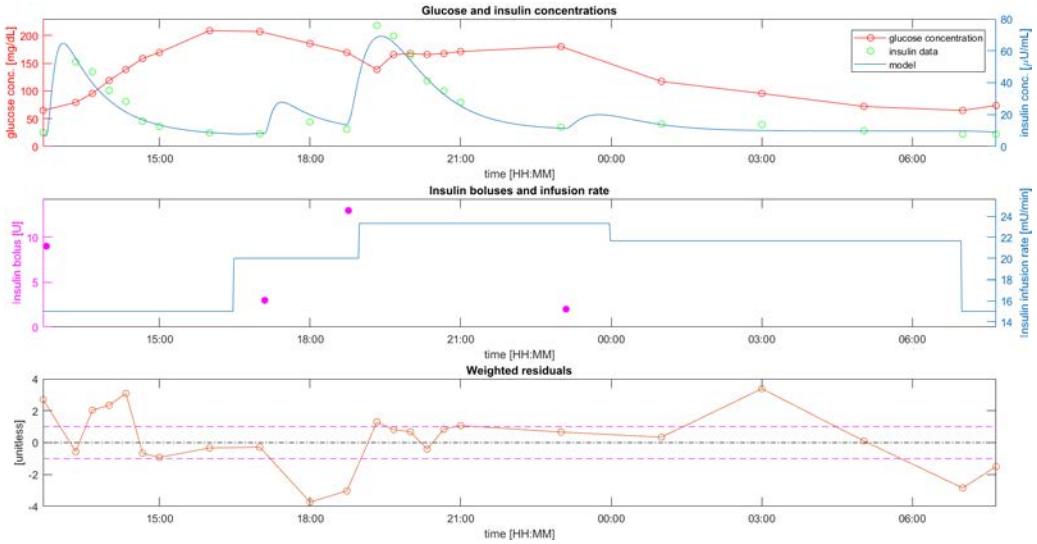

Figure 5.30: Model III: Subject 6

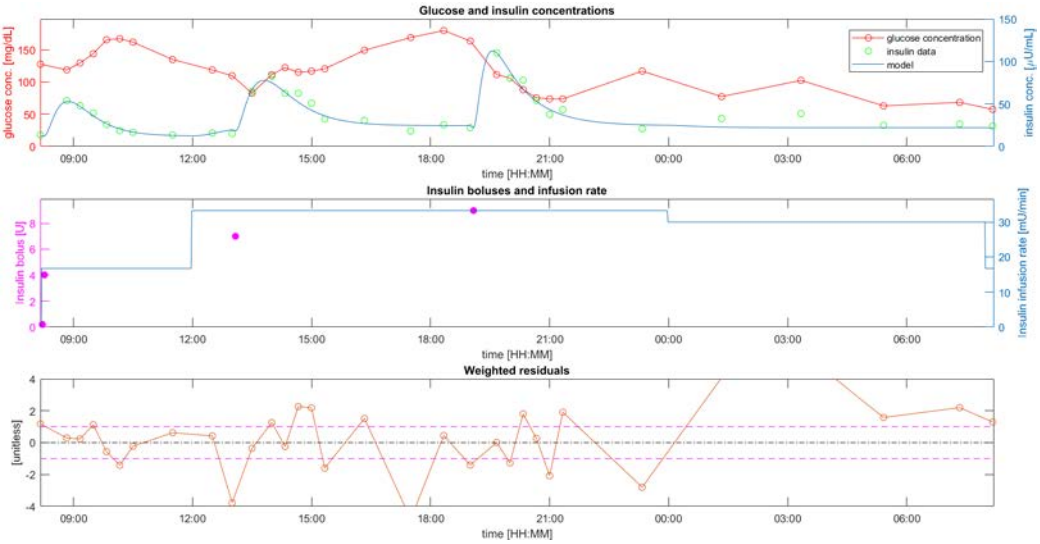

Figure 5.31: Model III: Subject 7

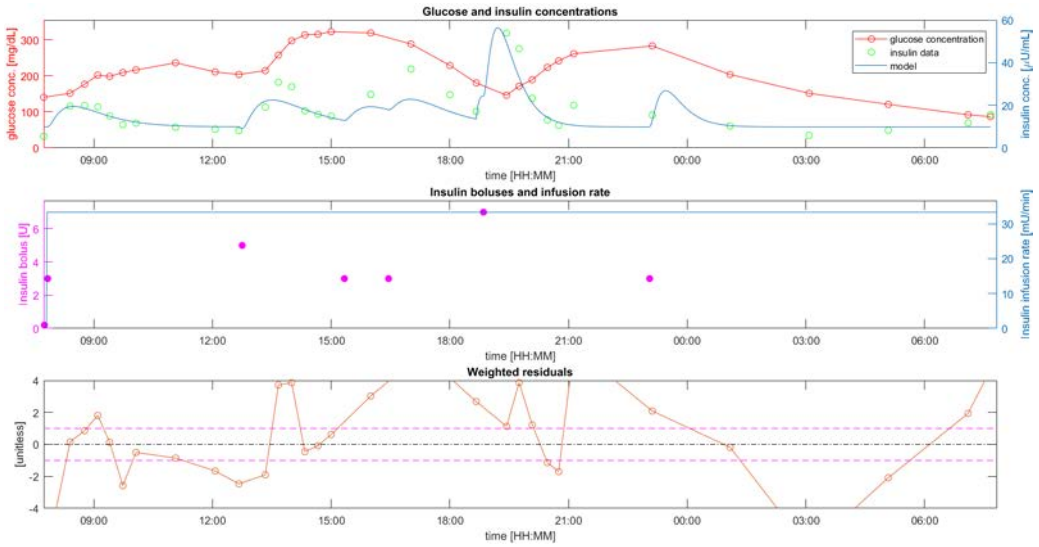

Figure 5.32: Model III: Subject 8

Model IV

The extension of a Michaelis–Menten kinetics in the absorption between the two IP compartments in Model IV did not improve the prediction of plasma insulin profiles with respect to the linear Model III. This was confirmed by the similar weighted residuals pattern (Figure 5.33–5.40). Further evidence stems from Table 5.4, in which model parameters and their precisions are reported. In particular, among the IP parameters, k_a is estimated, on average, with good precision (CV<100%) in all the three subintervals, while $V_{\max}$ and k_m are estimated, on average, with very poor precision in the first and third subinterval, and in detail, with CV>100% in 39% and 35% of the time, respectively. Then, V_i ($0.202 \pm 0.048\ L/Kg$) is estimated close to the prior value (around 0.131 L/Kg), the same applies to the fractional clearance (0.224 ± 0.068 with respect to the prior value around 0.131 min^{-1}). The variability of k_a in each of the three subintervals (k_{a1}, k_{a2} and k_{a3}) is quite small, since its dispersion (SD) is always lower than its average value (0.029 ± 0.016, 0.024 ± 0.014, $0.027 \pm 0.017\ min^{-1}$ respectively). The same considerations can be applied for the variability of $V_{\max}$ in the three subintervals (1017 ± 376, 838 ± 369, $788 \pm 235\ mU/min$ respectively). Finally, the variability of k_m is large only in the first subinterval (1633 ± 2093, 500 ± 247, $929 \pm 536\ mU$ respectively). In conclusion, the eventual saturation of the insulin in the first IP compartment, due to the rapid insulin absorption, seemed not occur.

Table 5.3: *Model III*: parameter estimates and their precisions (CV)

Subjects	*Parameters*							
	V_i (L/kg)	n (min^{-1})	k_{a1} (min^{-1})	k_{d1} (min^{-1})	k_{a2} (min^{-1})	k_{d2} (min^{-1})	k_{a3} (min^{-1})	k_{d3} (min^{-1})
1	0.166 (20)	0.272 (20)	0.036 (18)	0.068 (34)	0.029 (22)	0.050 (32)	0.030 (5)	0.030 (N/A)
2	0.173 (18)	0.179 (18)	0.042 (7)	0.042 (N/A)	0.076 (6)	0.076 (N/A)	0.066 (13)	0.218 (50)
3	0.135 (19)	0.290 (19)	0.064 (30)	0.199 (12)	0.024 (7)	0.501 (1)	0.026 (12)	0.913 (2)
4	0.171 (15)	0.311 (16)	0.014 (10)	0.223 (112)	0.035 (8)	0.035 (N/A)	0.012 (11)	0.062 (32)
5	0.160 (18)	0.148 (18)	0.028 (4)	0.028 (N/A)	0.023 (5)	0.023 (N/A)	0.012 (9)	0.284 (68)
6	0.135 (20)	0.237 (20)	N/A (N/A)	N/A (N/A)	0.019 (6)	0.175 (52)	0.028 (5)	0.028 (N/A)
7	0.158 (18)	0.123 (18)	0.038 (5)	0.038 (N/A)	0.032 (5)	0.032 (N/A)	0.021 (10)	0.120 (48)
8	0.207 (15)	0.234 (15)	0.028 (83)	0.031 (84)	0.025 (6)	0.025 (N/A)	0.053 (6)	0.053 (N/A)
Mean ± SD (CV)	0.163 ± 0.023 (18)	0.224 ± 0.068 (18)	0.036 ± 0.016 (22)	0.090 ± 0.084 (60)	0.033 ± 0.018 (8)	0.115 ± 0.164 (28)	0.031 ± 0.019 (9)	0.213 ± 0.298 (40)

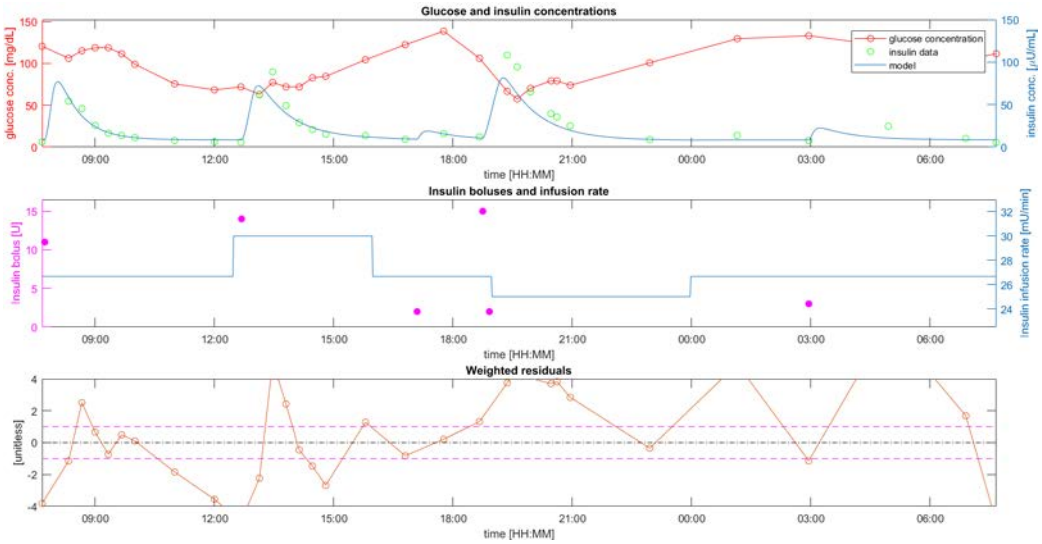

Figure 5.33: Model IV: Subject 1

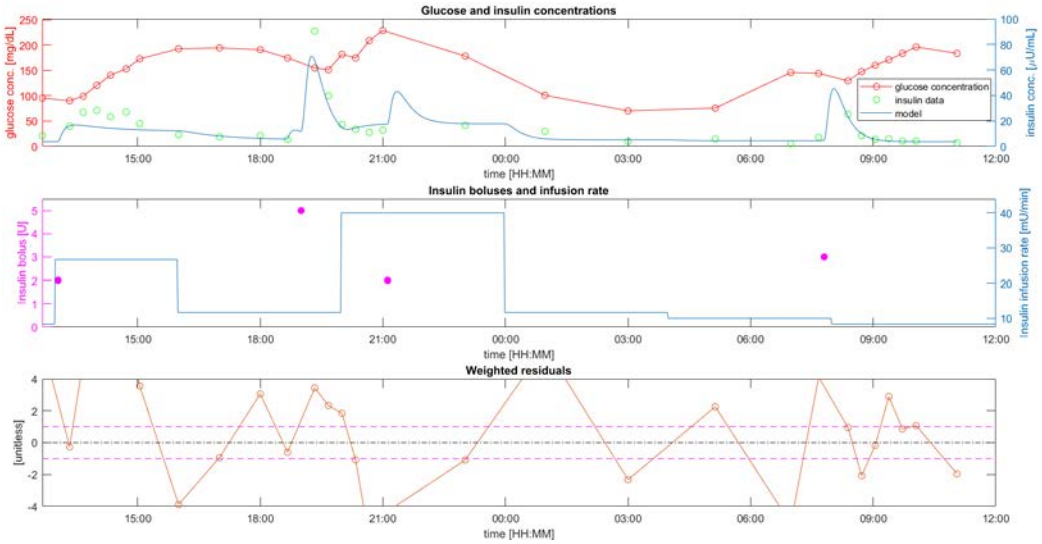

Figure 5.34: Model IV: Subject 2

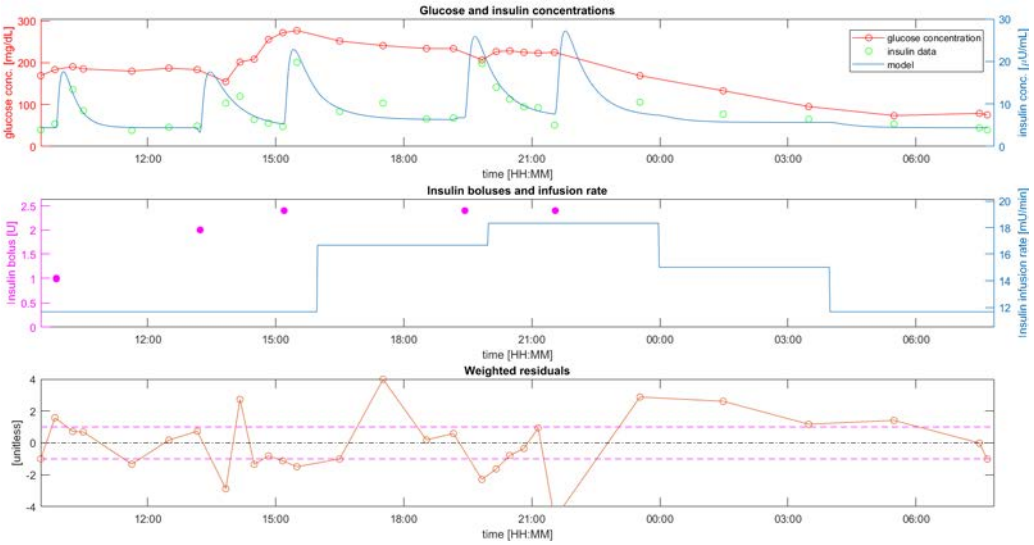

Figure 5.35: Model IV: Subject 3

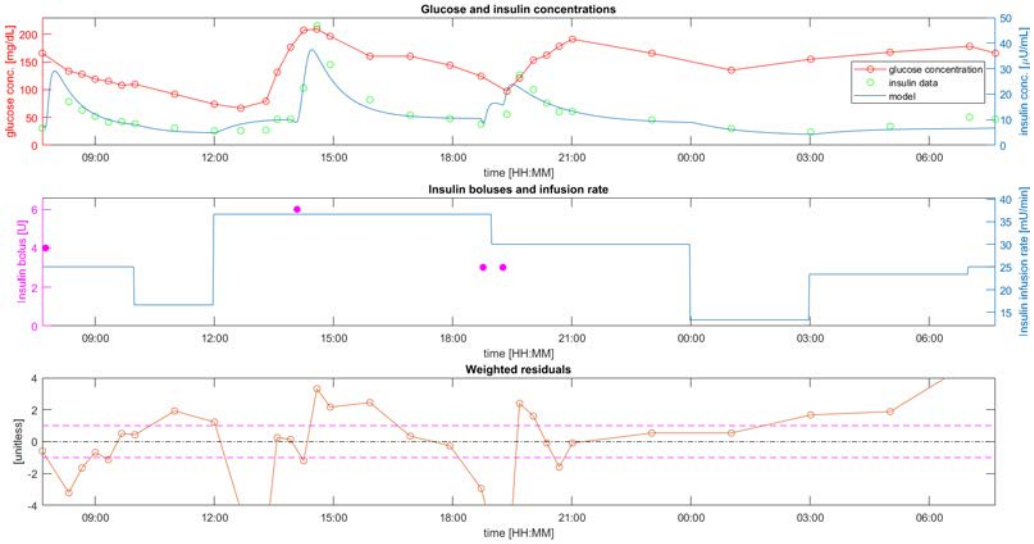

Figure 5.36: Model IV: Subject 4

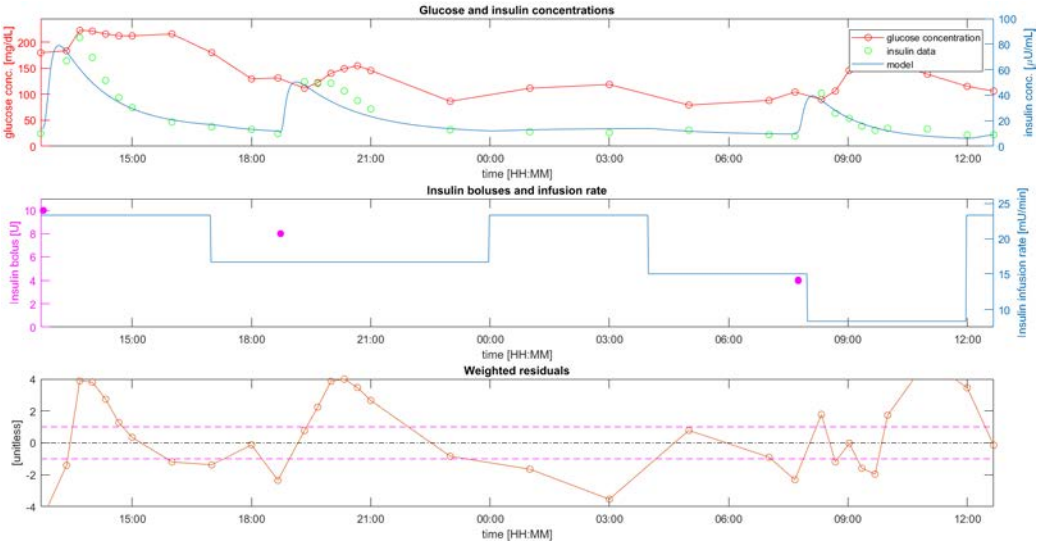

Figure 5.37: Model IV: Subject 5

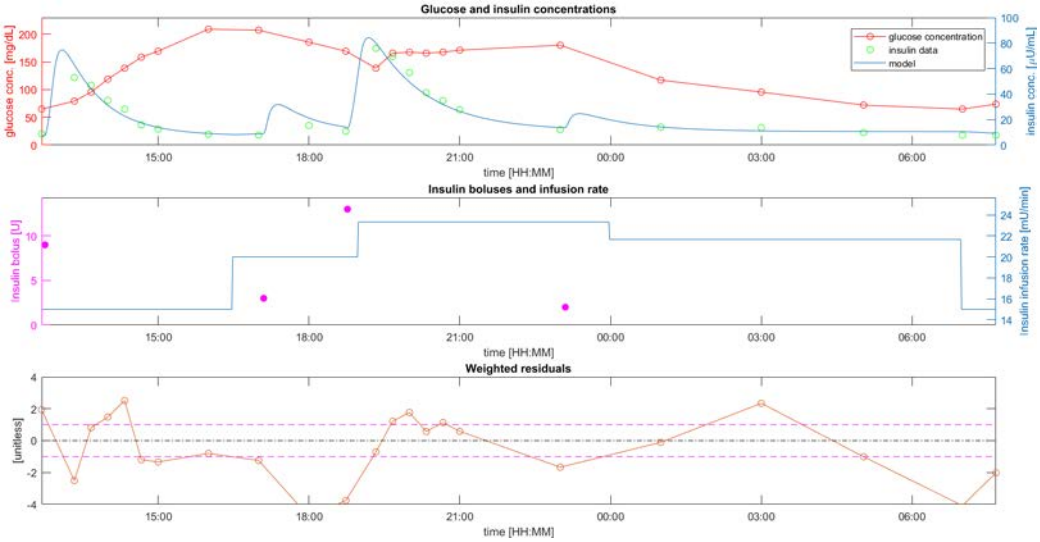

Figure 5.38: Model IV: Subject 6

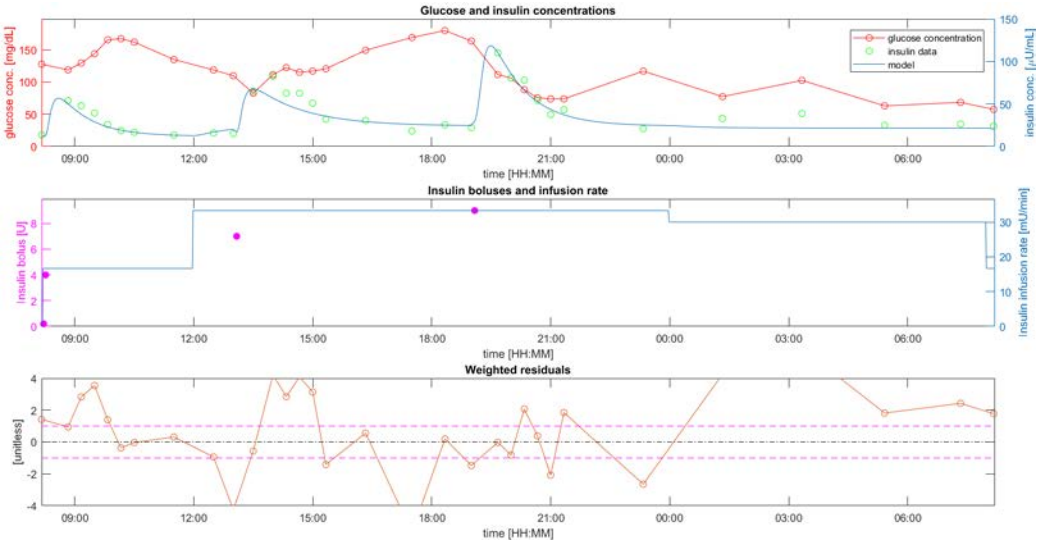

Figure 5.39: Model IV: Subject 7

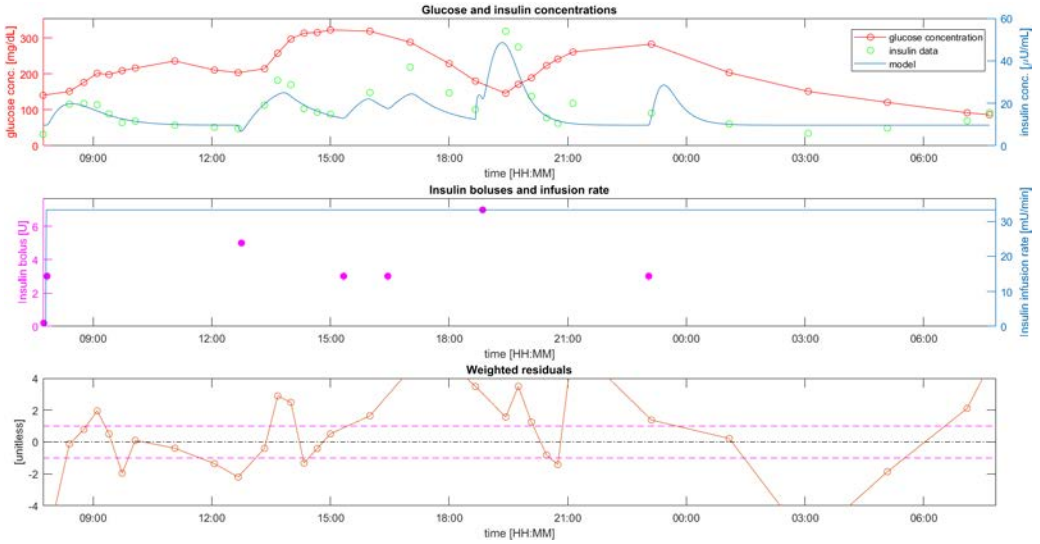

Figure 5.40: Model IV: Subject 8

Table 5.4: *Model IV*: parameter estimates and their precisions (CV)

Sub	*Parameters*										
	V_i (L/kg)	n (min^{-1})	k_{a1} (min^{-1})	$V_{\max 1}$ (mU/min)	k_{m1} (mU)	k_{a2} (min^{-1})	$V_{\max 2}$ (mU/min)	k_{m2} (mU)	k_{a3} (min^{-1})	$V_{\max 3}$ (mU/min)	k_{m3} (mU)
1	0.268 (20)	0.169 (20)	0.030 (9)	1037.2 (1058)	683.85 (3134)	0.020 (7)	909.60 (45)	599.75 (16)	0.019 (8)	761.70 (20)	490.71 (19)
2	0.252 (18)	0.128 (19)	0.016 (21)	976.53 (0)	671.39 (0)	0.056 (18)	732.78 (220)	597.58 (173)	0.062 (31)	696.99 (2575)	726.88 (2670)
3	0.198 (20)	0.191 (20)	0.061 (30)	1060.9 (38)	674.39 (44)	0.028 (15)	999.18 (49)	703.58 (36)	0.031 (11)	643.72 (200)	506.73 (191)
4	0.243 (20)	0.208 (20)	0.027 (10)	1268.6 (175)	1008.9 (174)	0.023 (18)	535.02 (29)	756.41 (22)	0.013 (18)	987.05 (0)	689.28 (2)
5	0.177 (19)	0.134 (19)	0.014 (7)	1500.8 (3)	1344.2 (5)	0.011 (10)	1307.6 (0)	245.15 (3)	0.015 (11)	1026.3 (2689)	1669.2 (2872)
6	0.184 (19)	0.159 (19)	N/A (N/A)	N/A (N/A)	N/A (N/A)	0.022 (1)	1006.9 (0)	690.49 (1)	0.015 (8)	952.26 (40)	594.81 (42)
7	0.162 (19)	0.123 (20)	0.021 (10)	1003.4 (0)	702.10 (0)	0.013 (18)	1084.2 (311)	309.45 (336)	0.019 (12)	917.50 (484)	888.47 (537)
8	0.131 (20)	0.375 (20)	0.037 (155)	276.16 (199)	6343.8 (227)	0.018 (17)	125.27 (17)	95.027 (29)	0.043 (22)	321.71 (52)	1868.3 (166)
Mean ± SD (CV)	0.202 ± 0.048 (19)	0.186 ± 0.082 (19)	0.029 ± 0.016 (34)	1017.6 ± 376.46 (211)	1632.7 ± 2092.67 (512)	0.024 ± 0.014 (13)	837.56 ± 368.70 (84)	499.68 ± 247.33 (77)	0.027 ± 0.017 (15)	788.40 ± 235.23 (758)	929.29 ± 536.15 (812)

Model V

The extension of a Langmuir kinetics in the absorption between the two intraperitoneal compartments in Model V did not significantly improve the prediction of plasma insulin profiles obtained with respect to the linear Model III. In fact, model fit, as well as weighted residuals pattern were similar (Figure 5.41–5.48) to those obtained in Model III, so the same considerations of Model IV can be applied here. In table 5.5, model parameters and their precisions are reported, in particular: among the IP parameters, k_a and α are estimated, on average, with poor precision (CV>100%) in the first subinterval, while their precision is good in the other two subintervals. On the other hand, β is estimated, on average, with very poor precision (CV $\gg$ 100%) in all the three subintervals and in detail, in 91% of the time. Then, V_i (0.167 $\pm$ 0.024 L/Kg) is estimated close to the prior value (around 0.131 L/Kg), the same applies to the fractional clearance (0.218 $\pm$ 0.060 with respect to the prior value around 0.131 min^{-1}). The variability of k_a in the first and third subinterval (k_{a1} and k_{a3}) is large since their standard deviation is greater than their average value (0.126 $\pm$ 0.164, 0.190 $\pm$ 0.298 min^{-1} respectively), while is quite small in the second subinterval (0.102 $\pm$ 0.083 min^{-1}). The same considerations can be applied for the variability of α in the three subintervals (0.070 $\pm$ 0.100, 0.033 $\pm$ 0.013 and 0.044 $\pm$ 0.045 min^{-1} respectively). Finally, the variability of β is very large in all the subintervals (399960 $\pm$ 488041, 241672 $\pm$ 337339 and 101064 $\pm$ 203519 mU respectively). In conclusion, neither the insulin concentration in the second IP compartment seemed to drive a saturation phenomenon in the IP absorption.

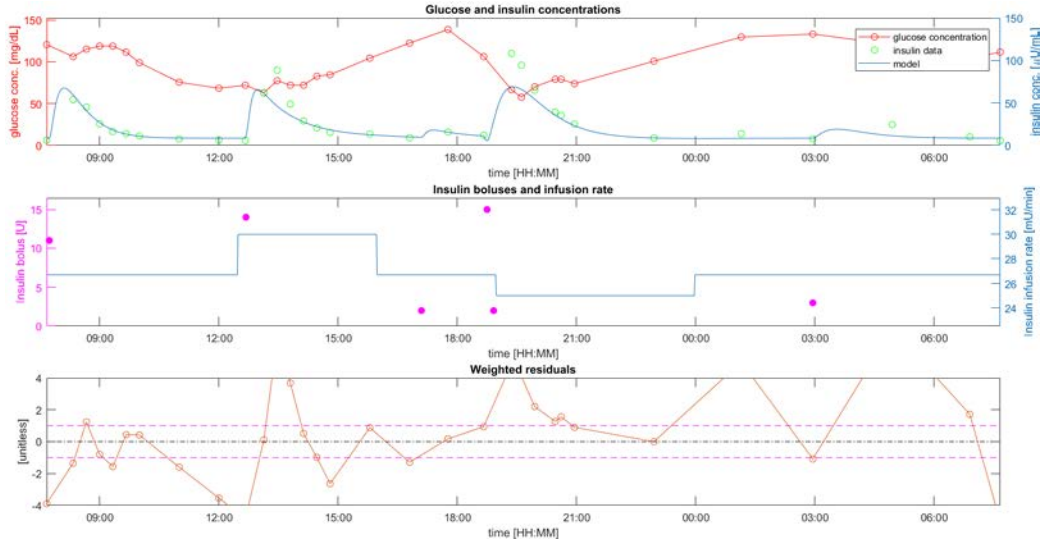

Figure 5.41: Model V: Subject 1

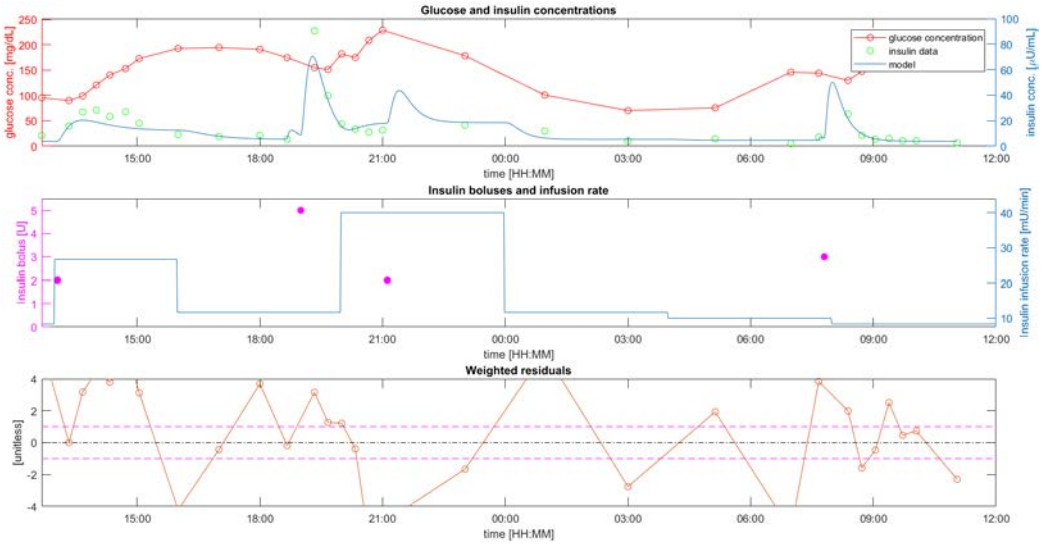

Figure 5.42: Model V: Subject 2

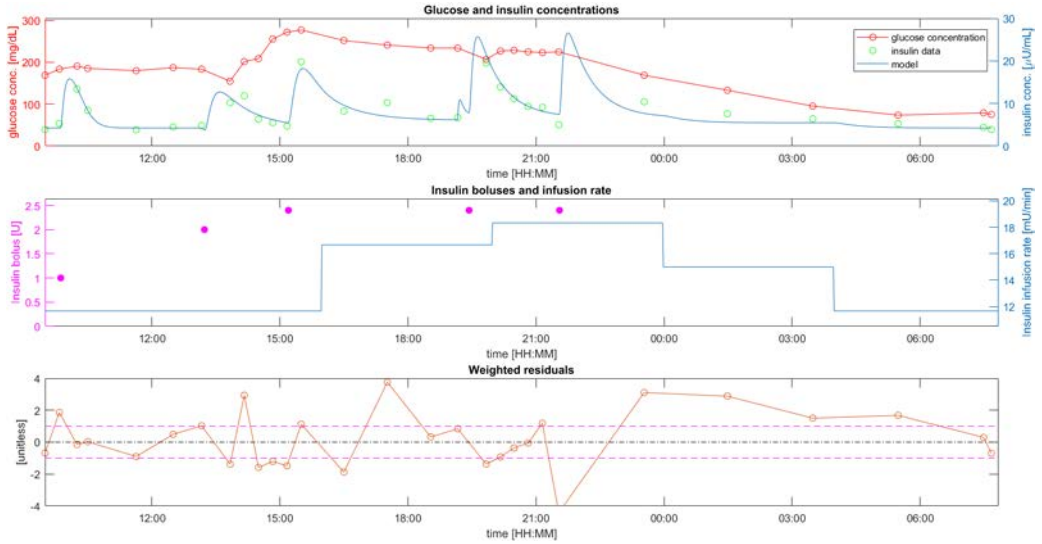

Figure 5.43: Model V: Subject 3

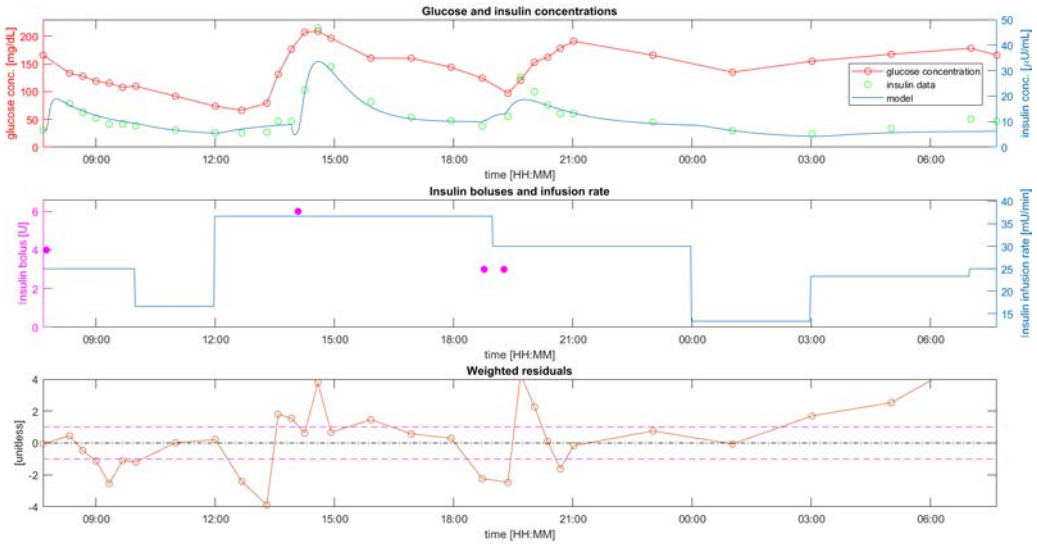

Figure 5.44: Model V: Subject 4

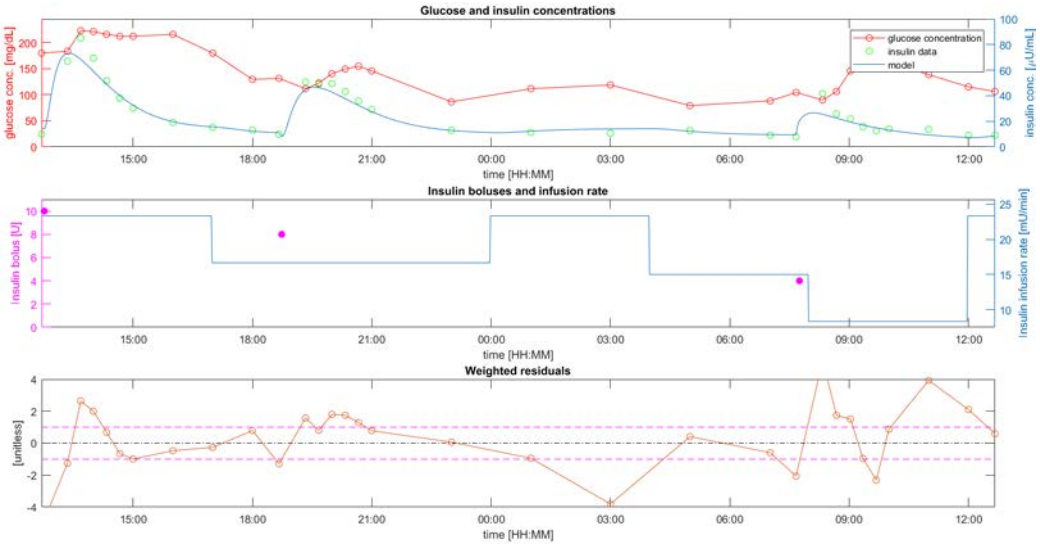

Figure 5.45: Model V: Subject 5

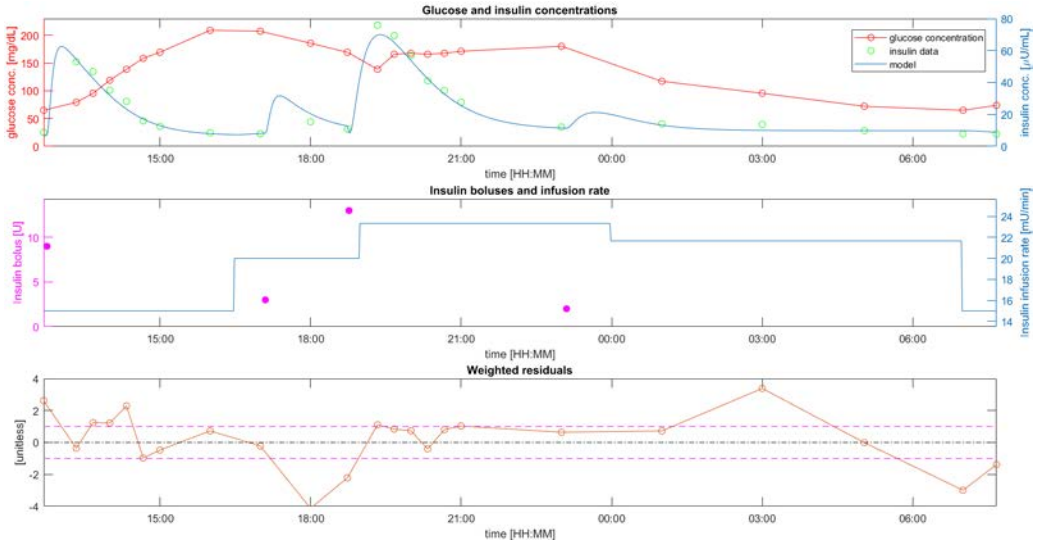

Figure 5.46: Model V: Subject 6

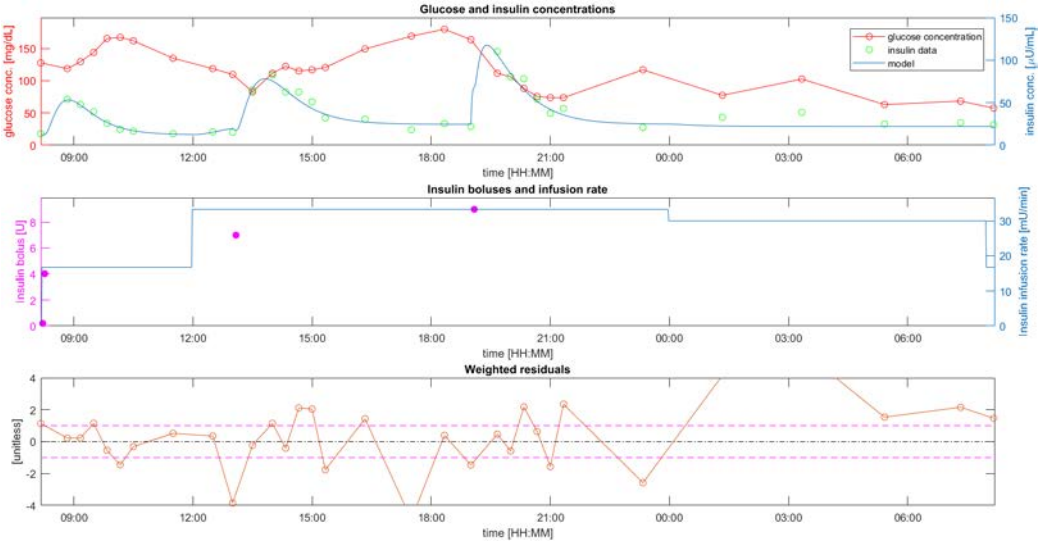

Figure 5.47: Model V: Subject 7

Table 5.5: *Model V*: parameter estimates and their precisions (CV)

Sub	*Parameters*										
	V_i (L/kg)	n (min^{-1})	k_{a1} (min^{-1})	β_1 (mU)	α_1 (min^{-1})	k_{a2} (min^{-1})	β_2 (mU)	α_2 (min^{-1})	k_{a3} (min^{-1})	β_3 (mU)	α_3 (min^{-1})
1	0.197 (20)	0.228 (20)	0.086 (55)	9875.7 (178)	0.042 (39)	0.240 (61)	138453 (3312)	0.018 (22)	0.029 (94)	48058.3 (493)	0.034 (56)
2	0.148 (20)	0.209 (20)	0.033 (41)	877810 (43503)	0.049 (53)	0.119 (44)	959217 (30905)	0.060 (53)	0.395 (109)	599756 (174105)	0.056 (49)
3	0.153 (20)	0.257 (20)	0.132 (546)	482.72 (477)	0.295 (453)	0.139 (108)	120016 (27538)	0.022 (76)	0.535 (90)	46554 (15717)	0.029 (49)
4	0.194 (20)	0.273 (20)	0.491 (100)	19734 (6490)	0.014 (53)	0.051 (78)	22835 (328)	0.029 (88)	0.059 (47)	83856 (2899)	0.013 (47)
5	0.169 (20)	0.138 (20)	0.046 (65)	6380.1 (106)	0.032 (40)	0.0198 (47)	8990 (105)	0.041 (83)	0.081 (55)	3493.6 (279)	0.012 (56)
6	0.126 (20)	0.251 (20)	N/A (N/A)	N/A (N/A)	N/A (N/A)	0.192 (52)	1766.4 (59)	0.032 (18)	0.035 (68)	19877 (176)	0.031 (79)
7	0.166 (20)	0.117 (20)	0.048 (76)	956240 (33065)	0.032 (99)	0.033 (206)	144933 (2340)	0.032 (244)	0.333 (216)	1886.2 (268)	0.028 (51)
8	0.180 (20)	0.271 (20)	0.048 (59)	929196 (31756)	0.022 (73)	0.025 (99)	537165 (11295)	0.025 (131)	0.053 (87)	5034.6 (47)	0.149 (260)
Mean ± SD (CV)	0.167 ± 0.024 (20)	0.218 ± 0.060 (20)	0.126 ± 0.164 (135)	399960 ± 488041 (16511)	0.070 ± 0.100 (116)	0.102 ± 0.084 (87)	241672 ± 337340 (9492)	0.033 ± 0.013 (89)	0.190 ± 0.200 (96)	101065 ± 203519 (24248)	0.044 ± 0.045 (81)

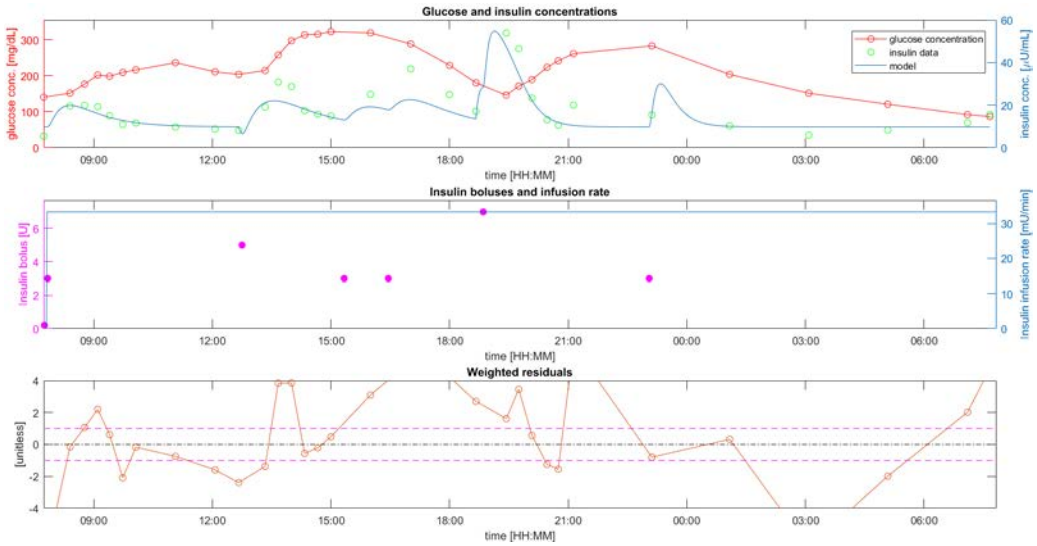

Figure 5.48: Model V: Subject 8

Model VI

Model VI did not significantly improve the prediction of plasma insulin profiles obtained with the linear Model III. Moreover, model fit in the third time interval (during the night) in subject 3, 4, 7 and 8 is still not so good, since the model is not able to describes these data, so over and/or underestimation is visible (Figures 5.51, 5.52, 5.55, 5.56). This is confirmed by the weighted residuals which are correlated with a larger amplitude than expected, i.e. $\pm$ 1. Model parameters and their precisions are reported in Table 5.6, in particular: among the IP parameters, k_a and k_d are estimated, on average, with good precision (CV<100%) in all of the three subintervals. The variability of k_a in each of the three subintervals (k_{a1}, k_{a2} and k_{a3}) is quite small, since its dispersion (SD) is always lower than its average value (0.035 $\pm$ 0.017, 0.028 $\pm$ 0.012, 0.028 $\pm$ 0.017 min^{-1} respectively). On the other hand, the variability of k_d is quite small only in the first subinterval (0.080 $\pm$ 0.079 min^{-1}), while in the other two subintervals, the variability in quite large (0.149 $\pm$ 0.188 and 0.261 $\pm$ 0.320 min^{-1} respectively). Then, V_i (0.142 $\pm$ 0.020 L/Kg) is estimated close to the prior value (around 0.131 L/Kg), a_G is estimated, on average, with poor precision (CV>100%) and its variability is large (0.0002 $\pm$ 0.0003 $min^{-1}dL/mg$). Finally, n_b (which together with a_G represents the fractional clearance in this Model VI), is estimated, on average, with good precision (CV < 100%) and its variability is small (0.264 $\pm$ 0.105 min^{-1}). In conclusion, fractional insulin clearance seemed not to be modulated by glucose concentration.

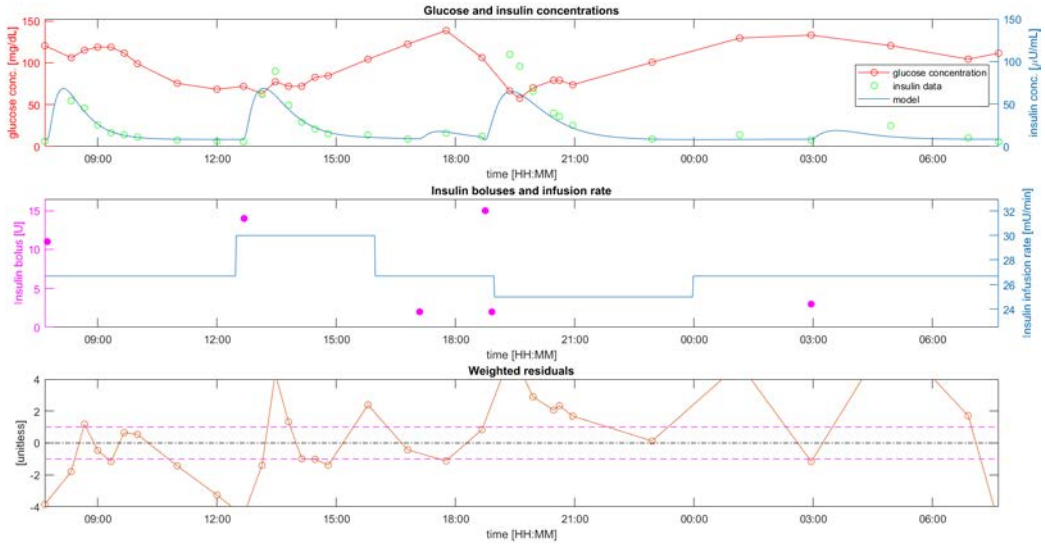

Figure 5.49: Model VI: Subject 1

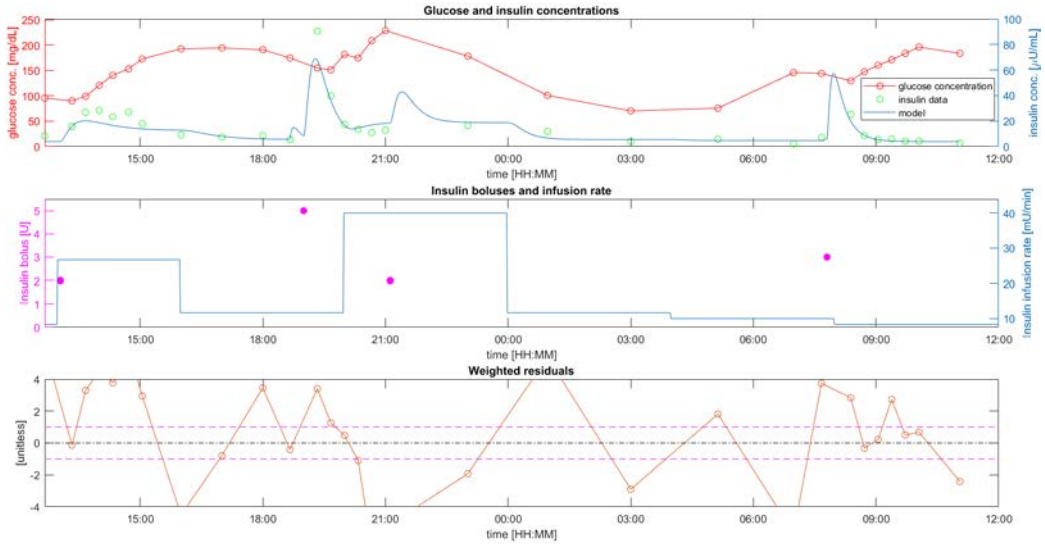

Figure 5.50: Model VI: Subject 2

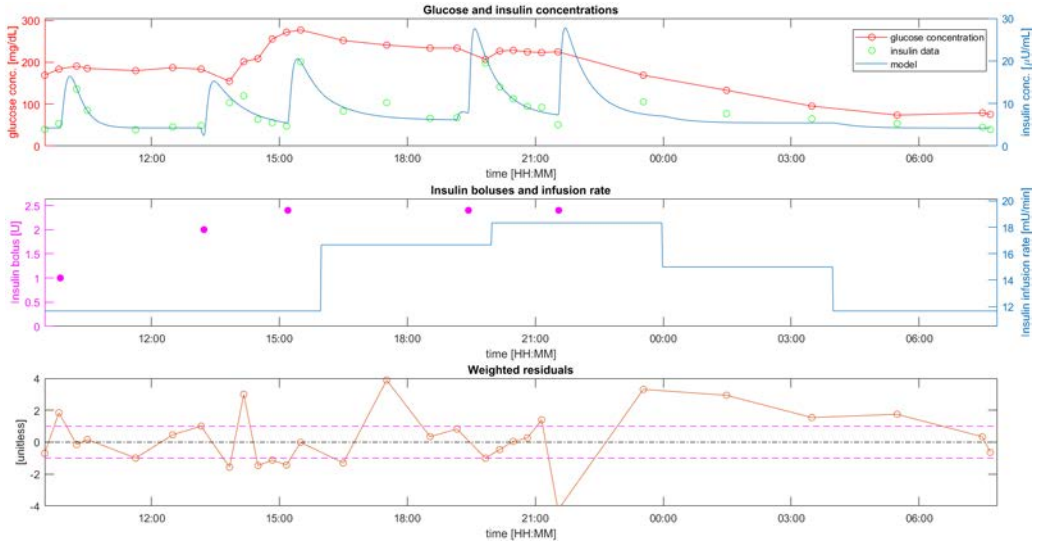

Figure 5.51: Model VI: Subject 3

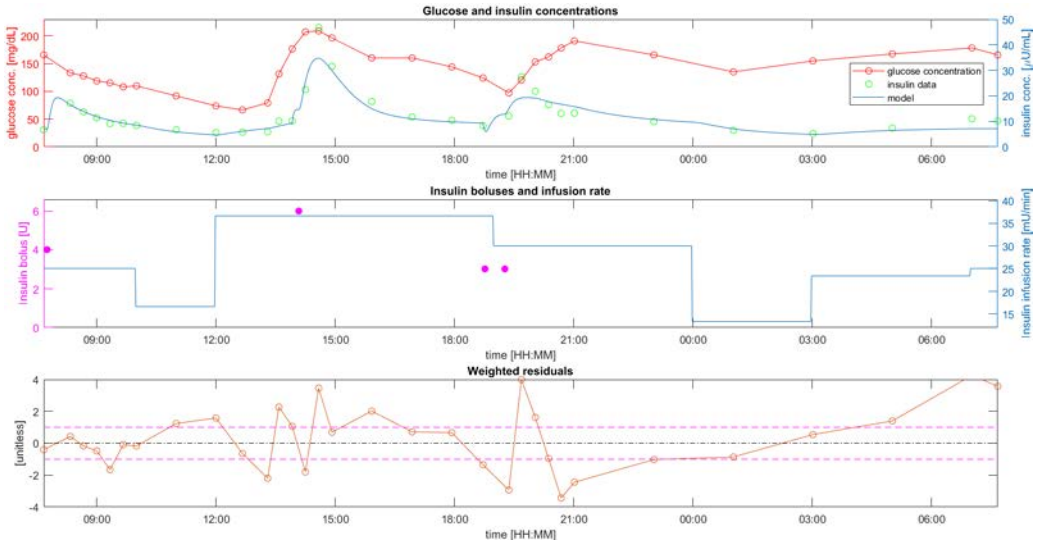

Figure 5.52: Model VI: Subject 4

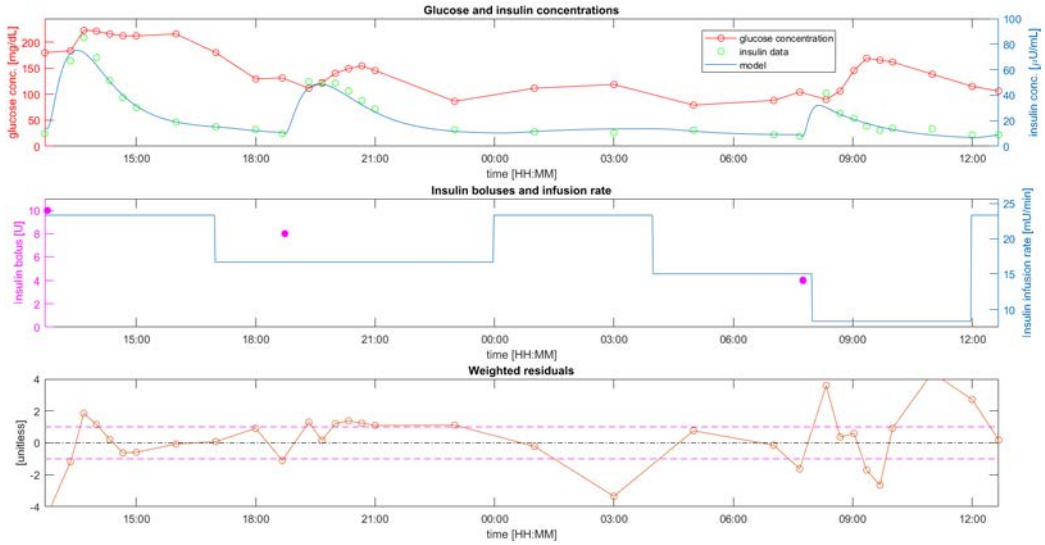

Figure 5.53: Model VI: Subject 5

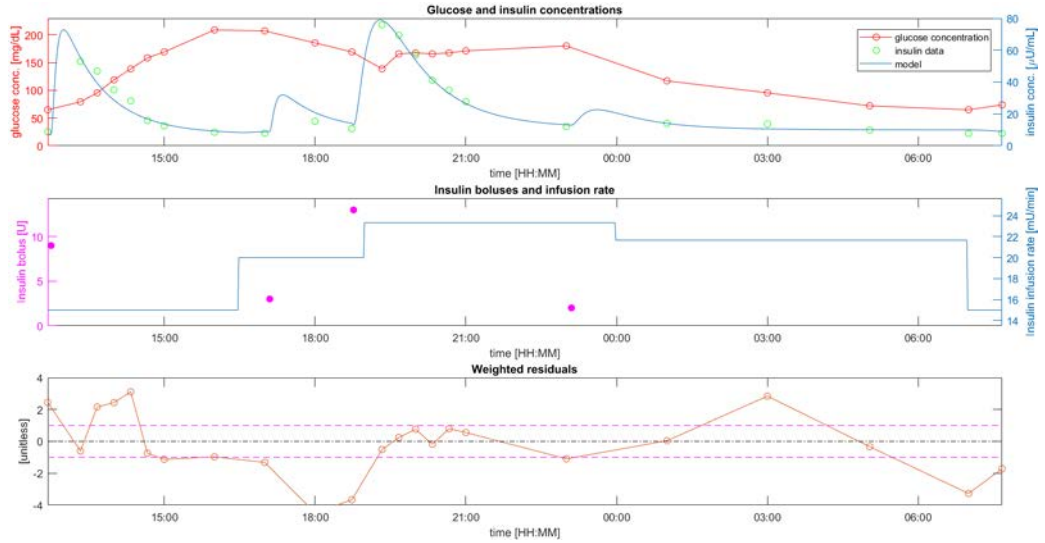

Figure 5.54: Model VI: Subject 6

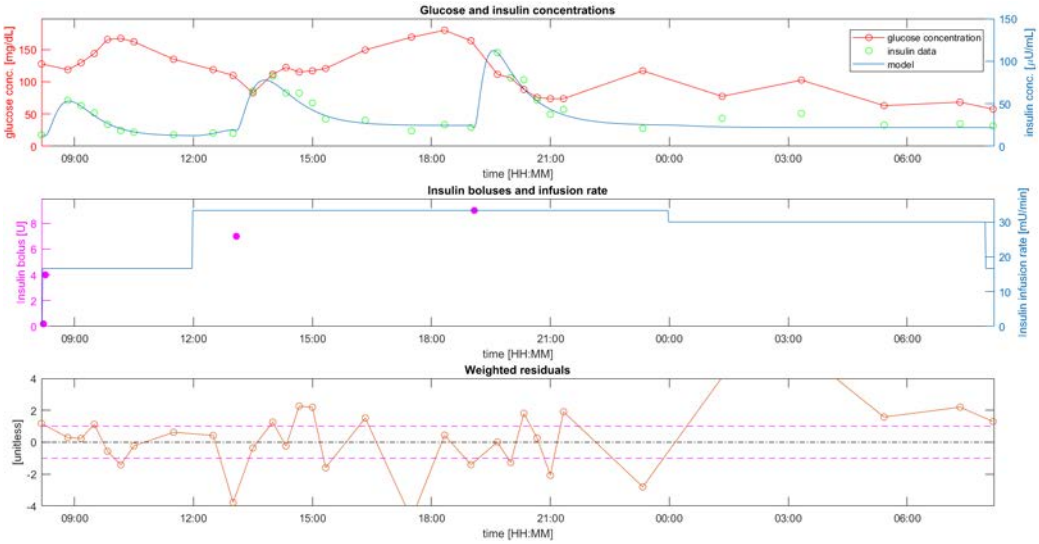

Figure 5.55: Model VI: Subject 7

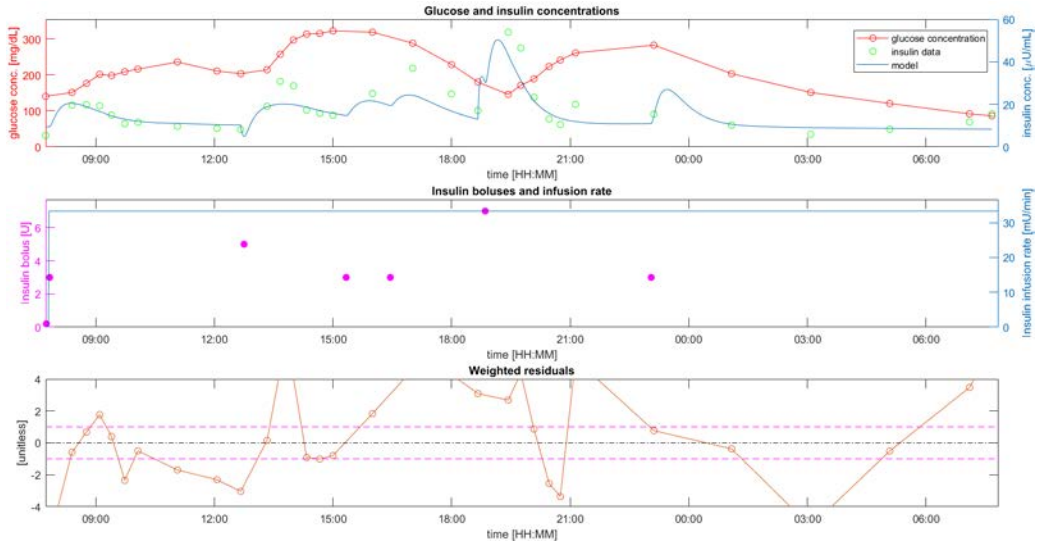

Figure 5.56: Model VI: Subject 8

Table 5.6: *Model VI*: parameter estimates and their precisions (CV)

Sub	*Parameters*								
	V_i (L/kg)	k_{a1} (min^{-1})	k_{d1} (min^{-1})	a_G $(min^{-1}dL/mg)$	n_b (min^{-1})	k_{a2} (min^{-1})	k_{d2} (min^{-1})	k_{a3} (min^{-1})	k_{d3} (min^{-1})
1	0.166 (20)	0.035 (17)	0.070 (33)	0.0001 (149)	0271 (20)	0.030 (22)	0.051 (32)	0.029 (5)	0.029 (N/A)
2	0.130 (20)	0.028 (4)	0.057 (18)	0.000002 (4886)	0.235 (20)	0.054 (9)	0.127 (13)	0.060 (13)	0.609 (297)
3	0.111 (16)	0.069 (40)	0.145 (64)	0.00002 (761)	0.352 (17)	0.023 (12)	0.304 (154)	0.030 (12)	0.902 (24)
4	0.149 (19)	0.014 (12)	0.242 (128)	0.0007 (28)	0.344 (20)	0.025 (16)	0.051 (20)	0.011 (10)	0.096 (47)
5	0.152 (19)	0.028 (4)	0.028 (N/A)	0.0001 (94)	0.157 (19)	0.023 (5)	0.023 (N/A)	0.012 (9)	0.206 (106)
6	0.152 (19)	N/A (N/A)	N/A (N/A)	0.0001 (109)	0.204 (19)	0.021 (7)	0.552 (5)	0.0174 (14)	0.073 (39)
7	0.158 (18)	0.038 (6)	0.038 (N/A)	0.0000001 (40152)	0.123 (18)	0.031 (5)	0.031 (N/A)	0.021 (10)	0.120 (55)
8	0.118 (12)	0.035 (10)	0.035 (N/A)	0.0006 (19)	0.430 (12)	0.014 (17)	0.046 (37)	0.042 (23)	0.051 (31)
MEAN ± SD (CV)	0.142 ± 0.020 (18)	0.035 ± 0.017 (13)	0.088 ± 0.079 (61)	0.0002 ± 0.0003 (5775)	0.265 ± 0.105 (18)	0.028 ± 0.012 (12)	0.148 ± 0.188 (44)	0.028 ± 0.017 (12)	0.261 ± 0.320 (85)

Model VII

The model VII was able to quite satisfactorily predict plasma insulin profiles in all the 8 subjects, slightly improving the model fit with respect to the linear Model III, as can be observed by weighted residuals, whose amplitude seems to be more comparable to the $[-1, +1]$ range (Figures 5.57–5.64). A saturation phenomenon concerning the fractional insulin clearance, which increases until a maximum value when the insulin concentration increases, seemed to occur. Thus, the model could better describe the data of the higher insulin absorption peaks, when a great amount of insulin could reach the liver and a saturation phenomenon could occur. Model fit in subject 1, 5 and 6, who were given significant insulin boluses ($> 10U$) are better described (Figures 5.57, 5.61, 5.62) than in linear Model III. In Table 5.7 model parameter estimates and their precisions are reported. Model parameters were overall estimated with precision: only in three cases, one for k_d, one for $V_{\max}$ and one for k_m (the latter two in the same subject 3), CV were greater than 100%. In addition, V_I (0.143 ± 0.019 L/Kg) is estimated close to the prior value (around 0.131 L/Kg). The variability of k_a in each of the three subintervals (k_{a1}, k_{a2} and k_{a3}) is quite small, since their dispersion (SD) is always lower than their average value (0.031 ± 0.025, 0.026 ± 0.015, 0.025 ± 0.017 min^{-1} respectively). On the other hand, the variability of k_d is small only in the third subinterval (0.164 ± 0.122 min^{-1}), while it is large in the first and second subintervals (0.256 ± 0.303 and 0.093 ± 0.097 min^{-1} respectively). Also the variability of $V_{\max}$ and k_m (which together represent the fractional clearance in this Model VII) is large (788 ± 1014 mU/min and 2657 ± 2692 mU respectively). Finally, one–way ANOVA was performed in order to test the *null hypothesis* that values in the k_{a1}, k_{a2} and k_{a3} columns (Table 5.7) are drawn from populations with the same mean values (using the F distribution). Since $F = 0.19 < F_{\text{crit}} = 3.49$, the null hypothesis was accepted, concluding that the differences between k_{a1}, k_{a2} and k_{a3} means are nonsignificant at the 5% significance level (the p–value is 0.8263). Then, one–way ANOVA was performed also to compare means of k_{d1}, k_{d2} and k_{d3}. Also in this case, $F = 1.38 < F_{\text{crit}} = 3.49$, the null hypothesis was accepted, concluding that the differences between k_{d1}, k_{d2} and k_{d3} means are nonsignificant at the 5% significance level (the p–value is 0.274).

Model VIII

Model VIII was able to satisfactorily predict plasma insulin profiles, as confirmed by the weighted residuals, whose amplitude is more comparable to the $[-1, +1]$ desired band than all the other models. However, a further analysis allows to detect some unphysiological pattern. In fact, for instance in subject 1 (Figure 5.65), it is evident how the absorption insulin peaks described by the models are quite difficult to be physiologically described. This particular model fit can be observed in all the sub-

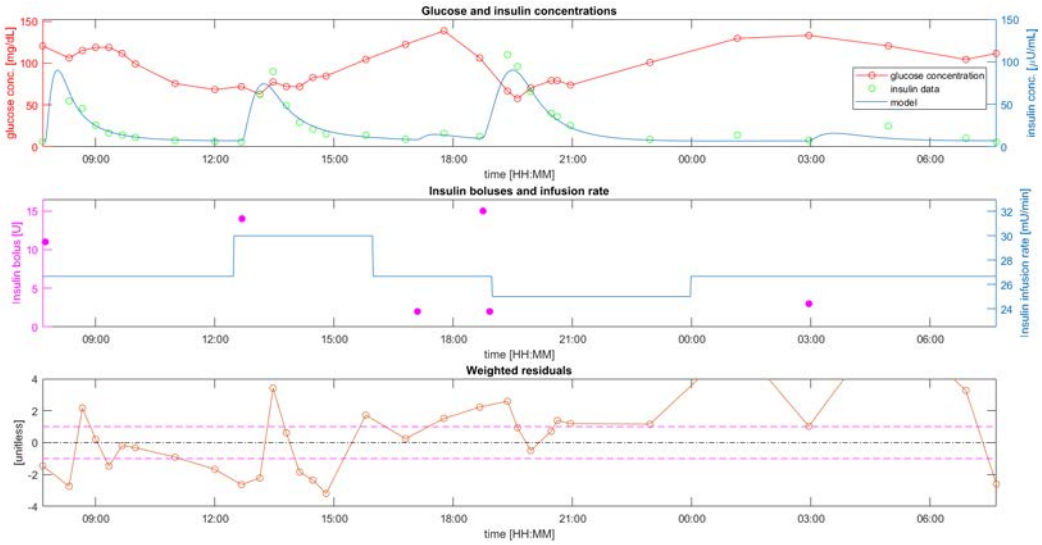

Figure 5.57: Model VII: Subject 1

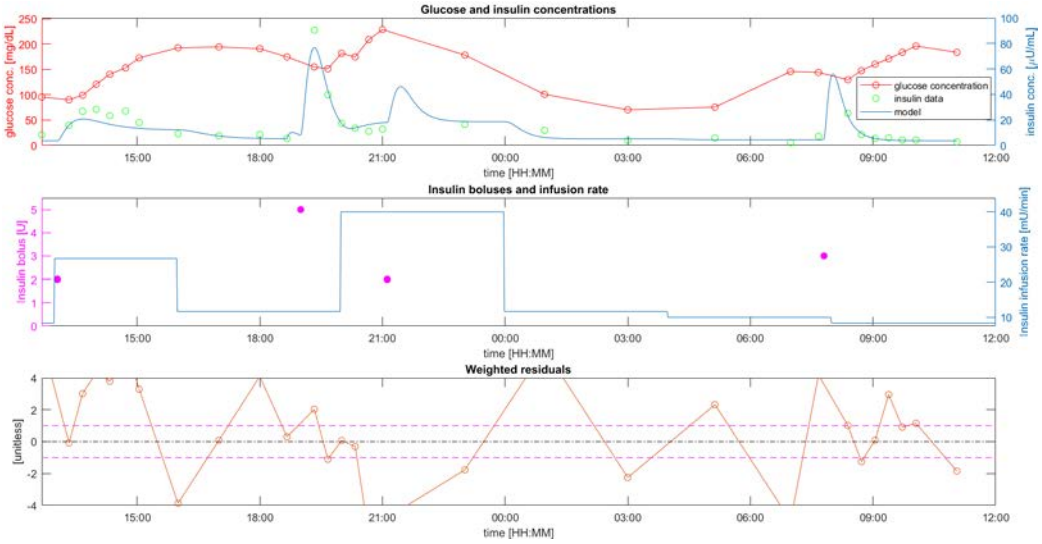

Figure 5.58: Model VII: Subject 2

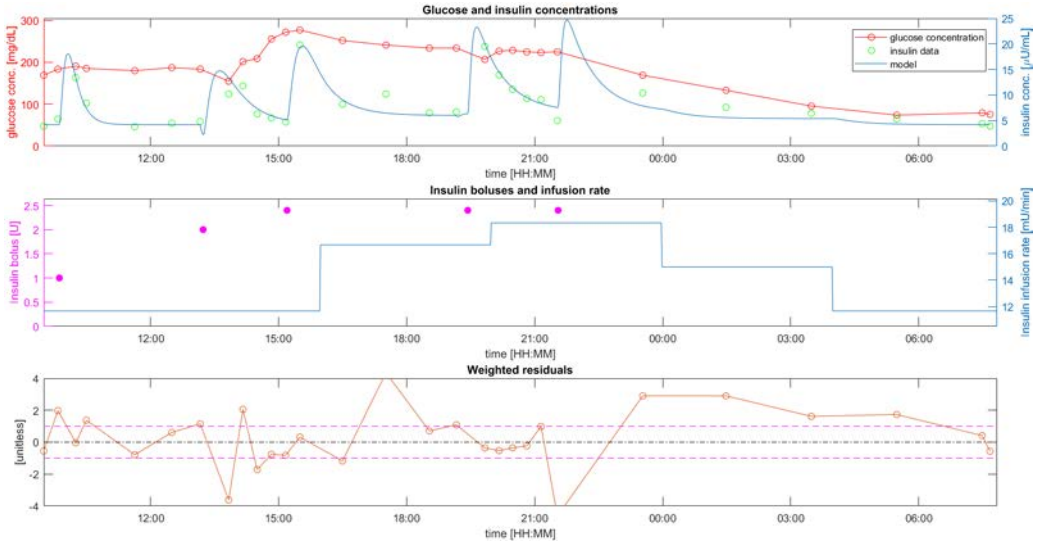

Figure 5.59: Model VII: Subject 3

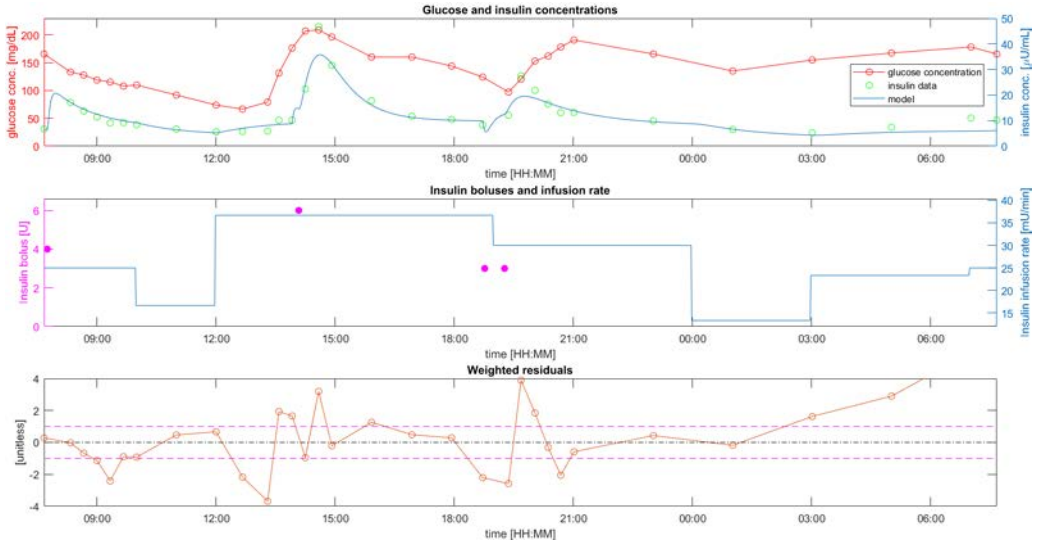

Figure 5.60: Model VII: Subject 4

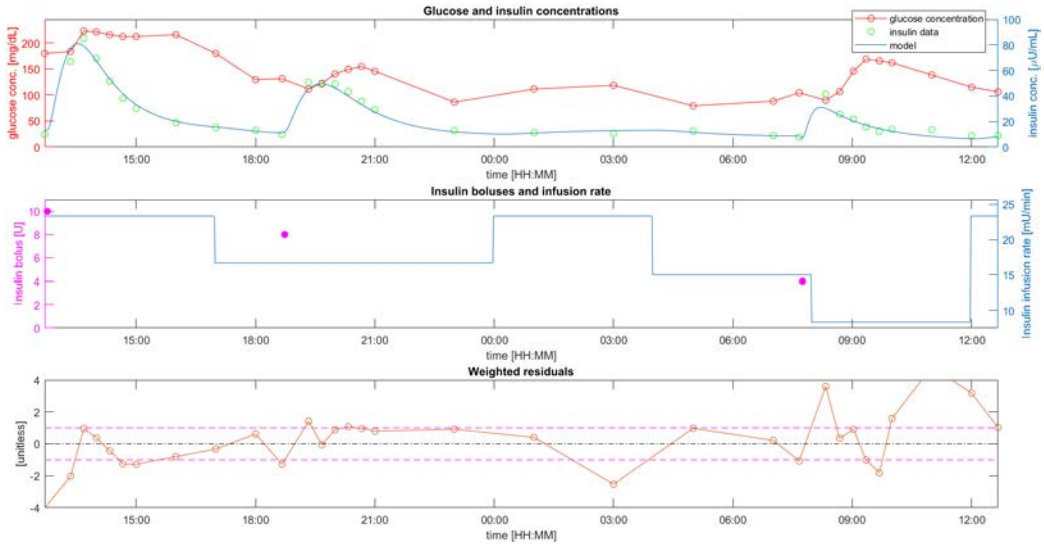

Figure 5.61: Model VII: Subject 5

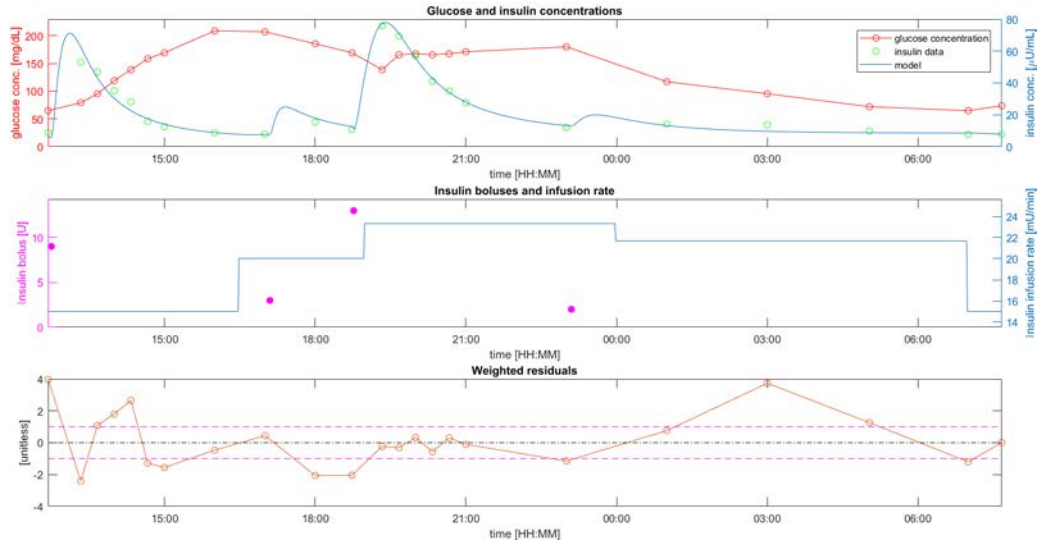

Figure 5.62: Model VII: Subject 6

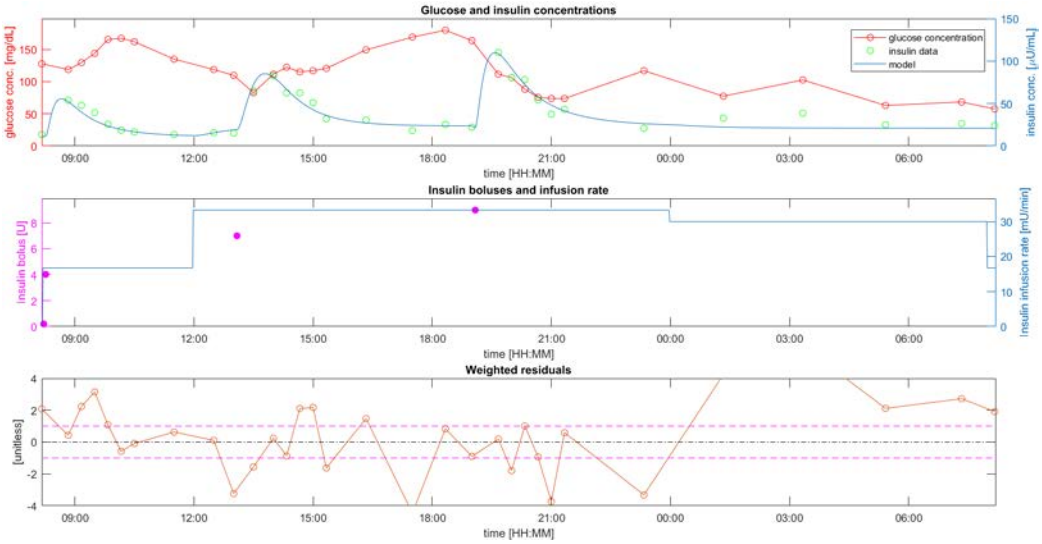

Figure 5.63: Model VII: Subject 7

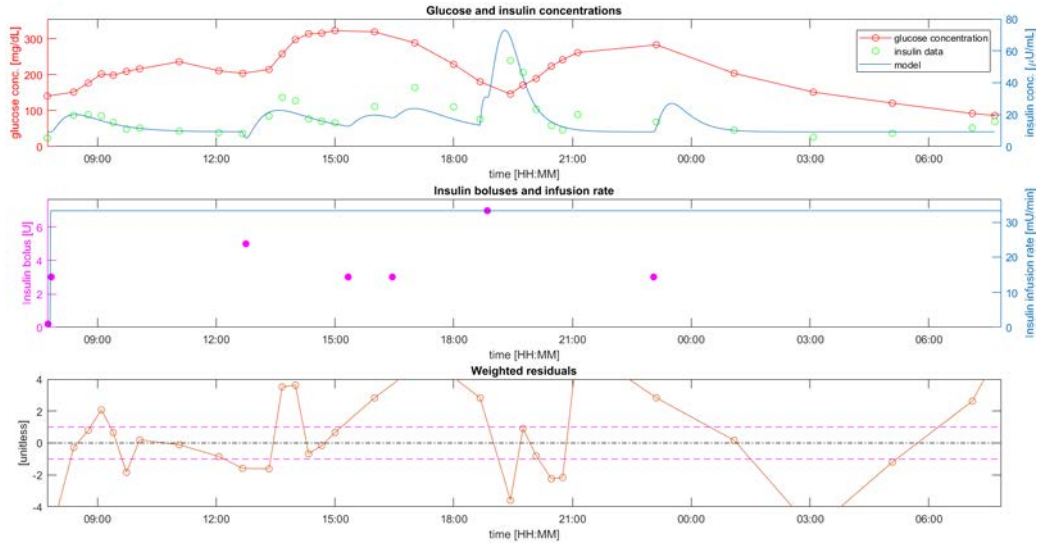

Figure 5.64: Model VII: Subject 8

Table 5.7: *Model VII*: parameter estimates and their precisions (CV)

Sub	*Parameters*								
	V_i (L/kg)	k_{a1} (min^{-1})	k_{d1} (min^{-1})	$V_{\max}$ (mU/min)	k_m (mU)	k_{a2} (min^{-1})	k_{d2} (min^{-1})	k_{a3} (min^{-1})	k_{d3} (min^{-1})
1	0.137 (19)	0.021 (7)	0.313 (49)	404.32 (13)	952.07 (27)	0.017 (9)	0.079 (21)	0.020 (25)	0.039 (33)
2	0.128 (19)	0.037 (47)	0.043 (51)	553.94 (81)	2143.8 (91)	0.062 (36)	0.091 (49)	0.057 (11)	0.282 (294)
3	0.110 (17)	0.084 (43)	0.157 (70)	3291.7 (1013)	9033.1 (1025)	0.030 (31)	0.088 (65)	0.026 (15)	0.345 (62)
4	0.145 (19)	0.013 (14)	0.887 (1)	445.53 (78)	1110.3 (91)	0.025 (55)	0.045 (97)	0.010 (14)	0.072 (38)
5	0.143 (19)	0.017 (17)	0.043 (27)	477.46 (29)	2580.3 (40)	0.021 (5)	0.021 (N/A)	0.012 (8)	0.152 (70)
6	0.142 (18)	N/A (N/A)	N/A (N/A)	312.55 (7)	1129.9 (15)	0.016 (5)	0.324 (12)	0.012 (8)	0.088 (29)
7	0.162 (19)	0.019 (12)	0.306 (39)	416.98 (70)	3061.9 (86)	0.020 (23)	0.061 (43)	0.015 (11)	0.285 (32)
8	0.175 (19)	0.022 (32)	0.043 (51)	402.61 (9)	1244.1 (20)	0.018 (8)	0.034 (17)	0.045 (14)	0.048 (16)
MEAN ± SD (CV)	0.143 ± 0.020 (19)	0.031 ± 0.025 (25)	0.256 ± 0.303 (41)	788.14 ± 1013.9 (163)	2656.9 ± 2691.7 (174)	0.026 ± 0.015 (22)	0.093 ± 0.097 (43)	0.025 ± 0.017 (13)	0.164 ± 0.122 (72)

jects except for subjects 2 and 3. In Table 5.8 model parameter estimates and their precisions are reported. Model parameters were overall estimated with good precision: only a_I in subject 3 was estimated with a very poor precision (CV $\gg$100%). The variability of k_a in each of the three subintervals (k_{a1}, k_{a2} and k_{a3}) is quite small, since its dispersion (SD) is lower than or equal to its average value (0.023 $\pm$ 0.019, 0.022 $\pm$ 0.022 and 0.016 $\pm$ 0.014 min^{-1} respectively). On the other hand, the variability of k_d is quite small only in the second subinterval (0.387 $\pm$ 0.340 min^{-1}), while in the other two subintervals, the variability in quite large (0.375 $\pm$ 0.431 and 0.322 $\pm$ 0.333 min^{-1} respectively). Then, V_i (0.112 $\pm$ 0.014 L/Kg) is estimated close to the prior value (around 0.131 L/Kg), a_I is estimated, on average, with poor precision (CV>100%) and its variability is quite small (0.004 $\pm$ 0.003 $min^{-1}mL/\mu U$). In addition, n_b (which, together with a_I, represents the fractional clearance in this Model VIII), is estimated, on average, with good precision (CV < 100%) and its variability is small (0.362 $\pm$ 0.090 min^{-1}). Finally, one–way ANOVA was performed in order to test the *null hypothesis* that values in the k_{a1}, k_{a2} and k_{a3} columns (Table 5.8) are drawn from populations with the same mean values (using the F distribution). Since $F = 0.26 < F_{\text{crit}} = 3.49$, the null hypothesis was accepted, concluding that the differences between k_{a1}, k_{a2} and k_{a3} means are nonsignificant at the 5% significance level (the p–value is 0.7722). Then, one–way ANOVA was performed also to compare means of k_{d1}, k_{d2} and k_{d3}. Also in this case, $F = 0.07 < F_{\text{crit}} = 3.49$, the null hypothesis was accepted, concluding that the differences between k_{d1}, k_{d2} and k_{d3} means are nonsignificant at the 5% significance level (the p–value is 0.9318).

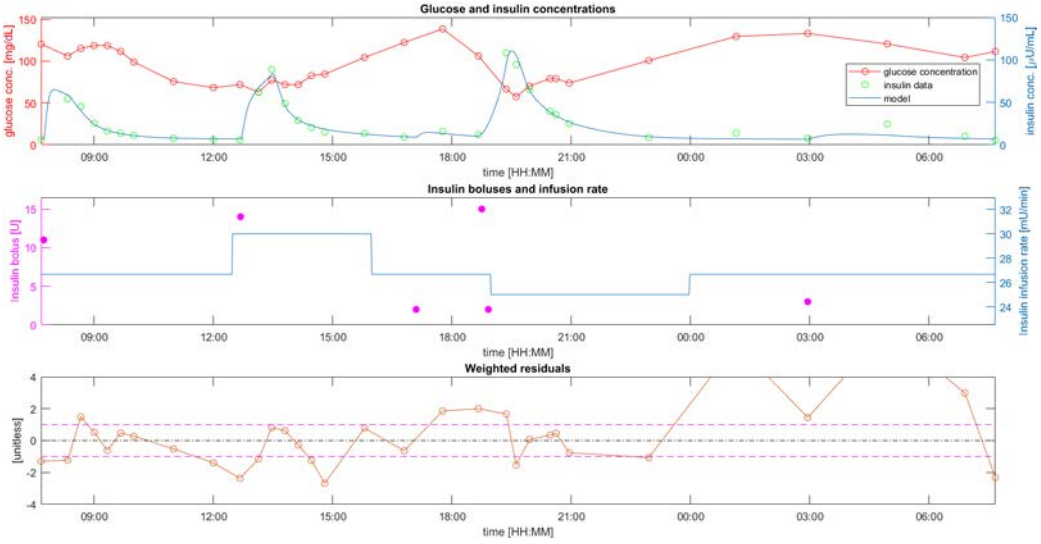

Figure 5.65: Model VIII: Subject 1

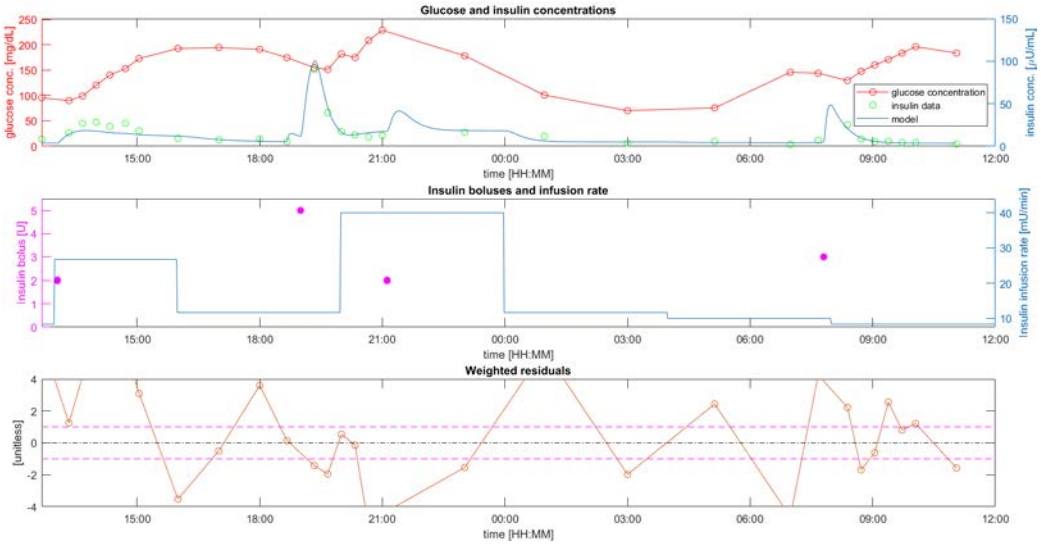

Figure 5.66: Model VIII: Subject 2

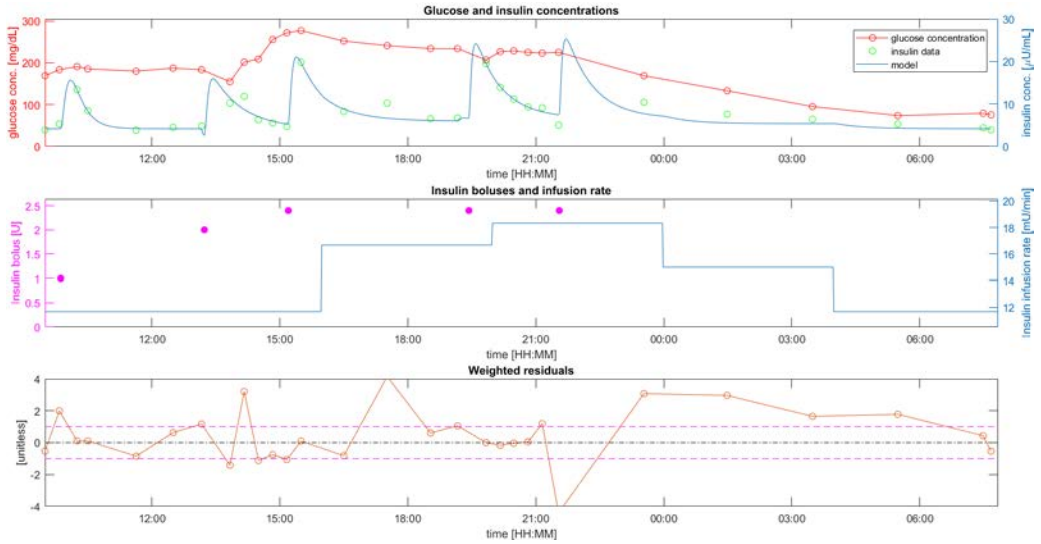

Figure 5.67: Model VIII: Subject 3

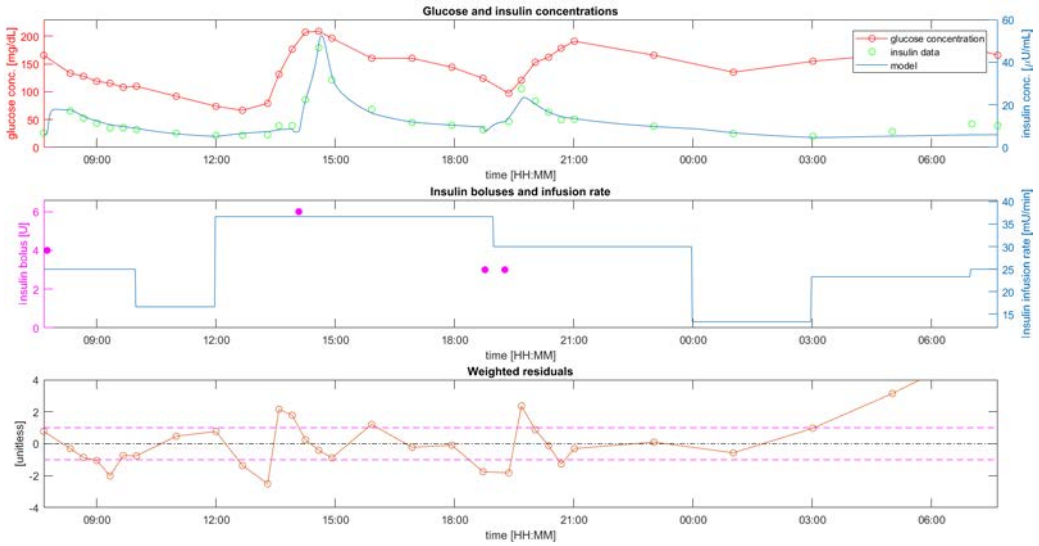

Figure 5.68: Model VIII: Subject 4

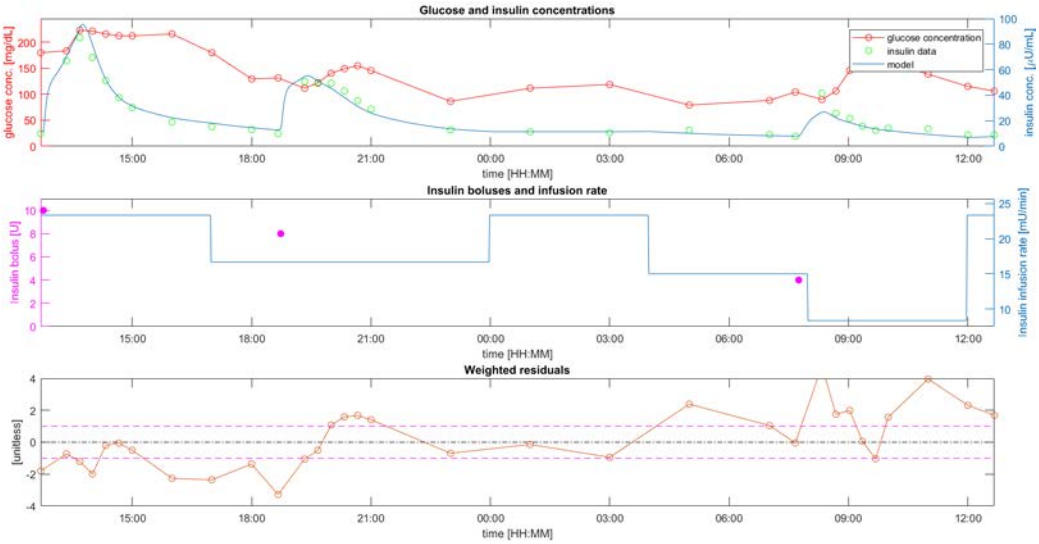

Figure 5.69: Model VIII: Subject 5

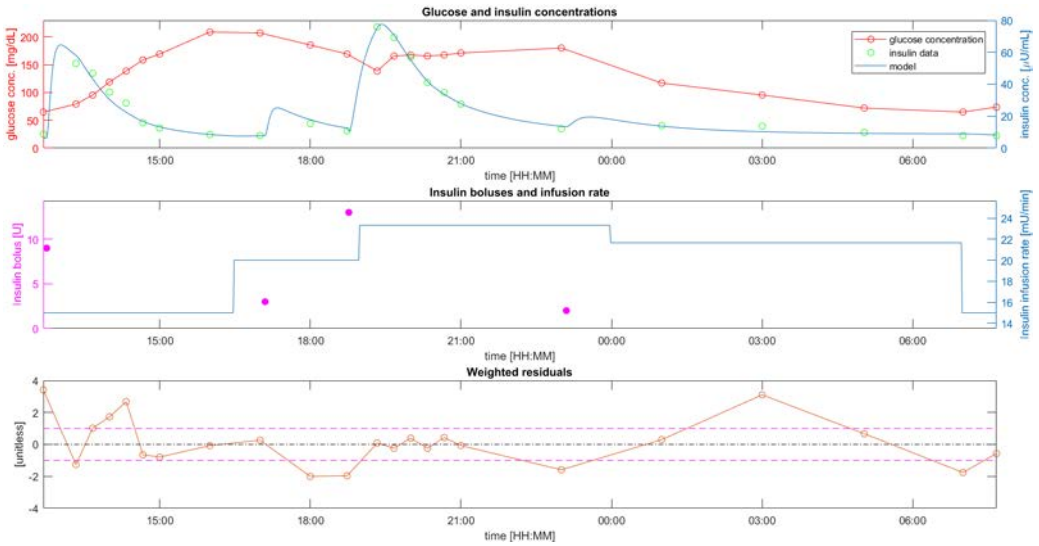

Figure 5.70: Model VIII: Subject 6

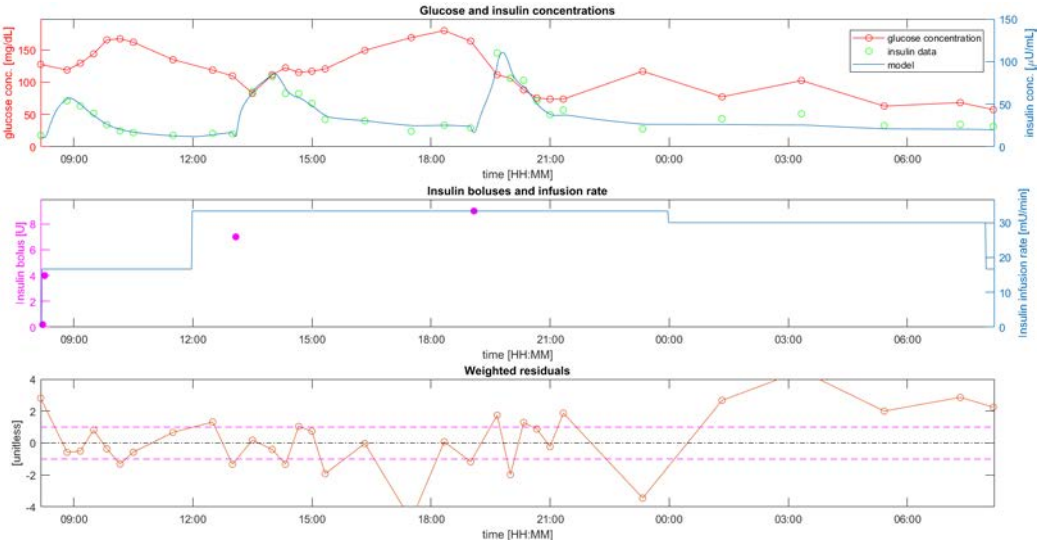

Figure 5.71: Model VIII: Subject 7

Table 5.8: *Model VIII*: parameter estimates and their precisions (CV)

Sub	*Parameters*								
	V_i (L/kg)	k_{a1} (min^{-1})	k_{d1} (min^{-1})	a_I $(min^{-1}mL/\mu U)$	n_b (min^{-1})	k_{a2} (min^{-1})	k_{d2} (min^{-1})	k_{a3} (min^{-1})	k_{d3} (min^{-1})
1	0.121 (16)	0.022 (8)	0.304 (61)	0.003 (18)	0.457 (16)	0.013 (8)	0.167 (77)	0.019 (8)	0.019 (N/A)
2	0.097 (17)	0.021 (20)	0.066 (35)	0.002 (68)	0.342 (17)	0.074 (12)	0.074 (N/A)	0.047 (12)	0.494 (18)
3	0.120 (20)	0.065 (31)	0.143 (5)	0.00004 (5097)	0.333 (20)	0.024 (11)	0.482 (1)	0.026 (16)	0.967 (0)
4	0.126 (17)	0.012 (14)	0.999 (0)	0.009 (23)	0.458 (17)	0.010 (31)	0.214 (91)	0.007 (19)	0.0997 (61)
5	0.101 (17)	0.007 (11)	0.988 (7)	0.003 (20)	0.290 (17)	0.008 (11)	0.784 (8)	0.008 (14)	0.086 (74)
6	0.121 (18)	N/A (N/A)	N/A (N/A)	0.002 (37)	0.287 (19)	0.0175 (9)	0.394 (16)	0.012 (16)	0.084 (39)
7	0.091 (14)	0.016 (13)	0.087 (42)	0.002 (16)	0.250 (15)	0.008 (20)	0.962 (2)	0.004 (29)	0.237 (7)
8	0.123 (17)	0.018 (26)	0.040 (49)	0.009 (17)	0.479 (17)	0.021 (6)	0.021 (N/A)	0.008 (12)	0.589 (2)
Mean ± SD (CV)	0.112 ± 0.014 (17)	0.023 ± 0.019 (16)	0.375 ± 0.431 (27)	0.004 ± 0.003 (662)	0.362 ± 0.090 (17)	0.022 ± 0.022 (15)	0.387 ± 0.340 (36)	0.016 ± 0.014 (16)	0.322 ± 0.333 (27)

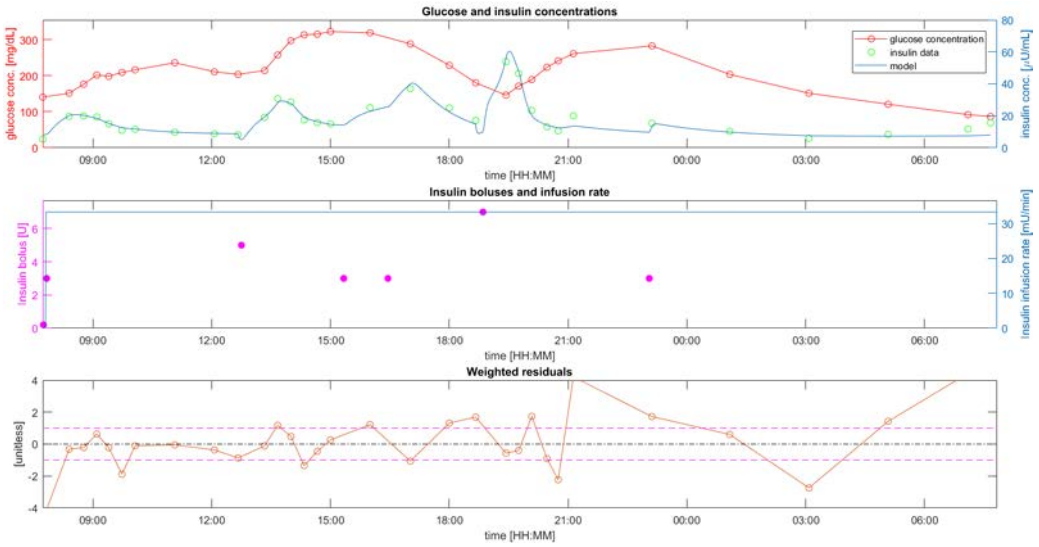

Figure 5.72: Model VIII: Subject 8

5.3 Model selection and statistical analysis

Model comparison is summarized in Table 5.9. Model I and II are not able to well describe the data, in fact their measure of the deviation of the experimental data from the predicted, represented by *WRSS*, is resulted to be very high with respect to the other models. This is also confirmed by the percentage of subjects who passed the Runs test equal to 75% for Model I and II and 88% for Model III, which instead quite well predicted the data. Among the models III – VIII which quite satisfactorily describe the data, WRSS results the lowest for Model VIII but it shows very unphysiological model predictions, so the model cannot be physiologically acceptable. Thus, the second lowest value is obtained with Model VII. Runs test, instead, does not allow to add statistical information in the model selection. The ability of the model to estimate model parameters with a satisfactory precision results, on average, lower than 100% for Models III (17%), VII(62%) and VIII (91%). In addition, the 62% in Model VII is mostly due to only two bad estimates in subject 3 which contributes in increasing the average precision. Then, if it is observed the percentage of subjects with all the CV below 100%, it is equal to 88% for model 3 (7/8 subjects), 75% for Model 7 (6/8 subjects) and 88% for Model 8 (7/8 subjects). Furthermore, in Model III, in 48% of the time, one model parameter (k_d) is virtually identical to k_a. In Model VII, this happened only 0.05% of the time. Finally, AICc is the lowest (149) in Model VIII, then in Model VII (188) and in Model III (197).
In summary, Model I and II are not able to reproduce the data, Model IV, V, VI are able to better describe the data but they are not numerically identifiable, with an

Table 5.9: Summary results of Model comparison

Model	Average precision of parameter estimates	WRSS	Residual randomness	AICc
I	6%	794.56	75%	799
II	13%	254.63	75%	261.55
III	17%	187.06	88%	196.67
IV	$> 100\%$	238.49	75%	251
V	$\gg 100\%$	191.08	100%	203.6
VI	$\gg 100\%$	186.19	88%	198.71
VII	62%	175.02	88%	187.55
VIII	91%	136.11	88%	148.64

average unacceptable precision of the estimates (CV>100%). Model VIII shows unphisyiological behaviour in insulin profiles. Model III and VII are able to reproduce the data with, on average, a good precision of parameter estimates in almost all subjects, a reasonable physiological interpretation of model parameters, but Model VII has a WRSS and AICc values lower than Model III. Therefore, taking together all the criteria, Model VII is selected as the best Model among the ones developed.

Chapter 6

Conclusions

Nowadays, insulin therapy in T1D is usually based on exogenous insulin administration via subcutaneous route through the common MDI or, more recently, CSII therapy. These SC insulin replacement strategies face problems associate to delays and intra–/inter–subject variability. In this regard, CIPII therapy mimics physiology more closely than standard therapies, restoring partially the positive portal to systemic insulin gradient, and it constitutes a last treatment option in cases of SC insulin resistance in subjects with T1D. Then, considering the mounting interest, among the researchers in this field, towards a fully automated and implantable AP, the IP insulin infusion seems to be the better solution in terms of mimicking the physiological insulin delivery route. In this regard, in order to better understand the underlying physiology in the IP route of insulin administration, in this thesis, a first model of the IP kinetics, able to describe plasma insulin data after IP administration and accurately estimate model parameters, was developed. To do this, we used a unique dataset of eight subjects treated by implanted pumps, who underwent a two–day closed–loop and one–day open–loop therapy. A battery of models, with increasing complexity, was developed and model selection was carried out applying well–accepted criteria of ability to describe the data, parameters identifiability, physiological plausibility and parsimony. In particular, assuming a mono–compartmental description of plasma insulin kinetics, eight models of intraperitoneal insulin absorption have been developed. In Model I a direct insulin absorption into circulation was proposed, but it was not able to well describe the data, resulting with the highest WRSS and the lowest runs test to assess whiteness of weighted residuals. Model II assumes a mono-compartment description for the intraperitoneal insulin absorption showing its inability to well describe the data as Model I. Model III assumes a two-compartment description for the intraperitoneal insulin absorption with a satisfactory description of the data, precise model parameters estimation leading to WRSS and AICc values among the lowest obtained. Models IV and V, which assume respectively a non–linear (Michaelis-Menten for Model IV and Langmuir for Model V) absorption between the two intraperitoneal

compartments, and Model VI, which assumes a relation between the glucose concentration and fractional insulin clearance, do not improve consistently the model fit and model parameters, on average, were estimated with poor precision (CV>100%). Model VII assumes a non–linear (Michaelis–Menten) fractional insulin clearance and allowed to accurately estimate model parameters and well describe the data. Finally, Model VIII, similarly to Model VII, assumes a relation between the insulin concentration and fractional insulin clearance, showing the lowest WRSS value but with unphysiological model predictions. Therefore, the two models which were able to well predict the data with physiological plausible parameters estimated with precision, resulted to be Models III and VII with the latter one chosen as best because of lowers values of WRSS and AICc. In further detail, in both models, the intraperitoneal parameter k_a, which has been estimated three times, one in each time subinterval, shows both a small inter–subject variability (SD is always lower than their average value) and a small intra–subject variability (confirmed by ANOVA test), so that, an average k_a value resulted to be equal to 0.033 min^{-1} in Model III and 0.027 min^{-1} in Model VII. On the other hand, k_d presents a quite large inter–subject variability but a small intra–subject variability (ANOVA test) in both Model III and VII. A possible limitation of the study can be related to the low number of the subjects. However, if consider the high experimental costs and the invasive procedure for pump insertion instead of the conventional SC insulin therapy, the dataset can be considered a satisfactory and unique tool.

Future challenges will include testing the models with the closed–loop data available in the database, in order to validate the model also in closed–loop, then, using another model for measurement error of insulin, such as with standard deviation known up to a proportionally constant a posteriori estimated. Finally, another next step will be adopting the two–compartmental model for the insulin kinetics, with the purpose to test the model selected as the best and include it in the UVA/Padova T1D Simulator, allowing to simulate IP route of insulin administration.

Bibliography

[1] M. A. Atkinson, G. S. Eisenbarth, and A. W. Michels. "Type 1 diabetes". In: *Lancet* 383 (2014), pp. 69–82.

[2] J.D. Bagdade, F.L. Dunn, et al. "Intraperitoneal insulin therapy corrects abnormalities in cholesteryl ester transfer and lipoprotein lipase activities in insulin-dependent diabetes mellitus". In: *Arteriosclerosis Thrombosis and Vascular Biology* 14 (1994), pp. 1933–1939.

[3] L. Bally, H. Thabit, and R. Hovorka. "Finding the right route for insulin delivery – an overview of implantable pump therapy". In: *Expert Opininion on Drug Delivery* 14 (2017), pp. 1103–1111.

[4] G. Bellu, M.P. Saccomani, S. Audoly, et al. "DAISY: A new software tool to test global identifiability of biological and physiological systems". In: *Computer Methods and Programs in Biomedicine* 88 (2007), pp. 52–61.

[5] R.M. Bergenstal, W.V Tamborlane, A. Ahmann, et al. "Effectiveness of sensor-augmented insulin-pump therapy in type 1 diabetes". In: *The New England Journal of Medicine* 363 (2010), pp. 311–320.

[6] M. Bisiacco and G. Pillonetto. *Sistemi e Modelli*. Bologna: Esculapio, 2015.

[7] J.C. Blair, A. McKay, C. Ridyard, et al. "Continuous subcutaneous insulin infusion versus multiple daily injection regimens in children and young people at diagnosis of type 1 diabetes: pragmatic randomised controlled trial and economic evaluation". In: *BMJ* 365 (2019).

[8] P.R. Bratusch–Marrain et al. "Hepatic disposal of biosynthetic human insulin and porcine C-peptide in humans". In: *Metabolism* 33 (1984), pp. 151–157.

[9] D.R. Burnett, L.M. Huyett, H.C. Zisser, et al. "Glucose sensing in the peritoneal space offers faster kinetics than sensing in the subcutaneous space". In: *Diabetes* 63 (2014), pp. 2498–2505.

[10] K.P. Burnham and D.R. Anderson. "Multimodel inference: understanding AIC and BIC in model selection". In: *Sociological Methods & Research* 33 (2004), pp. 61–304.

[11] M. Campioni et al. “Minimal model assessment of hepatic insulin extraction during an oral test from standard insulin kinetic parameters”. In: *American Journal of Physiology–Endocrinology and Metabolism* 297 (2009), pp. 941–948.

[12] C. Cobelli and E. Carson. *Introduction to Modeling in Physiology and Medicine*. Academic Press, 2019.

[13] C. Cobelli and E. Carson. *Modelling methodology for physiology and medicine*. Elsevier, 2014.

[14] C. Colette et al. “Effect of different insulin administration modalities on vitamin D metabolism of insulin-dependent diabetic patients”. In: *Hormone and Metabolic Research* 21 (1989), pp. 37–41.

[15] C. Dalla Man et al. “The UVA/PADOVA type 1 diabetes simulator: new features”. In: *Journal of Diabetes Science and Technology* 8 (2014), pp. 26–34.

[16] E. Dassau, E. Renard, J. Place, et al. “Intraperitoneal insulin delivery provides superior glycaemic regulation to subcutaneous insulin delivery in model predictive control-based fully-automated artificial pancreas in patients with type 1 diabetes: a pilot study”. In: *Diabetes, Obesity and Metabolism* 19 (2017), pp. 1698–1705.

[17] E. Ferrannini and C. Cobelli. “The kinetics of insulin in man. II. Role of the liver”. In: *Diabetes/Metabolism Reviews* 3 (1987), pp. 365–397.

[18] J.B. Field. “Extraction of insulin by liver”. In: *Annual Review of Medicine* 24 (1973), pp. 309–314.

[19] A.L. Fougner, K. Kolle, N.K. Skjarvold, et al. “Intraperitoneal glucose sensing is sometimes surprisingly rapid”. In: *Modeling, Identification and Control* 37 (2016), pp. 121–131.

[20] R. Garcia-Verdugo, M. Erbach, and O. Schnell. “A new optimized percutaneous access System for CIPII”. In: *Journal of Diabetes Science and Technology* 11 (2017), pp. 814–821.

[21] M.J. Haardt, J.L. Selam, G. Slama, et al. “A cost–benefit comparison of intensive diabetes management with implantable pumps versus multiple subcutaneous injections in patients with type I diabetes”. In: *Diabetes Care* 17 (1994), pp. 847–851.

[22] H. Hanaire–Broutin, C. Broussolle, N. Jeandidier, et al. “Feasibility of intraperitoneal insulin therapy with programmable implantable pumps in IDDM. A multicenter study. The EVADIAC Study Group. Evaluation dans le Diabète du Traitement par Implants Actifs”. In: *Diabetes Care* 18 (1995), pp. 388–392.

[23] C.A. Hedman et al. “Intraperitoneal insulin delivery to patients with type 1 diabetes results in higher serum IGF-I bioactivity than continuous subcutaneous insulin infusion”. In: *The Journal of Clinical Endocrinology & Metabolism* 81 (2014), pp. 58–62.

[24] N. Jeandidier, S. Boullu, E. Delatte, et al. “High antigenicity of intraperitoneal insulin infusion via implantable devices: preliminary rat studies”. In: *Hormone and Metabolic Research* 33 (2001), pp. 34–38.

[25] V. Lassmann–Vague, D. Raccah, M. Pugeat, et al. “SHBG (sex hormone binding globulin) levels in insulin dependent diabetic patients according to the route of insulin administration”. In: *Hormone and Metabolic Research* 26 (1994), pp. 436–437.

[26] S. Lee and P. Narendran. “A New Optimized Percutaneous Access System for CIPII”. In: *BMJ Case Reports* (2014).

[27] A. Liebl, R. Hoogma, E. Renard, et al. “A reduction in severe hypoglycaemia in type 1 diabetes in a randomized crossover study of continuous intraperitoneal compared with subcutaneous insulin infusion”. In: *Diabetes, Obesity and Metabolism* 11 (2009), pp. 1001–1008.

[28] S. J. Livingstone, H. M. Colhoun, et al. “Estimated life expectancy in a Scottish cohort with type 1 Diabetes, 2008-2010”. In: *JAMA* 313 (2015), pp. 37–44.

[29] S.J.J Logtenberg, E. van Ballegooie, H. Israêl–Bultman, et al. “Glycaemic control, health status and treatment satisfaction with continuous intraperitoneal insulin infusion”. In: *The Netherlands Journal of Medicine* 65 (2007), pp. 65–70.

[30] S.J.J Logtenberg, N. Kleefstra, S.T. Houweling, et al. “Health-related quality of life, treatment satisfaction, and costs associated with intraperitoneal versus subcutaneous insulin administration in type 1 diabetes: a randomized controlled trial”. In: *Diabetes Care* 33 (2010), pp. 1169–1172.

[31] S.J.J Logtenberg, N. Kleefstra, S.T. Houweling, et al. “Improved glycemic control with intraperitoneal versus subcutaneous insulin in type 1 diabetes: a randomized controlled trial”. In: *Diabetes Care* 32 (2009), pp. 1372–1377.

[32] J.J Meier, J.D. Veldhuis, and P.C. Butler. “Pulsatile insulin secretion dictates systemic insulin delivery by regulating hepatic insulin extraction in humans”. In: *Diabetes* 54 (2005), pp. 1649–1656.

[33] F. Piccinini et al. “A model for the estimation of hepatic insulin extraction after a meal”. In: *IEEE Transactions on Biomedical Engineering* 63 (2016), pp. 1925–1932.

[34] E. Renard. “Analysis of "A new optimized percutaneous access system for CIPII"”. In: *Journal of Diabetes Science and Technology* 11 (2017), pp. 822–824.

[35] E. Renard et al. “Artificial beta-cell: clinical experience toward an implantable closed-loop insulin delivery system”. In: *Diabetes & metabolism* 32 (2006), pp. 497–502.

[36] E. Renard, J. Place, M. Cantwell, et al. “Closed–Loop insulin delivery using a subcutaneous glucose sensor and intraperitoneal insulin delivery”. In: *Diabetes Care* 33 (2010), pp. 121–127.

[37] E. Renard, D. Apostol, D. Lauton, et al. “Quality of life in diabetic patients treated by insulin pumps”. In: *QoL Newsletter* 28 (2002), pp. 11–13.

[38] G. Ruotolo, M. Parlavecchia, M.R. Taskinen, et al. “Normalization of lipoprotein composition by intraperitoneal insulin in IDDM. Role of increased hepatic lipase activity”. In: *Diabetes Care* 17 (1994), pp. 6–12.

[39] M. P. Saccomani and L. D’Angiò. “Examples of testing global identifiability with the DAISY software”. In: *IFAC Proceedings Volumes* 42 (2009), pp. 48–53.

[40] C.V. Saudek, J.L. Selam, H.A Pitt, et al. “A preliminary trial of the programmable implantable medication system for insulin delivery”. In: *The New England Journal of Medicine* 321 (1989), pp. 574–579.

[41] M. Schiavon, C. Dalla Man, and C. Cobelli. “Modeling subcutaneous absorption of fast-acting insulin in type 1 Diabetes”. In: *IEEE Transactions on Biomedical Engineering* 65 (2018), pp. 2079–2086.

[42] O. Schnell, E. Gerlach, B. Hillebrand, et al. “A case of diabetic pregnancy controlled with a percutaneous access device for intraperitoneal insulin infusion”. In: *Diabetes Care* 17 (1994), pp. 1354–1355.

[43] J.L. Selam, D. Raccah, N. Jean–Didier, et al. “Randomized comparison of metabolic control achieved by intraperitoneal insulin infusion with implantable pumps versus intensive subcutaneous insulin therapy in type I diabetic patients”. In: *Diabetes Care* 15 (1992), pp. 53–58.

[44] G. Toffolo et al. “A minimal model of insulin secretion and kinetics to assess hepatic insulin extraction”. In: *American Journal of Physiology–Endocrinology and Metabolism* 290 (2006), pp. 169–176.

[45] P.R. van Dijk et al. “After 6years of intraperitoneal insulin administration IGF-I concentrations in T1DM patients are at low-normal level”. In: *Growth Hormone & IGF Research* 25 (2015), pp. 316–319.

[46] P.R van Dijk, S.J.J Logtenberg, K.H. Groenier, et al. “Complications of continuous intraperitoneal insulin infusion with an implantable pump”. In: *World Journal of Diabetes* 3 (2012), pp. 142–148.

[47] P.R. van Dijk, S.J.J Logtenberg, K.H. Groenier, et al. "Continuous intraperitoneal insulin infusion in type 1 diabetes: a 6–year post-trial follow–up". In: *BMC endocrine disorders* (2014), pp. 14–30.

[48] P.R van Dijk, K.H. Groenier, J.H. DeVries, et al. "Continuous intraperitoneal insulin infusion versus subcutaneous insulin therapy in the treatment of type 1 diabetes: effects on glycemic variability". In: *Diabetes technology & therapeutics* 17 (2015), pp. 379–384.

[49] P.R. van Dijk, S.J.J Logtenberg, R.O.B. Ganst, et al. "Intraperitoneal insulin infusion: treatment option for type 1 diabetes resulting in beneficial endocrine effects beyond glycaemia". In: *Clinical Endocrinology* 81 (2014), pp. 488–497.

[50] R. Visentin et al. "The UVA/PADOVA type 1 diabetes simulator goes from single meal to single day". In: *Journal of Diabetes Science and Technology* 12 (2018), pp. 273–281.

Vorrei innanzitutto ringraziare la Professoressa Dalla Man per avermi dato l'opportunità di cimentarmi in questo lavoro di Tesi, per la Sua grande disponibilità e cortesia e per la Sua professionalità nel seguirmi durante tutti questi mesi. Porgo un ringraziamento particolare anche a Michele Schiavon che mi ha sempre supportato con entusiasmo, pazienza e dedizione, aiutandomi a costruire un metodo di lavoro rigoroso e dispensando utili consigli.
Dedico questo lavoro alla mia famiglia, che mi è sempre stata vicino, al mio nipotino Tommaso, che durante questi suoi primi mesi di vita mi ha regalato tanti sorrisi, ai fioi di Conegliano, in particolare ad Enric, Silve e Pala, per i tanti momenti di spensieratezza e serate magiche, a Met e Cri, perché, in modo diverso, sono stati per me un grande ed insostituibile punto di riferimento, ai miei coinquilini, in particolare Toso, Vitu e Samu, che mi hanno sempre rallegrato, aiutato e occupato abusivamente la camera. Infine, alla mia super compagnia universitaria, Giulia C., Giulia N., Jess e Manu per i tanti bei momenti passati insieme a lezione, gli aperitivi e le tante risate.

One inch at a time.